PLASTO-HYDRODYNAMIC PRESSURE DUE TO THE FLOW OF VISCOUS FLUID THROUGH A CONFINED PASSAGE

by

IBRAHIM ALNATOUR (B.Eng)

This thesis is submitted as the fulfilment of the requirement for the award of Master of engineering (MEng) by research to the

DUBLIN CITY UNIVERSITY

Sponsoring Establishment :

Scientific Studies and Research Centre
Damascus-Syria

August 1989

DECLARATION

I declare that all unreferened work described in this thesis is entirely my own, and no portion of the work referred to in this thesis has been submitted in support of an application for another degree or qualification of this or any other university or other institute of learning.

SIGNED ____________

Ibrahim Al Natour

August 1989

CONTENTS Page

CONTENTS Page

CONTENTS Page

CONTENTS

ABSTRACT

PLASTO-HYDRODYNAMIC PRESSURE DUE TO THE FLOW OF VISCOUS FLUID THROUGH A CONFINED PASSAGE

I. AL Natour

A combined geometry plasto-hydrodynamic pressure unit has been investigated theoretically and experimentally. Previous investigators have used either stepped parallel or tapered bore pressure unit for die-less drawing and/or coating of wires, tubes and stripes. In the present study a combined parallel and tapered bore unit has been used in conjunction with polymer melts as pressure fluid.

In this present work a pressure unit is heated to convert the polymer feed into a viscous melt and the pressure in the fluid is generated by hydrodynamic action when a wire is drawn through it. Experimental work has been carried out on different pressure units with similar external but different internal geometries to investigate the performance of new pressure unit. Different types of polymer were used as the pressure medium. In this work analytical models based on Newtonian and pseudo-Newtonian characteristics have been developed to investigate the performance of the pressure unit and to optimise the process. The predicted results showed reasonable agreement those observed experimentally in magnitudes of maximum pressure. Experimental and theoretical results, showed that there exists a gap ratio (optimum) for which the pressure is maximum. For greater or smaller values of the gap ratio than the optimum value, a decreased magnitude for the maximum pressure was obtained. The maximum pressure at that gap ratio(optimum) is much higher compared to those obtained using either stepped or tapered bore pressure unit at similar conditions.

ACKNOWLEDGEMENTS

The author wishes to express his gratitude and sincere thanks to Professor M.S.J. Hashmi, Head of school of mechanical engineering for his support and helpful supervision and guidance during this research. Thanks are also due to Mr.T.walsh and other technical staff for their support at various stages of this work.

The author acknowledges the assistance given by the Scientific Studies and Researches Centre in Syria for providing financial support towards this research.

Finally, a word of thanks to my wife for her patience and support towards completion of my work.

LIST OF FIGURES

LIST OF FIGURES

LIST OF FIGURES

LIST OF FIGURES

LIST OF FIGURES

LIST OF FIGURES

LIST OF FIGURES

LIST OF FIGURES

LIST OF PLATES

NOMENCLATURE

L_1	Length of the first part of the pressure unit unit
L_2	Length of the second part of the pressure unit
	Viscosity of the fluid
P'_1	Pressure gradient in the first part of the pressure unit
P'_2	Pressure gradient in the second part of the pressure unit
Pms	Pressure at the step
Pmax	Maximum pressure in the pressure unit
Q_1	Flow of fluid in the first part of the unit
Q_2	Flow of fluid in the second part of the unit
σ_x	Axial stress in the wire
τ_1	Shear stress in the fluid in the first part of the unit
τ_2	Shear stress in the fluid in the second part of the unit
τ_{c1}	Shear stress on the wire in the first part of the unit
τ_{c2}	Shear stress on the wire in the second part of the unit

u_1 Velocity of fluid in the first part of the unit

u_2 Velocity of fluid in the second part of the unit

h_1 Initial radial gap in the first part of the unit

h_2 Middle radial gap at the step of the unit

h_3 Final radial gap in the second part of the unit

CHAPTER-1

INTRODUCTION

1.1 Hydrodynamic Phenomenon

Hydrodynamic means dynamics of fluid and under certain flow condition the hydrodynamic action generates very high pressure inside the passage through which the fluid is flowing. A common situation is when the fluid is flowing through a converging surface (like Journal Bearing). The magnitude of this hydrodynamic pressure is dependent on the viscosity of the fluid, the geometrical configuration of the confined passage and the relative speed of the solid surfaces. The effect of such action is less apparent for thin oil type fluids. However for plastics processing and food and mineral processing industries the pressure generation due to hydrodynamic phenomenon could be a significant design factor for the processing equipment and pipe works. It has been observed experimentally that when a solid rod is pulled through a stepped or conical gap, which is filled with a viscous fluid (like polymer melt) then the pressure generated is so high that the outer casing may rapture if the wall-thickness is not large enough. Furthermore, if the casing is very strong then the rod may suffer permanent deformation if it is not made of very hard metal.A number of studies have been carried out applying this phenomenon to plastically reduce the diameter of steel, copper and aluminum wires, and tubes when pulled through a strong casing of stepped bore or taper bored geometry. In these processes no contact takes place between the metallic casing and the the wire or tube. The deformation is caused by the fluid pressure generated through hydrodynamic action.

1.2 THE DRAWING PROCESS

In a conventional drawing process,the reduction in the area of wires, strip and tubes is accomplished by pulling the material through a shaped die.For wires and tubes conical dies are used as shown in Fig. 1. and wedge shaped dies are used for strip drawing.In the drawing process the die is used to particularly change the cross-section of the material to a specific size with an acceptable surface finish. In the drawing process, metal to metal contact takes place causing friction which leads to a reduction in die life due to wear. In order to reduce die wear lubricants are used. The use of such lubricants is very important for a number of metal forming processes because the lubrication leads to a reduction in the drawing load and die wear and hence improve the machine life and surface finish of the product. Generally two types of lubrication are used in the drawing process. These are (1) Liquid lubrication and (2) Solid lubrication. Both the liquid and solid lubrication are employed in metal working processes involving generation of pressure at the interfaces. The action of these lubricants under boundary lubrication conditions is to form a film on the friction surface.

In conventional drawing process, friction between the products and the die is of the boundary type where metal to metal contact takes place in spite of the presence of a lubricant.This results in excessive die wear.Hydrodynamic lubrication action however, refers to a regime where a thick lubricant film separates two metal surfaces previously in contact. To create such a regime a certain product speed and lubricant pressure must be achieved and maintained in order to keep the surfaces continuously apart. Prior to hydrodynamic lubrication action boundary lubrication is the dominant regime. The film thickness produced in solid lubrication is greater than that in boundary lubrication but less than that in hydrodynamic lubrication (1,2) Boundary lubrication methods have been used in the metal drawing process since the inception of the process itself. However, the need to produce drawn metal with satisfactory physical properties and the demands for an increase in both production and quality of product lead to a number of investigations during recent years

1.3 BACKGROUND LITERATURE OF HYDRODYNAMIC PHENOMENON

In recent years attempts have been made to make use of hydrodynamic action in drawing processes .One of the earliest successful attempt to employ hydrodynamic action in a metal forming process was described by CHRISTOPHERSON and NAYLOR(3) They published a paper which showed the development of hydrodynamic lubrication action in wire drawing. They employed a long tube, having a length of up to 500 times the diameter of the wire, with a narrow gap between the tube and the wire, was attached firmly to the entrance side of the die as shown in Fig. 2 The fluid adhered to the wire and was dragged into the clearance between the tube and the wire. At about 182.8 m/min. the pressure built-up at the approach to the die reached between 68.950 and 275.8 MN/m^2 .It should be noted that only after a critical speed is attained the hydrodynamic effect is developed. Thus, during starting and stopping at the beginning and end of each wire drawing run the fluid film is broken. Lubricants of high viscosity ensure hydrodynamic lubrication at lower speeds and with shorter tubes. This adaptation of a tube with liquid lubricant has not become a practical means for providing hydrodynamic lubrication in wire drawing.

WISTREICH(4) conducted experimental work on the forced lubrication based on a pressure tube system. Soap powder was used as the lubricant in a short nozzle (2 inch in Length) which was attached to the entry side of the die. The experimental results showed that the speed, temperature and tube gap had a direct effect on the film thickness produced. He also showed that when the soap powder was replaced by oil, an increase rather than a decrease in film thickness was observed. The schematic diagram of the (B.I.S.R.A) unit is shown in Fig. 3

TATTERSAL(5) published a detailed analysis of plasto-hydrodynamic lubrication action in wire drawing taking some rheological and metallurgical properties of the process into account.More recently CHU(6)using the work of TATTERSAL, has presented a chart for the inlet tube he designed.

KALMOGOROV et al(7)also conducted experimental work on tube sinking under conditions of hydrodynamic action . In contrast to similar devices for wire drawing. There was no seal between the nozzle and the die, because the lubrication pressure in tube sinking was much lower. Soda-soap powder was used as the lubricant in that work. BLOOR et al(8) produced a theoretical analysis for elasto-plasto hydrodynamic lubrication action for strip drawing through wedge shaped dies. They took account of elastic component in the strip at entry and exit to the die and the pressure and viscosity characteristics of the lubricant. It was shown by comparing the magnitude of the predicted lubricant film thickness that hydrodynamic lubrication could be accomplished during the process.

1.4 BACKGROUND LITERATURE OF POLYMER MELT AS A NON-NEWTONIAN FLUID IN DRAWING PROCESS

Polymers have recently been considered as a lubricant in the drawing process. There are many important differences between the rheology of molten polymer and conventional lubricants such as oil.The most obvious of these is the very high viscosity of polymer melts at temperatures which would preclude the use of oil as a lubricant. Non-newtonian lubricants have been previously investigated for journal bearings(9) and they have been found to be advantageous to bearings subjected to oscillatory load which induce fatigue loading. The use of a polymer melt as a lubricant in the drawing process was suggested by SYMMONS and THOMSON(10).They investigated the adherence of a polymer coat onto the drawn wire. Hydrodynamic lubrication action of polymer on the wire was claimed to be achieved successfully. STEVENS(11)conducted some limited experimental work on wire drawing and polymer lubrication and investigated the coating features of the polymer. The practical results showed a decrease in the coating thickness with an increase in drawinq speed which gave some correlation with his Newtonian solution. CRAMPTON(12) carried out an in depth study of the wire drawing process using a unit similar to the one adopted by STEVENS. Again polymer melt was used as a lubricant and the apparatus consisted of a pressure tube connected to the forward end of a conventional die. The polymer melt was dragged into the tube by the motion of the wire, generating high pressures which resulted in hydrodynamic lubrication and coating of wire during the drawing process. A section view of the unit is shown in Fig. 4. Other experimental work carried out by HASHMI et al (13-15) has shown that effective reduction of the wire diameter should be possible using a polymer melt in conjunction with a stepped bore tubular unit only. PANWHER et al(16) reported work carried out on the dieless tube sinking process and presented an analytic solution based upon NEWTONIAN characteristics. Subsequently PANHWER(17) analysed the system taking account of the NON-NEWTONIAN characteristics of the polymer melt. Subsequentaly SYMMONS et al (18-19) presented analyses of a dieless wire drawing process using a viscosity-pressure and viscosity temperature relationship of experimental form. Their aim was to examine individually the effect of pressure and temperature on the viscosity of polymer melt and consequently on the process performance.

1.5 THE PRESENT WORK AND ITS AIM

In previous studies the investigators have studied the hydrodynamic action in the drawing process by using either a stepped bore reduction unit which consists of two parallel portions, or a tapered bore reduction unit.Their aims were (i) to reduce the diameter of the material to a specific size with an acceptable surface finish and (ii) to generate sufficient pressure as to cause a thick hydrodynamic film which would prevent excessive contact and friction between the die and material.This would result in no metal to metal contact, and would reduce die wear. A thick hydrodynamic film can be generated by high viscosity lubricants .In the present work the effect of the geometry of the pressure unit on pressure distribution has been studied. The unit consist of two parts.The first part is made parallel and the second part is tapered. According to the theoretical analysis developed for the geometry of this unit, the maximum pressure occurs after the step of the unit.This is not in line with previous studies which showed that the maximum pressure occurs at the step of the reduction unit. In this present work a polymer is used as the pressure fluid and the pressure unit is heated to convert the polymer feed into a viscous melt and the required pressure in the polymer is generated by hydrodynamic action produced by the motion of the wire. The effect of drawing wire through the pressure unit is to drag in a thick film of polymer and coat the wire. When the polymer melt has adhered to the surface of the wire, it could be used to protect the wire against corrosion in storage.

The radial gap between the die and the wire controls the thickness of the polymer melt coating, However, in this form of wire coating, a very thick coat is required and conditions are created in which adhesion is not achieved therefore the polymer melt can be easily stripped from the wire. The objectives of the present work are:(a)- to investigate the performance of a combined geometry hydrodynamic pressure unit, (b) to formulate a theoretical model for predicting the results for the hydrodynamic pressure and (c) to establish the correlation between the experimental results and the theoretical prediction. The results of this investigation should be useful for

(A)-Plasto-hydrodynamic die-less drawing and coating of wires, strips, tubes and composite wire-ropes (B)-Hydrodynamic lubrication in rotary system since, higher pressure would prevent metal to metal contact of the bearing systems

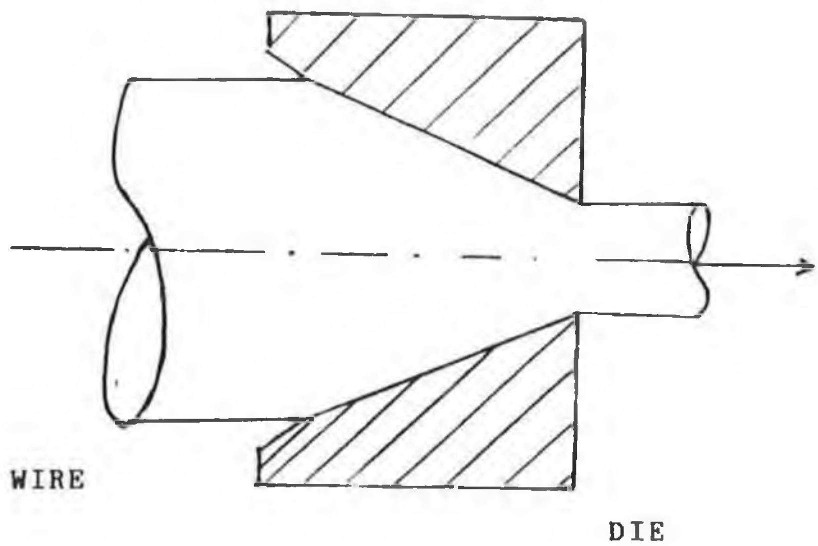

FIG (1) WIRE THROUGH A CONICAL DIE

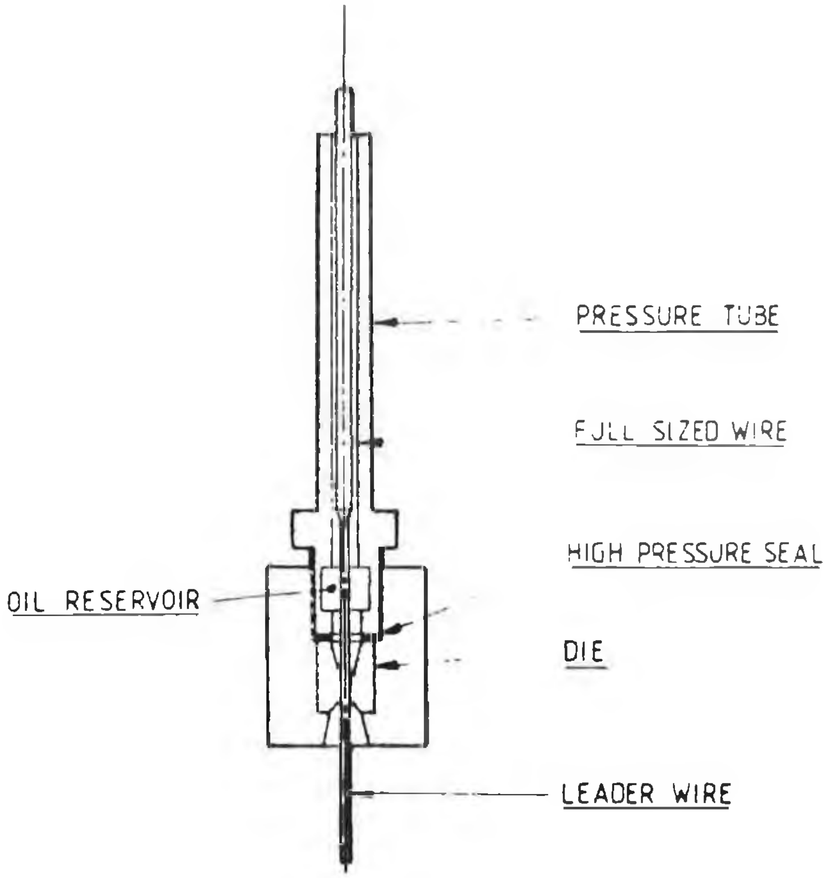

FIG 2 - TYPICAL INLET TUBE AND DIE

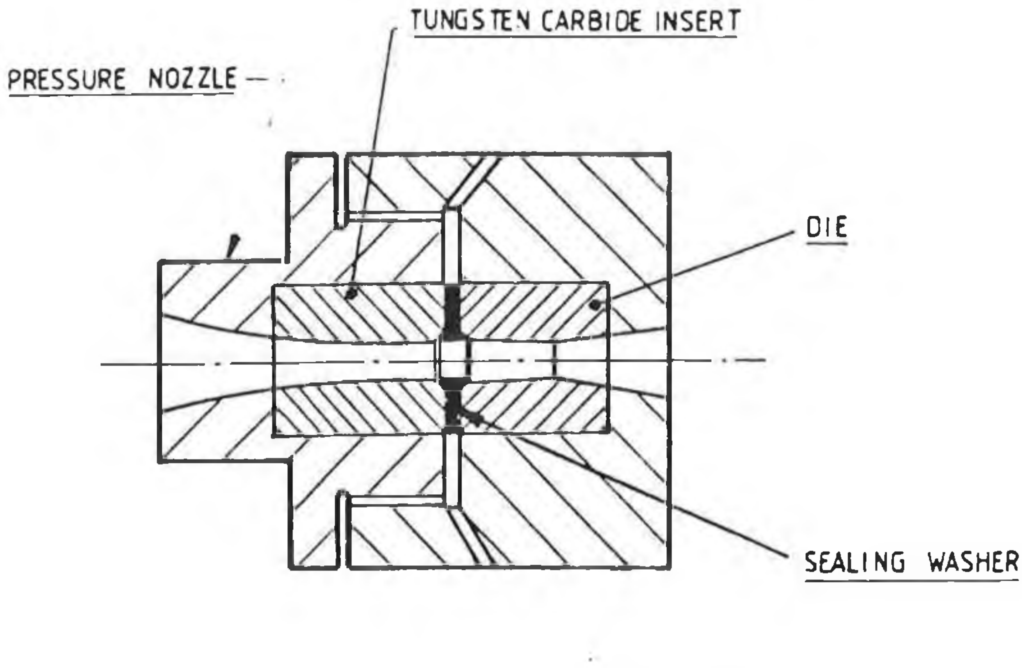

FIG 3 - B.I.S.R.A. NOZZLE-DIE UNIT

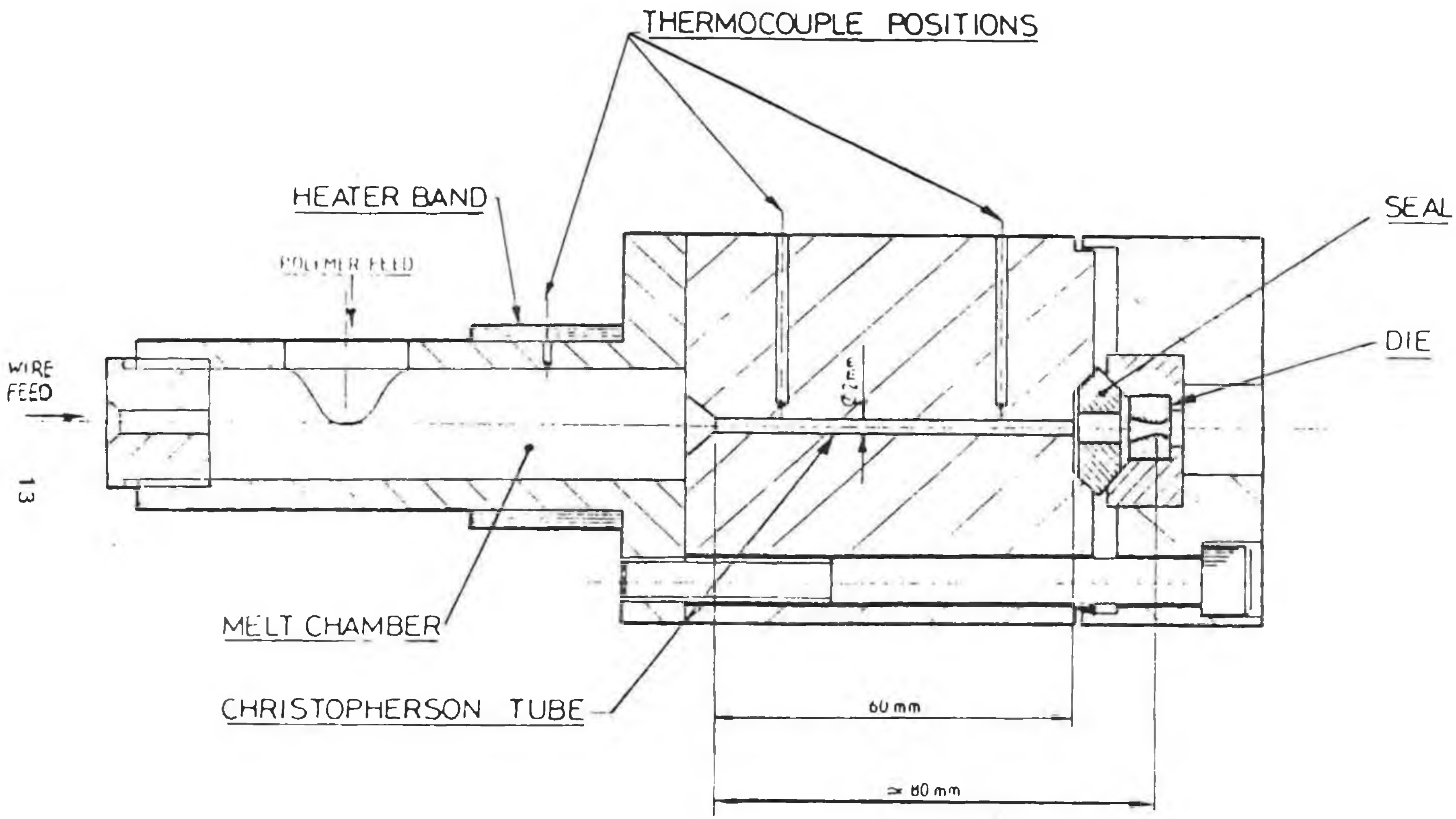

FIG(4) PLASTO-HYDRODYNAMIC TUBE-DIE ASSEMBLY

CHAPTER-2

RHEOLOGY OF POLYMER MELT

2.1 INTRODUCTION

Polymers generally consist of very long molecular chains. One form of bonding between the molecules is cross-linking which is referred to as thermo-setting polymer. The forces of attraction between the molecules are the Van der Waals forces and polymers with this type of bonding are commonly called thermo-plastic polymers. A useful image of the structure is a mass of randomly distributed long strands of sticky wool. When the polymers are heated the inter-molecular forces are weakened so that they become soft and flexible and eventually, at high temperatures, they turn into a viscous melt. If the applied stress together with an increase in temperature is high enough to overcome the Van der Waals forces, a relative molecular motion takes place causing the polymer to flow. The type of flow depends on the mobility of the molecular chains and the forces holding them together. In thermoplastic polymers long molecules take up a non-random configuration under a stress which is partially recovered when the stress is removed. The thermo-setting polymers show distinct brittle behaviour. The flow characteristics of polymer melts are very different from those of conventional lubricants such as oil. In this chapter, discussions are made of the flow characteristics of the polymer melts, which are influenced by many factors in relation to the present work.

2.2 THE EFFECT OF TEMPERATURE ON VISCOSITY

An increase in the temperature of a molten polymer decreases its viscosity by varying extents which is dependent on the type of the polymer. Figure 5 shows typical extrapolated viscosity against the reciprocal of absolute temperature at ZERO shear rates. The slope of each line is a measure of the activation energy for each polymer. A temperature increase in polymers with higher activation energies has more deterious effect on viscosity compared to those of lower activation energies. Polyethylene, which is the most non-polar of all the materials shown, has a very low activation energy because the forces between the chains are very weak.DIENES (20) suggested that as the temperature increases, the molecular arrangements within the polymer changes more towards a random configuration, making it easier for the polymer to flow at higher temperatures. Figure 6 shows the variation of viscosity with temperature for polyethylene (ALKATHENE WV G23), POLYPROPYLENE (KM61), RIGIDEX AND POLYSTYRENE at ZERO shear rate. These graphs don't represent the complete behaviour since viscosity measurements are affected by pressure, shear rate, temperature, etc. and it is necessary to include these effects on viscosity of polymer melts.

2.3 THE EFFECT OF SHEAR STRESS AND STRAIN ON VISCOSITY

An outstanding characteristic of polymer melts is their non-Newtonian behaviour whereby the apparent viscosity decreases as the rate of shear increases. Figures 7-10 show the effect of shear rate on viscosity where the influence of temperature may be noted (12,17). These curves were produced by extruding polymer melts (ALKATHENE WVG23, POLYPROPYLENE KM61, RIGIDEX HDP, and POLYSTYRENE) through an extrusion rheometer at different temperatures. A non-linear relationship is seen to exist between shear stress and shear rate. The viscosity of the polymer may be calculated at any known shear rate by measuring the slope of the curve. A Newtonian fluid under shear stress conditions exhibits a linear relationship with shear rate where the slope of the line represents the viscosity of the fluids. Figures 11-14 show another way of representing the effect of shear rate on viscosity. In these figures the viscosity may be read off directly for known shear rate values.(For a Newtonian fluid this curves would be a horizontal straight line).

2.3.1 CRITICAL SHEAR STRESS

At low rates of shear, polymer melts flow through capillaries to produce smooth strands. At higher rates of shear certain kinds of flow instabilities can develop in which the surface of the extruded strand becomes rough or non-uniform in cross-section, and the rate of flow is no longer steady but pulsating (21-25). The flow irregularities were shown to take the form of spiral, ripple, bamboo, zigzag or helix for different types of polymers. The terms melt fracture, elastic turbulence and distortion have been used to describe this effect. This phenomena have been investigated by a number of workers (26-30) and there is general agreement on the following points:

1- Critical shear stress is independent of die length and diameter of the capillary

2-Critical shear stress has values in the region of 0.1-1.0 MN/m^2

3-Critical shear stress does not very widely with temperature.

4-A discontinuity in the viscosity-shear stress curves occured.

5- A flow defect always took place when

non-Newtonian fluids were involved.

6-The flow defect is often associated with the die inlet.

2.4 THE EFFECT OF PRESSURE ON VISCOSITY

Several theories suggest that the viscosity of a liquid polymer is determined by its free volume (31-35). The free volume of a liquid polymer is defined in various ways, but a common definition is the difference between the actual volume and the volume in which such a close-packing of the molecules occurs so that no motion can take place. The greater is the free volume the easier it is for flow to take place. Free volume increases with temperature because of thermal expansion. However, the most direct influence on free volume should be of the pressure. An increase in hydrostatic pressure decreases free volume and increases the viscosity of a liquid. Viscosity by definition, is the internal resistance to shearing stress due to inter-molecular forces of attraction. It was thought that when molecular attraction is encouraged, the apparent viscosity of the polymer which is one of the most important properties of these materials, may be increased. However, the effect of hydrostatic pressure on the apparent viscosity and other flow properties of polymer melts is not as well investigated as the effects of temperature and shear rate. WESTOVER (36) has described a double piston apparatus for measuring viscosity as a function of pressure at up to 25000 psi.(172 MN/m^2) He found the viscosity of polystyrene to increase by a factor over a hundred times and the viscosity of polyethylene to increase by a factor of five at a constant rate of shear as the pressure was increased. MAXWELL and JUNG (37) found that the viscosity of Polystyrene increased by a factor of 135 when the pressure was increased from 0 to 18000 psi (124 MN/m^2) at 196°C. The viscosity of Polyethylene increased by 14 times in the same pressure range at 149 °C. COGSWELL (38) suggested that the effect of an increase in pressure may be likened to that due to a drop in temperature.He observed that for low density Polyethylene, an increase in pressure of 100 MN/m^2 had the same effect on viscosity as that due to a drop in temperature of 35 °C within the melt range. It had been noted that at high pressure(over 150 MN/m^2)the melt tended to recrystallise and consequently, the melt acted like a solid plug (36). For this reason, pressure-viscosity measurement are often conducted at relatively high temperature. Most of the experimental work carried out by WESTOVER (39) was on a branched 0.92 density Polyethylene with pressure varying from 14 M.N/M^2 to 170 M.N/M^2.Since the work carried out by

WESTOVER was found to be the most comprehensive these have been used to determine the pressure coefficient of viscosity in the present work. Figure 15 shows the effect of pressure on shear stress-shear rate curves and.Figure (16) shows how the shear rate affects the influence of pressure on viscosity.

2.5 THE EFFECTS OF THE POLYMER FLOW CHARACTERISTICS

In the present work the polymer melt is subjected to very high pressures, much greater than those capable of being investigated in any extrusion rheometer. CRAMPTON (12) concluded that the decrease in coating thickness was due to the pressure of a critically low shear stress at low shear rates. However, it is also believed that, the poor performance of the units at higher drawing speed is related to a combination of factor such as shear rate, melt flow instability, partial crystallization, compressibility etc. The high pressures generated are believed to have the effect of increasing the melt viscosity in the unit. Temperature was maintained at a steady value when the tests were conducted minimising the effects inherent with changing temperature. However, more investigation is needed to understand these effects fully.

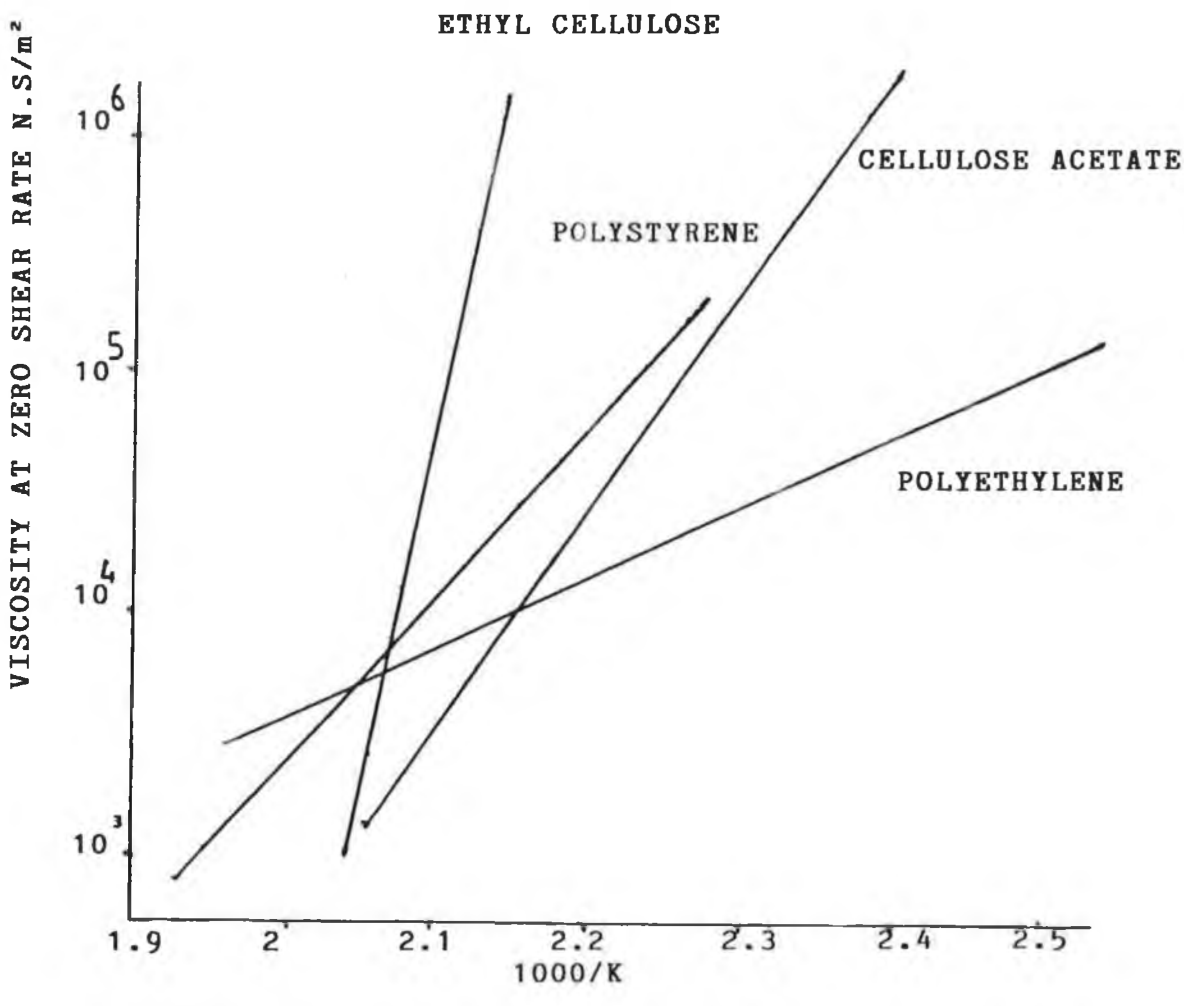

FIG(5) EFFECT OF TEMPERATURE ON VISCOSITY OF POLYMERS

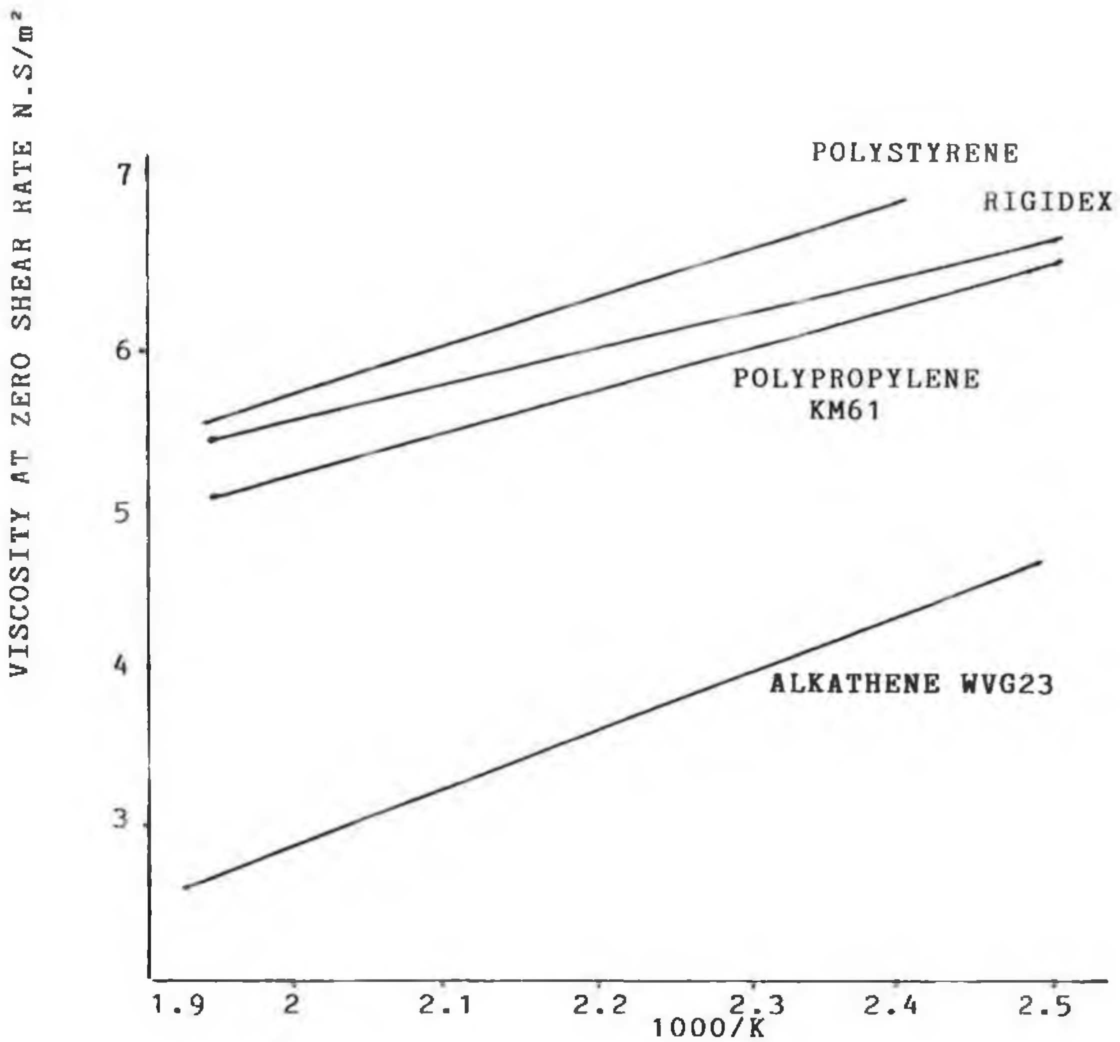

FIG (6) EFFECT OF TEMPERATURE ON VISCOSITY OF WVG23 KM61, RIGIDEX AND POLYSTYRENE

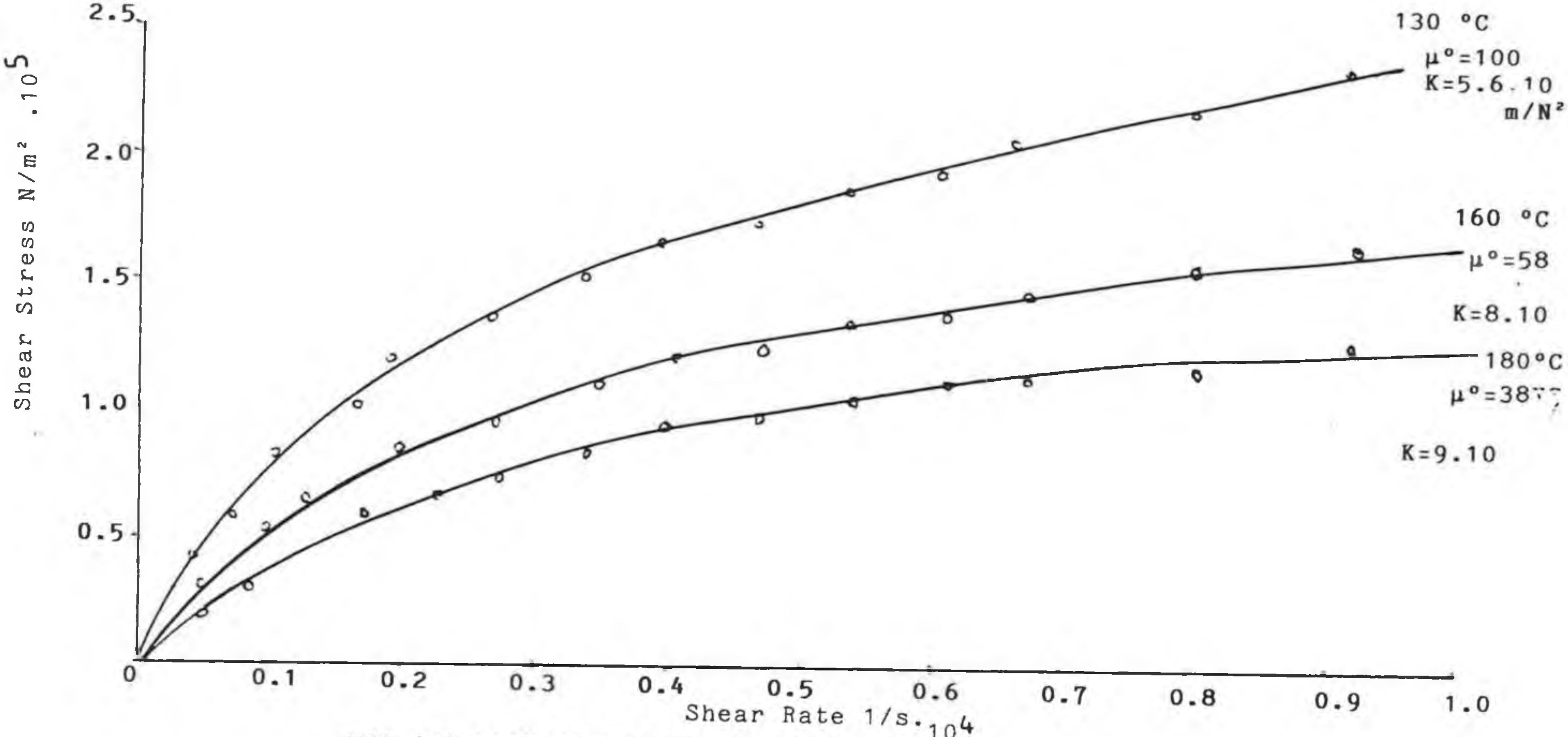

FIG (7) FLOW CURVES FOR ALKATHENE WVG23

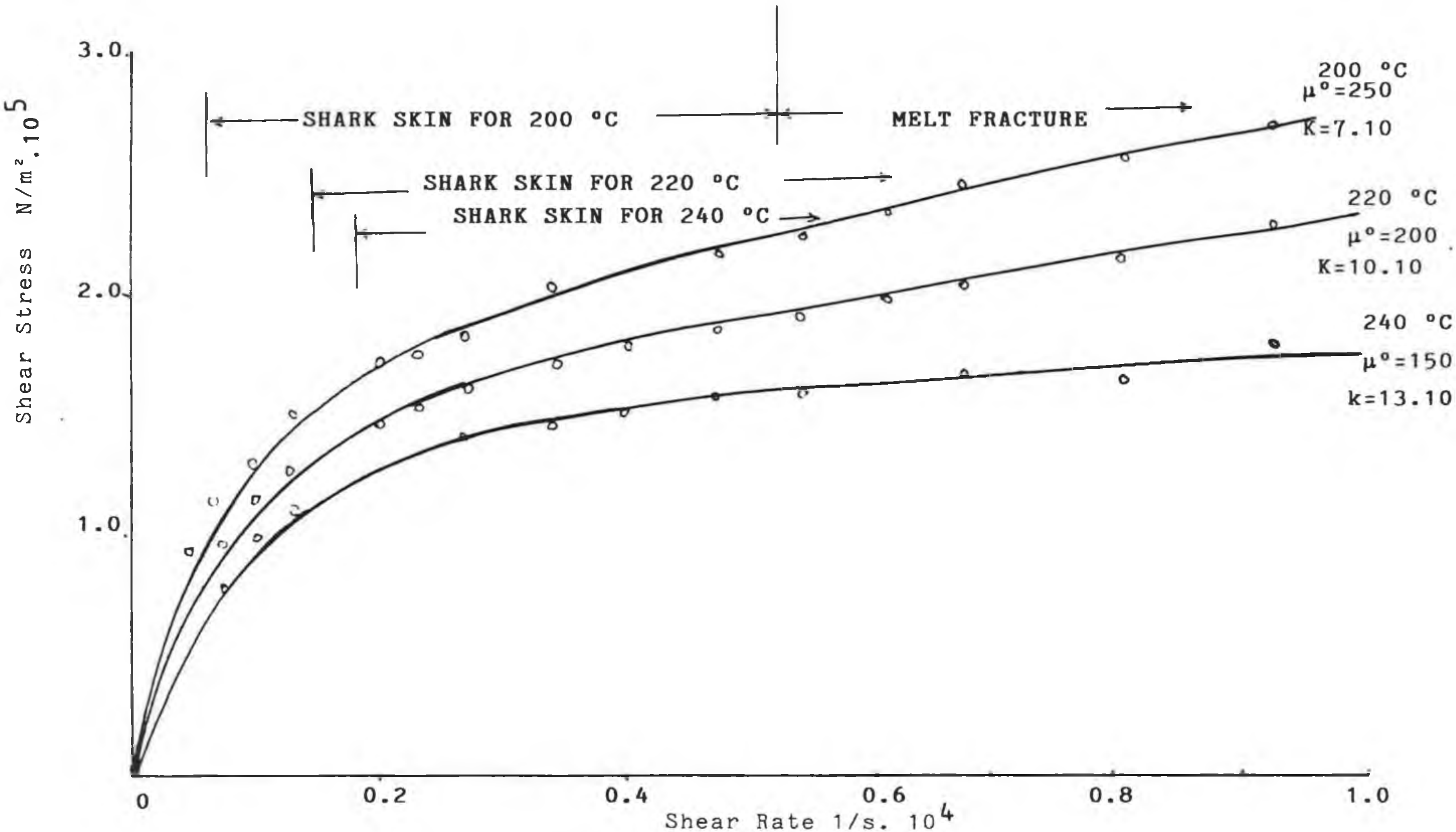

FIG (8) FLOW CURVES FOR POLYPROPLENE KM61

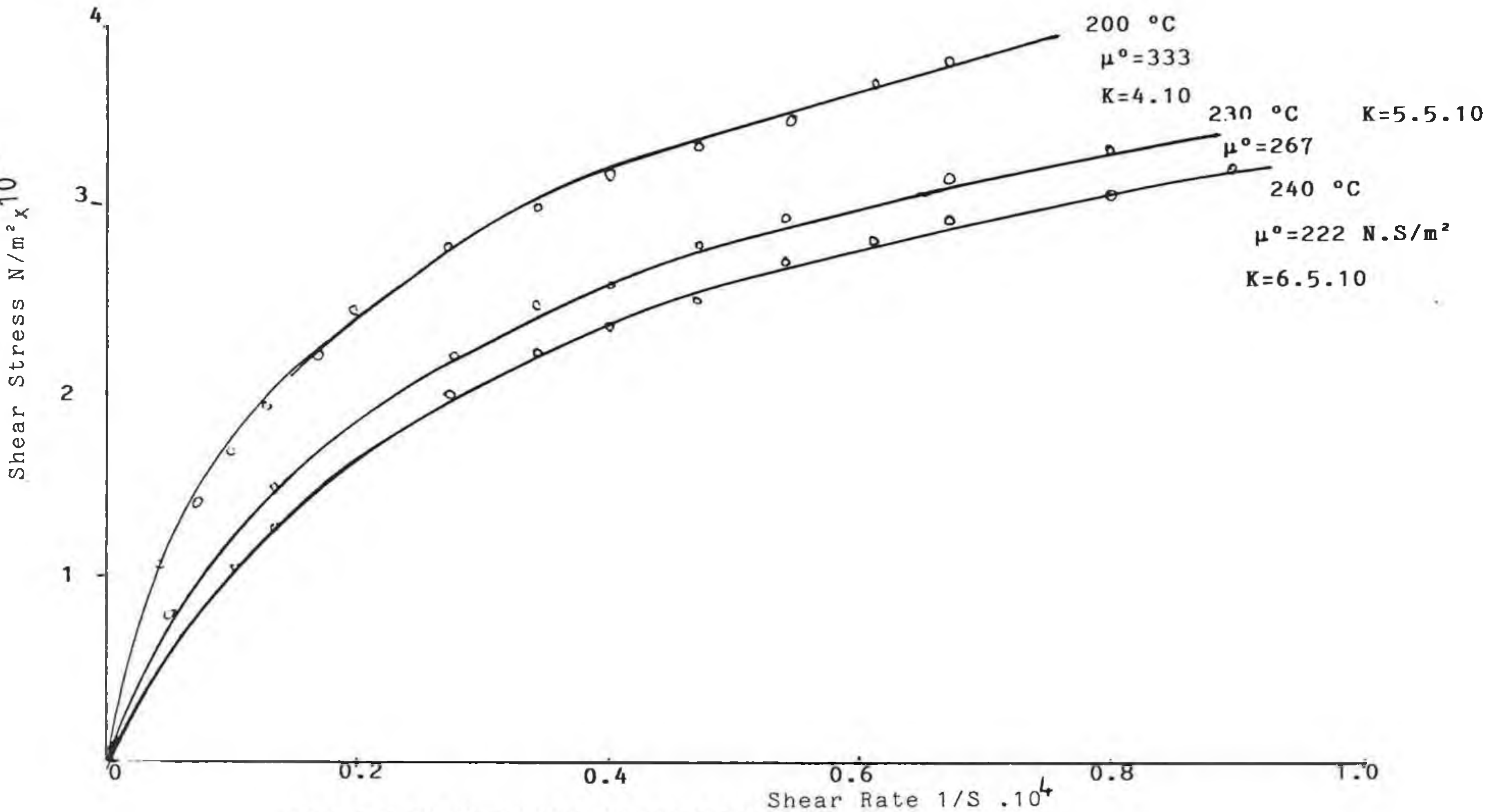

FIG (9) FLOW CURVES FOR RIGIDEX

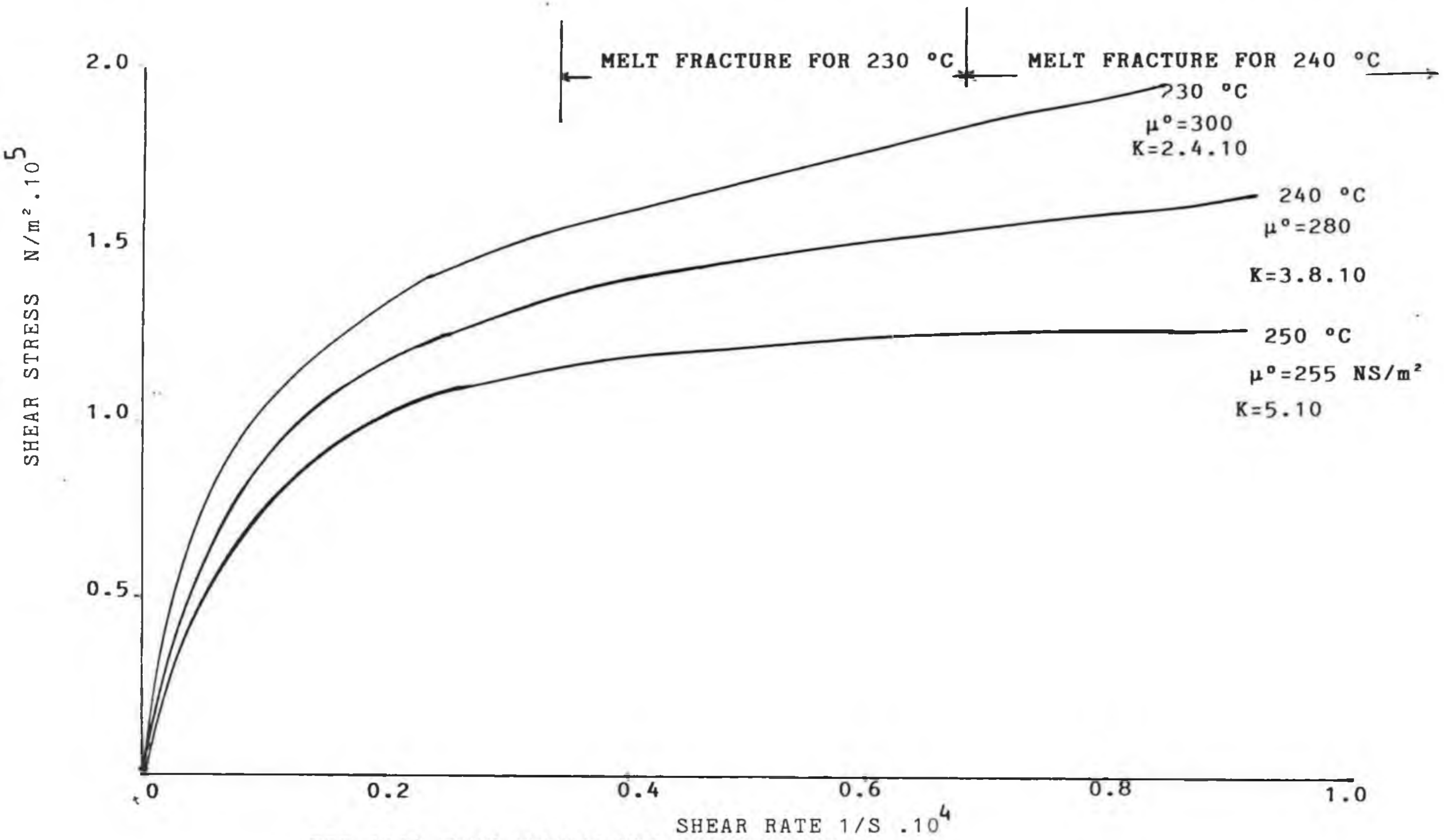

FIG (10) FLOW CURVES FOR POLYSTYRENE

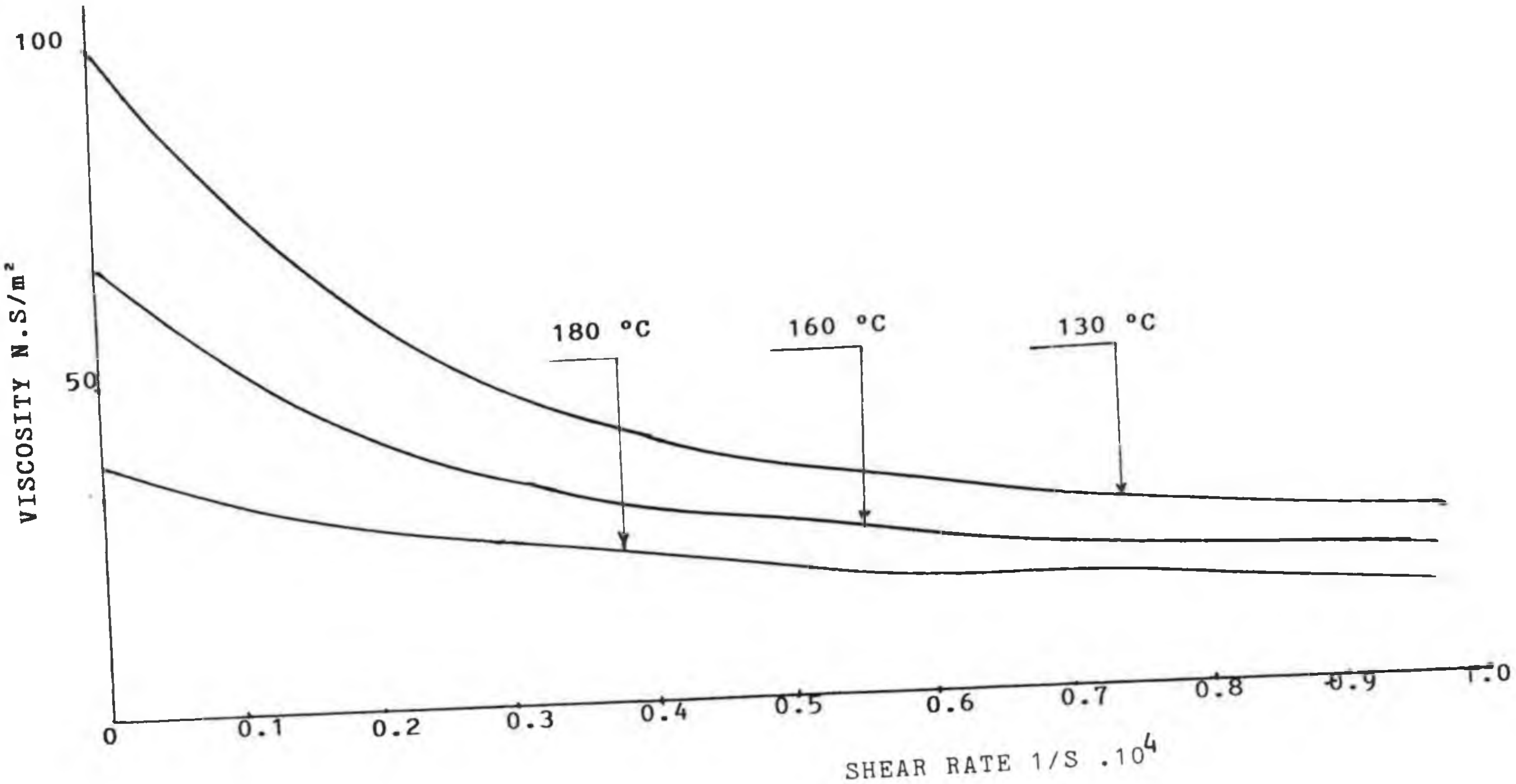

FIG(11) EFFECT OF SHEAR RATE ON VISCOSITY OF ALKATHENE WVG23

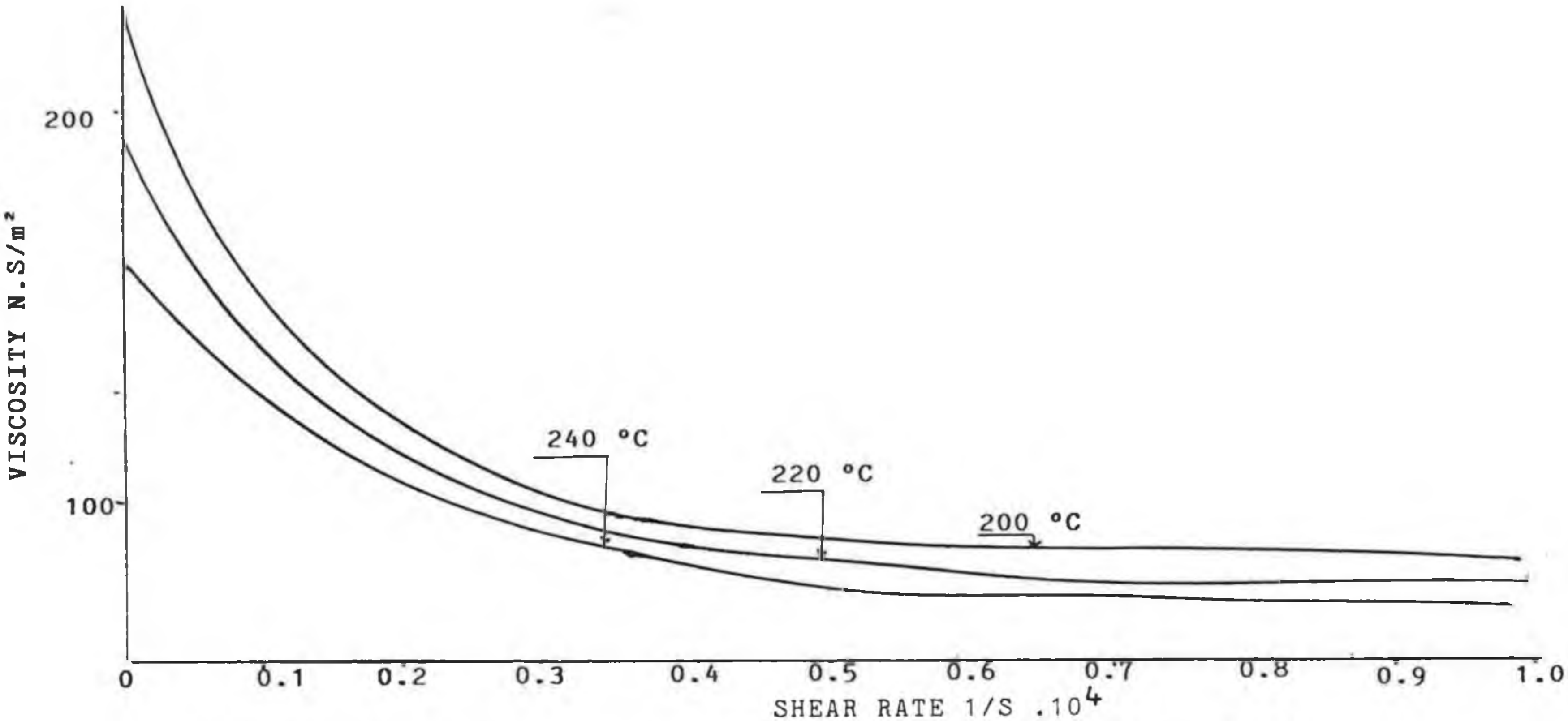

FIG (12) EFFECT OF SHEAR RATE ON VISCOSITY OF POLYPROPYLENE KM61

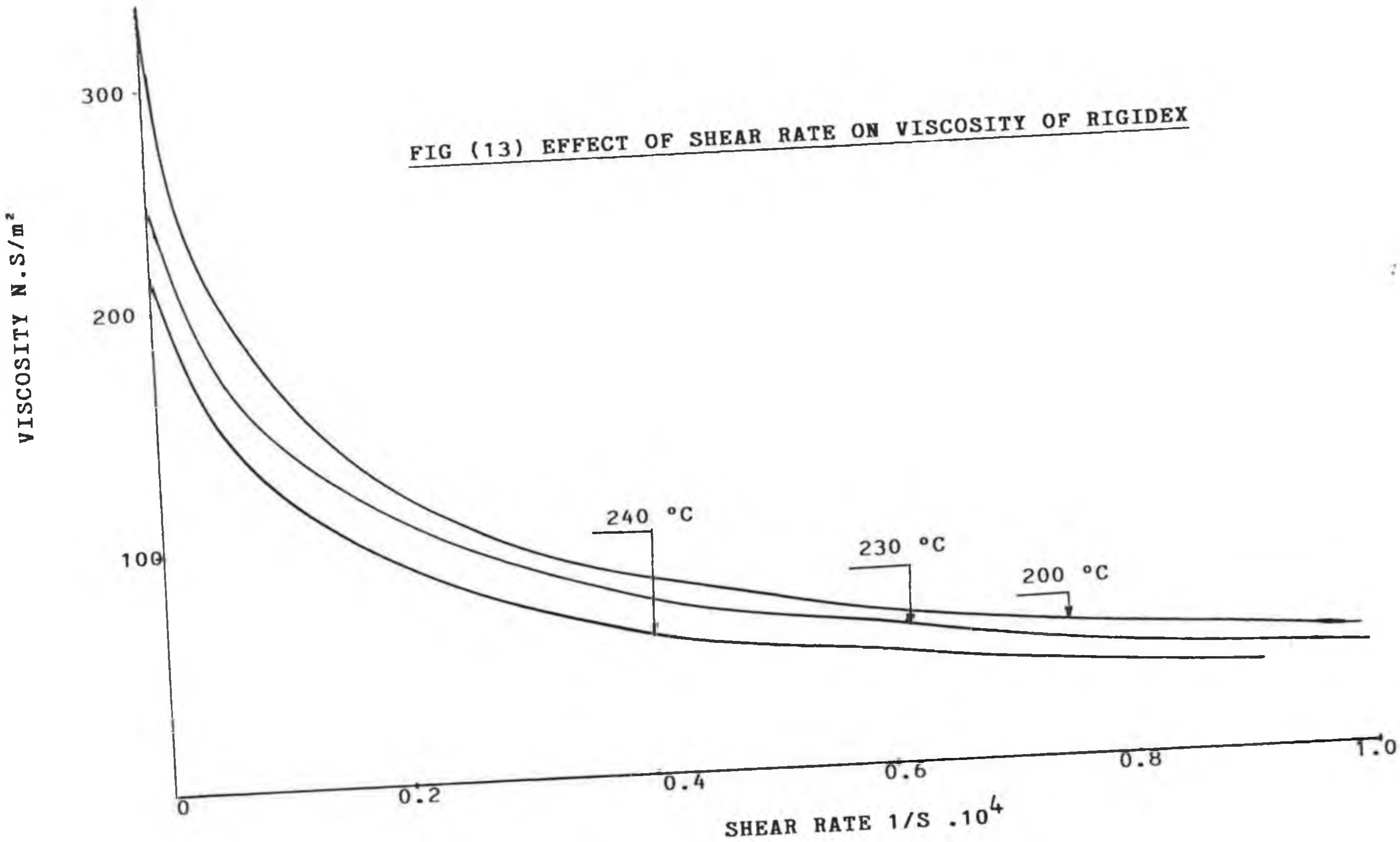

FIG (13) EFFECT OF SHEAR RATE ON VISCOSITY OF RIGIDEX

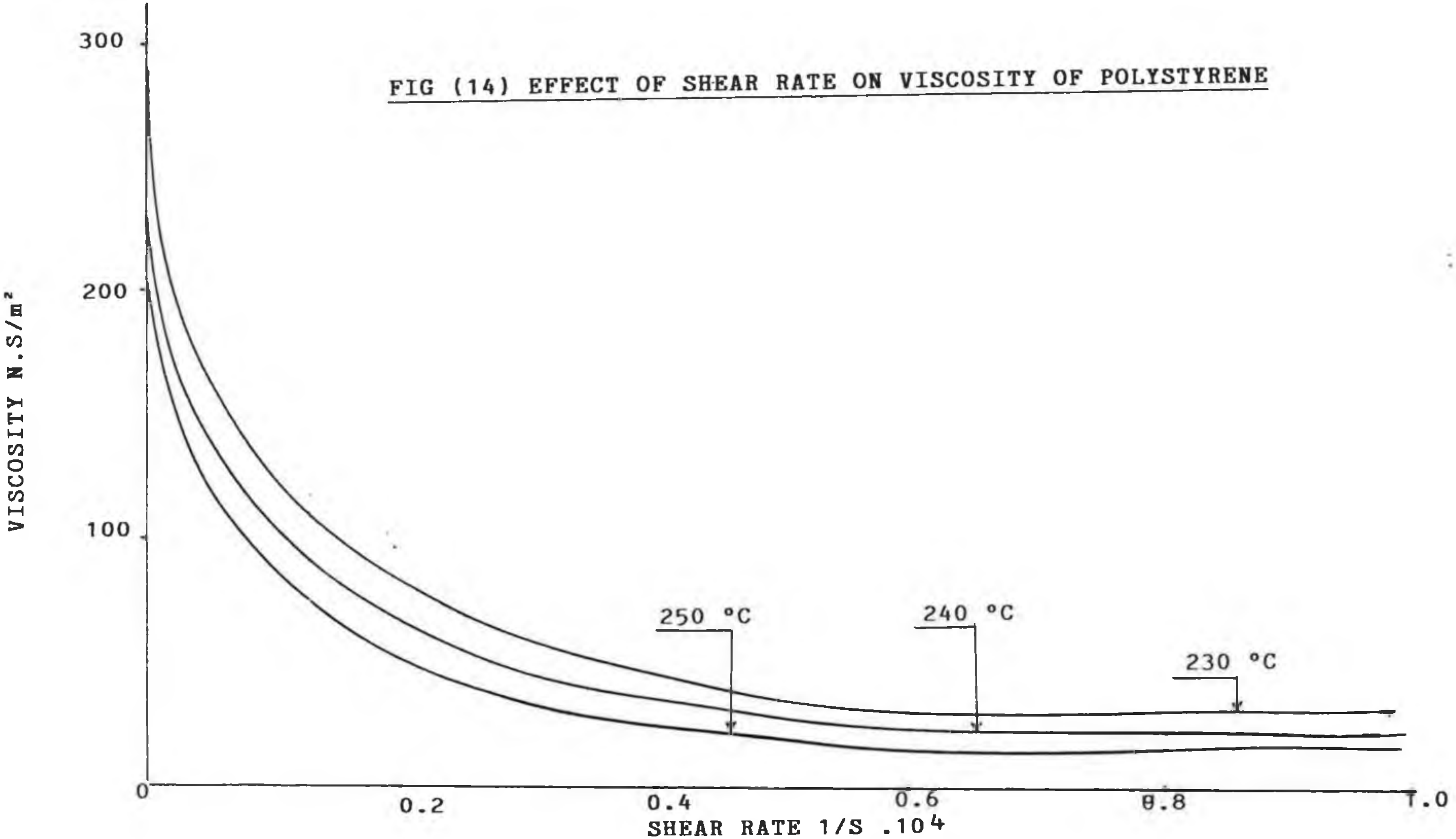

FIG (14) EFFECT OF SHEAR RATE ON VISCOSITY OF POLYSTYRENE

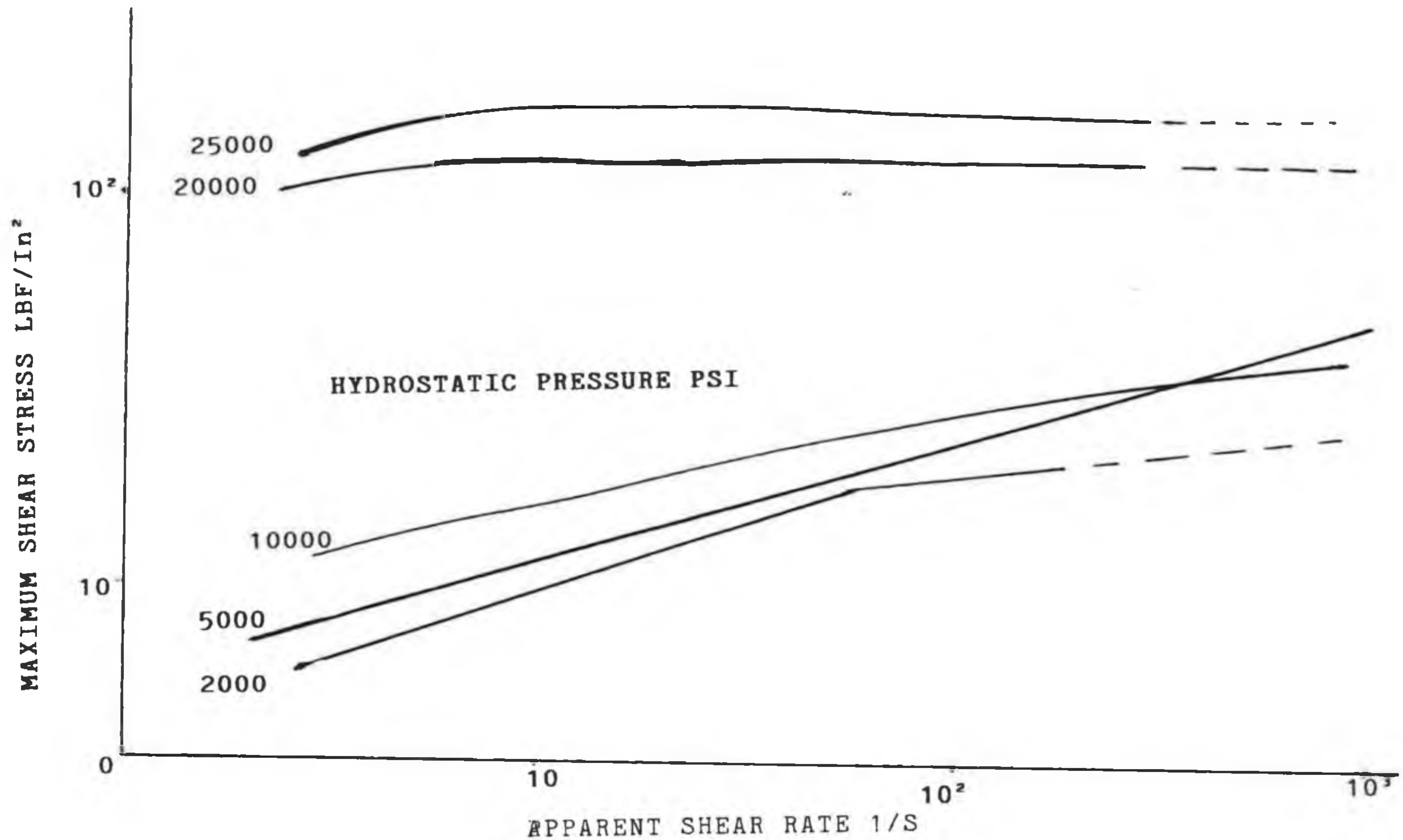

FIG (15) FLOW CURVES FOR 0.92 POLYETHYLENE AT 130 °C AFTER WESTOVER (36)

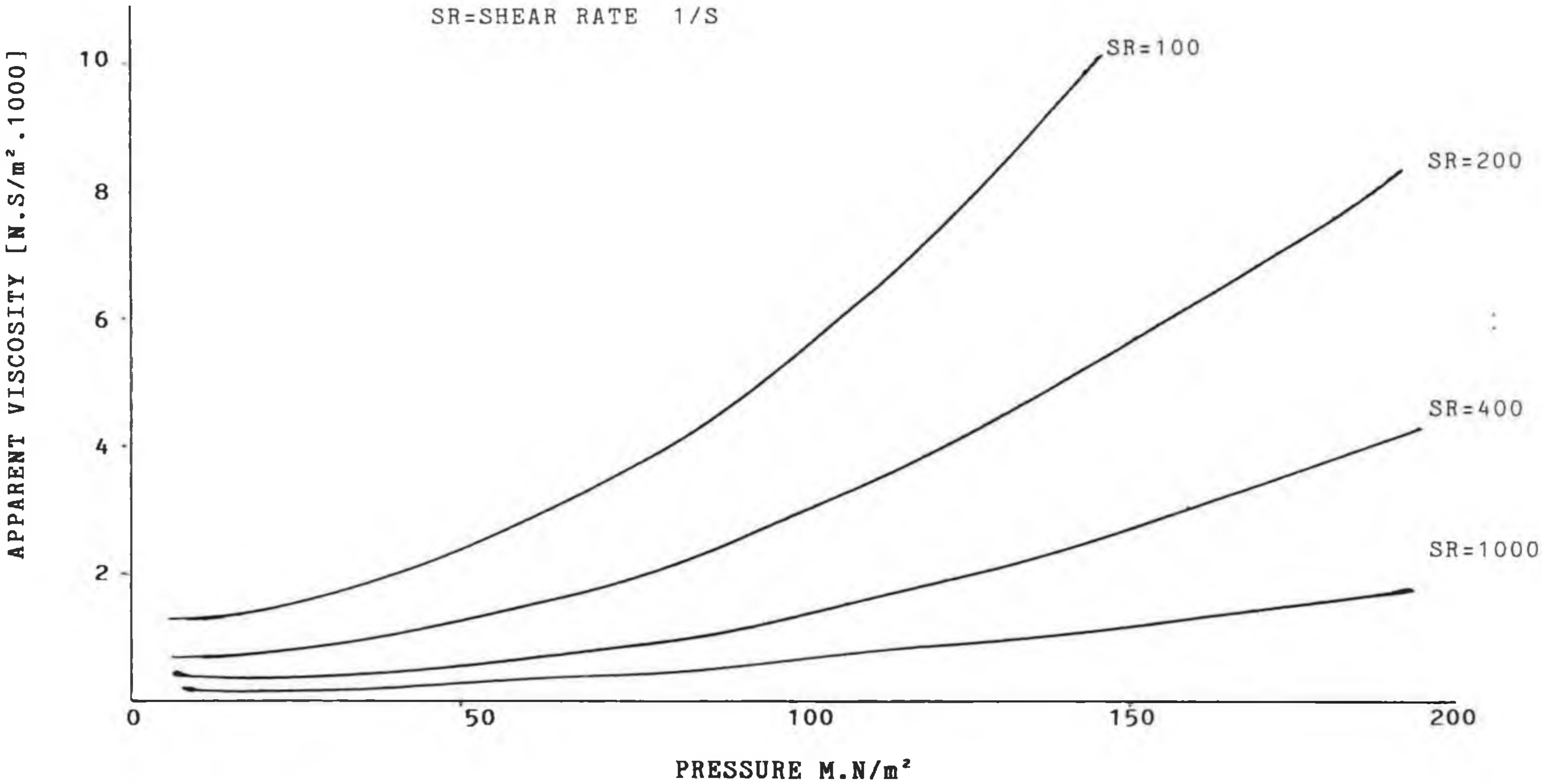

FIG (16)VISCOSITY VERSUS PRESSURE FOR DIFFERENT SHEAR RATES (0.92 POLYETHYLENE AT 130 °C)

CHAPTER-3

EXPERIMENTAL EQUIPMENT AND MATERIAL

3.1 General Description

Experiments were carried out using a general purpose drawing bench which has been adopted and modified. The general view of the drawing bench is shown in plate (3) and Fig. 17 The total length of the draw bench is approximately 2 m. The machine is driven by means of an electric motor (Type: Squirrel Cago 3 kW/3, 80 V/ 3 phase). The power is transmitted from the motor to the pulley block via a coupling (Type RM 12 F/F Fenner coupling with taper lock bushing), with integral speed reduction worm gear box (David Brown Gear box Type A237 10/1 L Position 1) using another coupling (Fenner Type RM 12 with taper lock bushing).The build-up of speed is determined by the accelerator time set on the frequency inverter which varies the motor speed settings. Actual motor speed (rev./min.) is obtained using a remote hand held digital tachometer (SHIMPO Type DT-205) which measures the speed of the rotating mark on the out put shaft of the motor

The above arrangement facilitated drawing speeds infinitely variable between 0.05 to 2.01 m/s. The accelerator time and remote hand held digital tachometer are shown in Plate (1). The polymer was heated by means of an electric heater band and the temperature was controlled thermostatically within ±4 °C of the pre-set temperature using a temperature regulator. The temperature was monitored continuously by means of thermo-couples. One Piezo electric quartz pressure transducer was mounted at different locations in turn on the pressure unit, which enabled the pressure variation along the unit to be measured. The output from the transducer was fed into a recorder via a charge amplifier. The drawing force was measured by means of a quartz load washer(KISTLER Type 9001). The output from the load washer was fed into a recorder via another charge amplifier.

3.2 Instrumentation of the experimental equipment

3.2.1 Pressure transducer

A HIGH-PRESSURE quartz transducer (KISTLER Type 6203 SN 285267) was used for this experimental work to measure the pressure in the pressure unit. The maximum pressure that this transducer could measure is 5000 bar and the working temperature at which this pressure transducer could be used is between -50 °C and + 200 °C. The schematic diagram in Fig 21 and Plate (2) shows the locations of the pressure transducer on the pressure unit.

3.2.2 Heater bands

Hollow cartridge heater bands (clampable type) were used for these experiments for hopper, pressure unit and the melt chamber . The dimensional details are given as follow :

Heater band for pressure unit

Type	I.D(m.m)	Width(m.m)	Volts	Watts
Clampable	56	112	240	750

Heater band for hopper

Type	I.D(m.m)	Width(m.m)	Volts	Watts
Clampable	56	60	240	500

Heater band for melt chamber

Type	I.D(m.m)	Width(m.m)	Volts	Watts
Clampable	25	30	240	200

The heater bands are shown in Fig(21) and plate(2)

3.2.3 Recorder

The output from the pressure transducer and the quartz load washer were fed into a recorder via two charge amplifiers. This recorder is made by LINSEIS (Type L 6514-4) and the charge amplifiers are supplied by FYLDE(Type FE-128-CA). Plate(4)shows the arrangements for the recorder and charge amplifiers.

3.2.4.Load cell

A quartz load washer(KISTLER Type 9001 S.N 330425) consists of one or twocylindersof quartz crystal, an electrode and a housing with plug (see Fig. 19) The force to be measured must act uniformly on the annular surface. Owing to the mechanical compressive stress an electrical charge is developed which is proportional to the change in force applied and does not depend on the dimensions of the quartz discs(longitudinal piezoelectric effect). The charge produced is picked up by the electrode and transferred to the plug connection. The polarity is arranged so that a compressive force produces a negative charge, which is then converted into a positive voltage in the charge amplifier. When a load washer is unloaded, a positive charge results provided the negative charge generated previously under load is dissipated by shorting on the plug. The maximum load capacity of the load washer used in this work is 7.5 kN.

3.2.5. Temperature Controller

An electronic ON-OFF temperature controller relay (type West 3300) was used for these experiments to control the pre-set temperature . The controller is designed to be used with thermo-couples type J, K and T. to monitor the temperature. A relay changeover contact within the controller operates at a pre determined temperature previously set by a panel mounted digital temperature indicator model RS 258-186. The operating temperature range for type J thermo-couple is -25°C to +625°C. The temperature controller is shown in plate (5)

3.2.6 Thermo-couple

Fibre glass insulated,2 mm insulation diameter. thermocouples type J were used for these experiments to monitor the temperature continuously. Their operating temperature range is 0-450 °C. These thermo-couples are shown in plate (6).

3.3 Design of the pressure unit

3.3.1 The unit

A number of units with similar external diameter but different internal geometries were used. All the units were made from Orvar supreme BH13(5% chromium-molibdenum-vanadium hot working steel). Each pressure unit was fixed on the stands. Detailed external dimensions of each unit are shown in Fig. 18. Four locations were made on the pressure unit to measure the generated pressures in the unit. The dimensions and position of holes for the pressure transducer are also shown in Fig(18).

3.3.2 Melt Chamber and Hopper

The melt chamber was made from Orvar supreme BH13 steel which was machined down to the size on a lathe machine and then bored out to form the cavity. An outlet hole was also machined for attaching the hopper. The melt chamber and the pressure unit were held together with three socket cap screws. The dimension of the screw holes are shown in Fig. 20 The heater bands were used for heating the polymer and the unit. Each heater band had a 25 mm inside diameter and a 30 mm width for the melt chamber and a 55 mm inside diameter and 60 mm width for the hopper. The positions of the heater bands are shown in Plate (2). The hopper for feeding the polymer was made from Orver supreme steel BH13 bar material.The dimensional details of the hopper are shown in Fig. 20

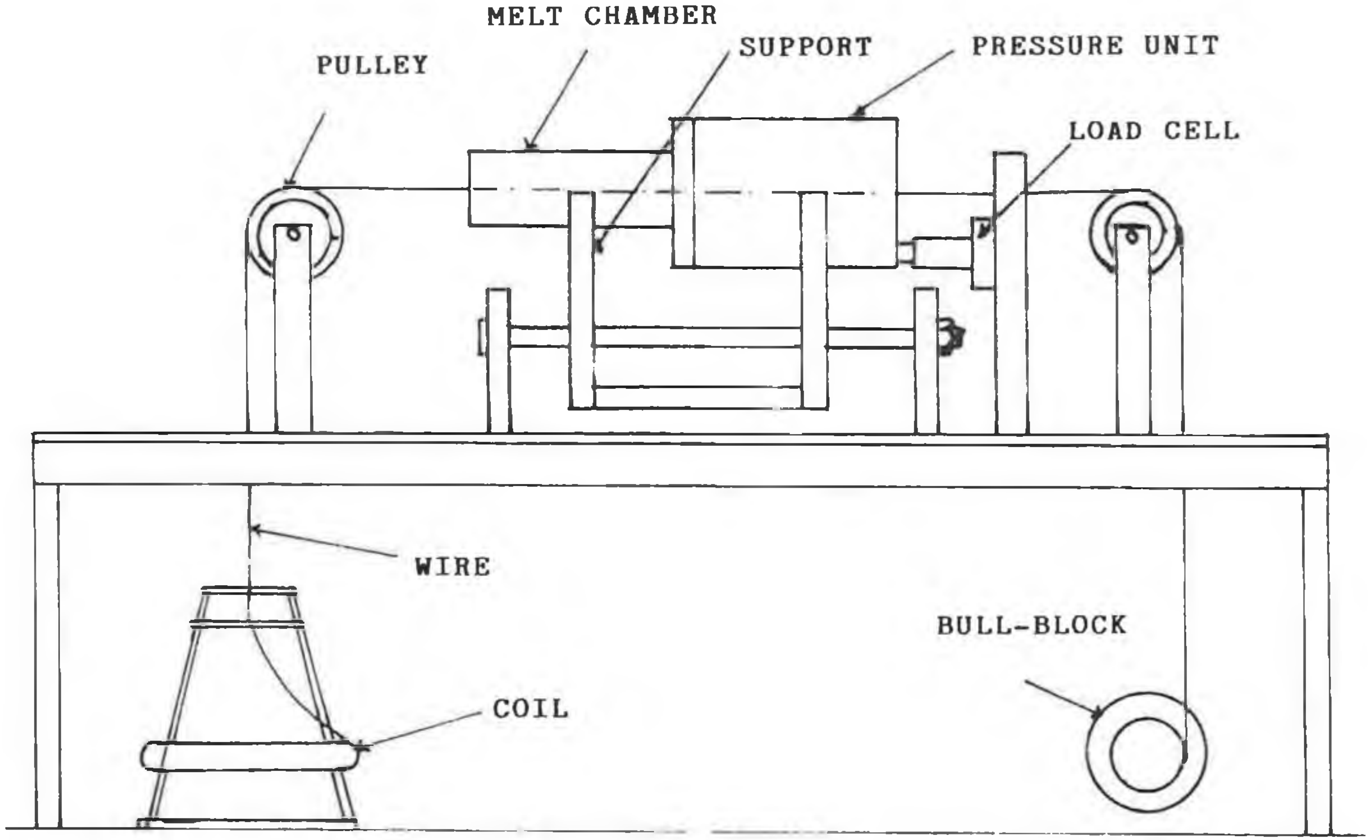

FIG (17) SCHEMATIC DIAGRAM SHOWING THE WIRE DRAWING ARRANGEMENT

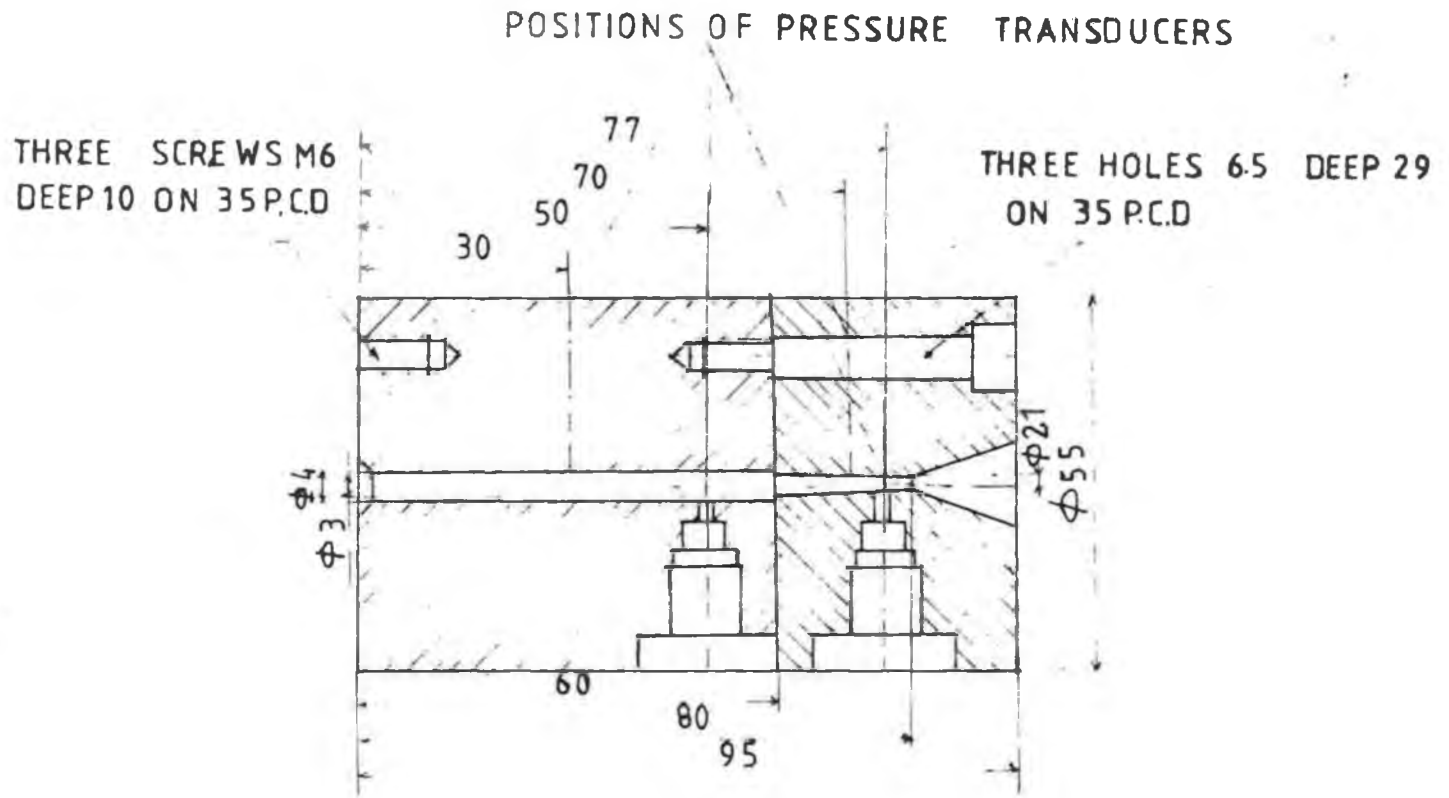

DIMENSIONS ARE IN MM

FIG (18) PRESSURE UNIT

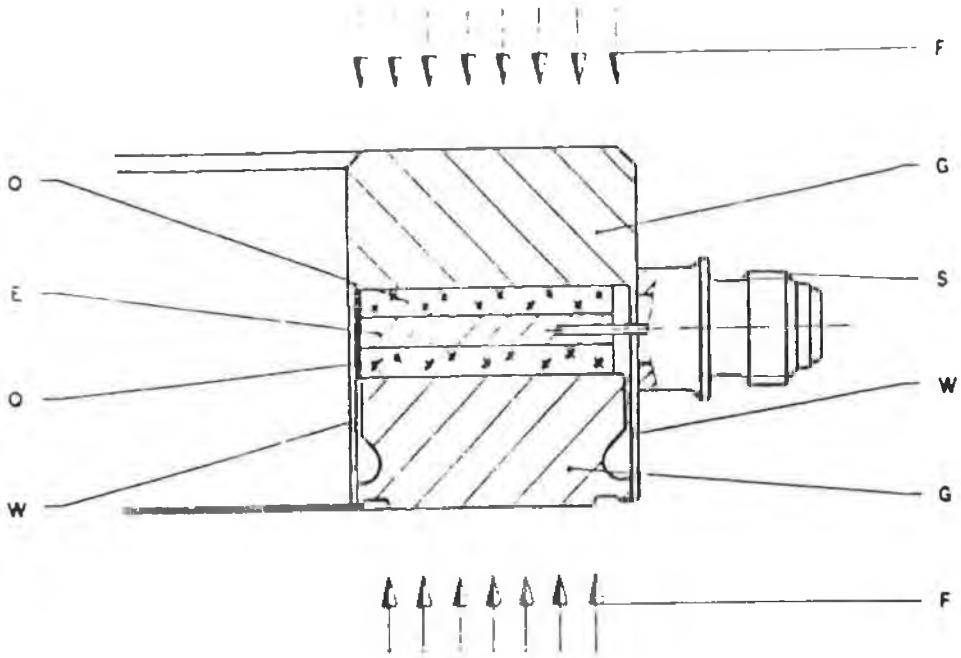

Q = quartz disk
E = electrode
W = elastic wall
G = housing
S = plug

FIG(19) SCHEMATIC SECTION THROUGH A QUARTZ LOAD WASHER

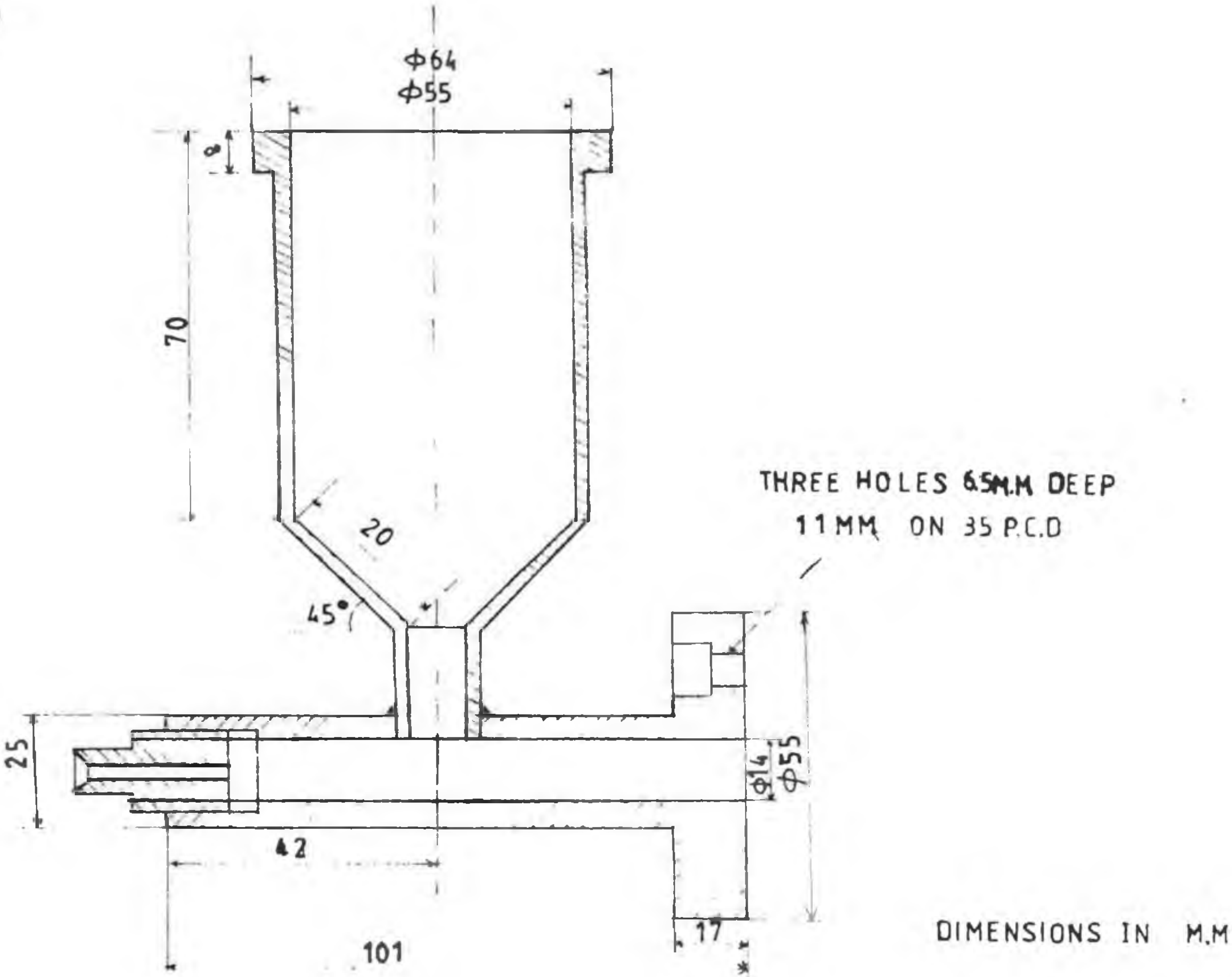

FIG(20) MELT CHAMBER AND HOPPER ASSEMBLY

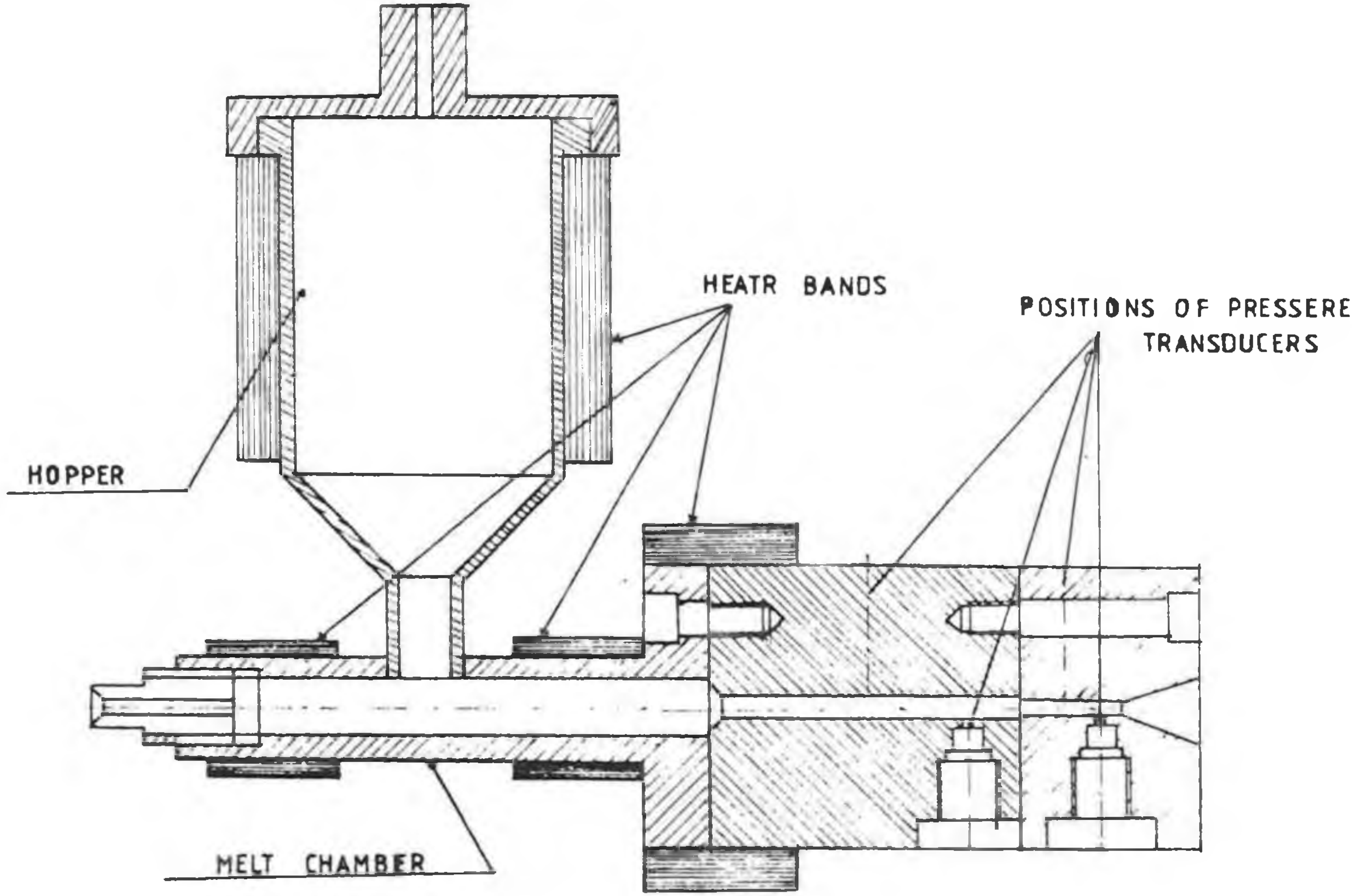

FIG (21)PRESSURE UNIT ASSEMBLY

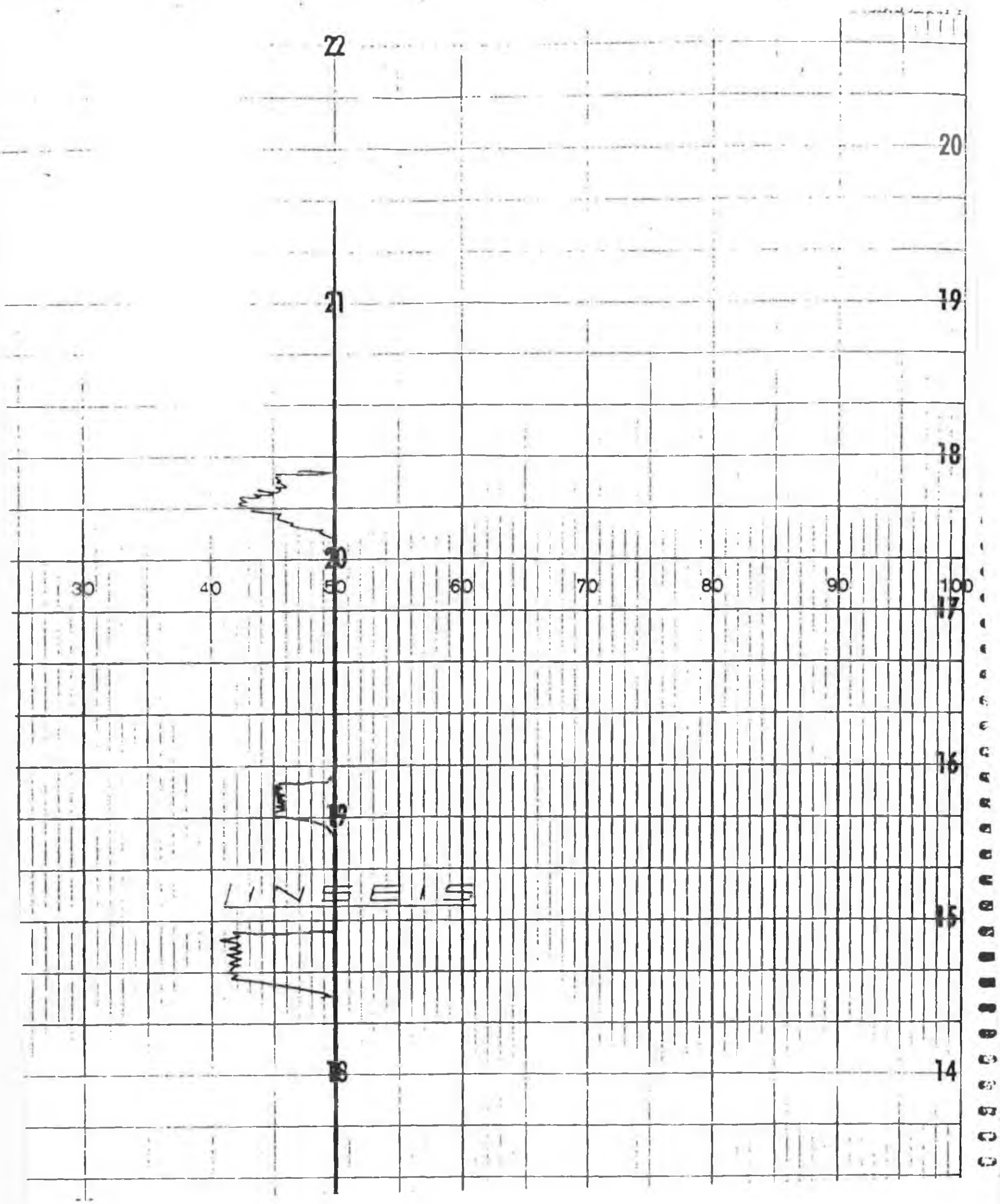

FIG (22) TYPICAL RECORDER TRACE FOR MEASURED PRESSURES

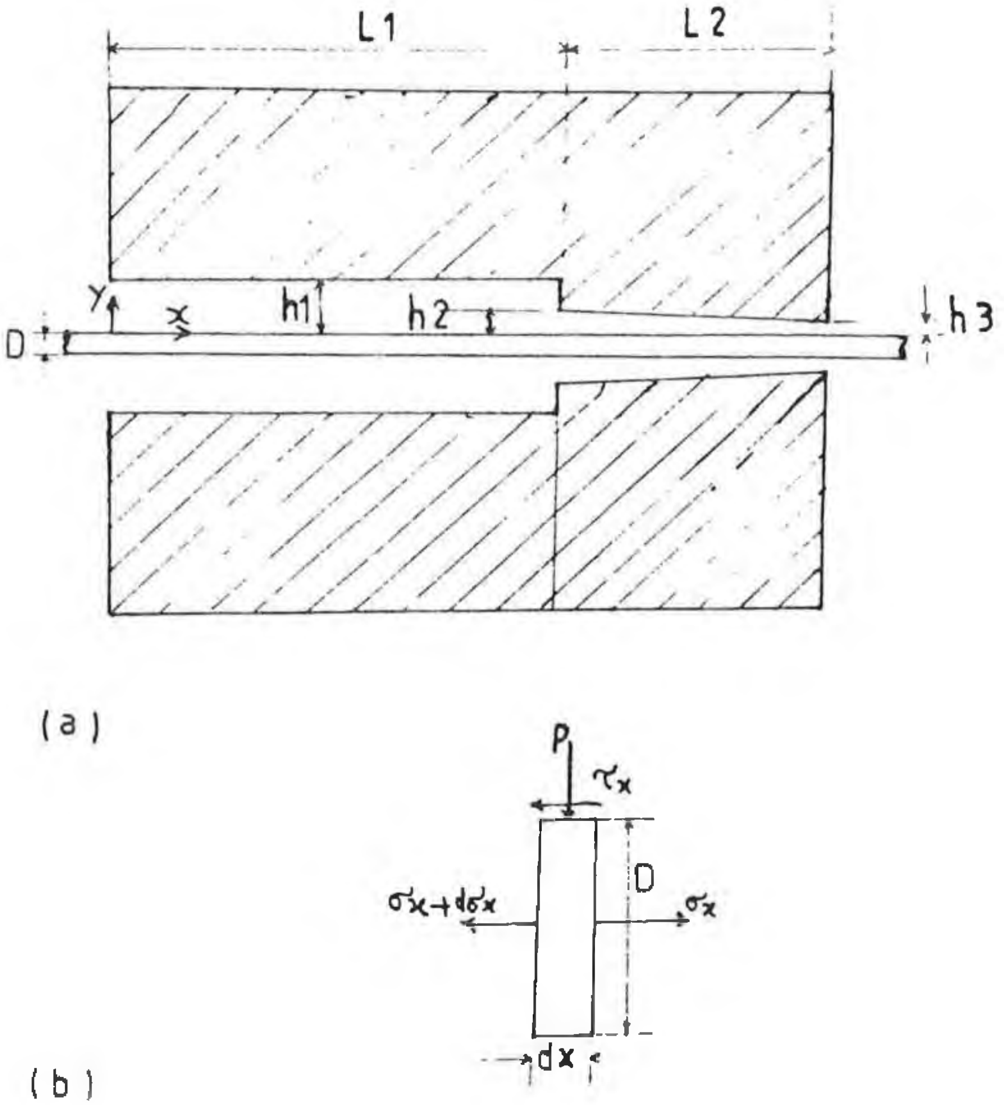

FIG (23) (a) GEOMETRICAL CONFIGURATION OF THE PRESSURE UNIT AND THE WIRE

(b) STRESSES ACTING ON A SMALL ELEMENT OF THE WIRE


REMOTE HAND HELD DIGITAL TACHOMETER
FREQENCY INVERTER
DT-205
SHIMPO

PLATE 1

PLATE 2

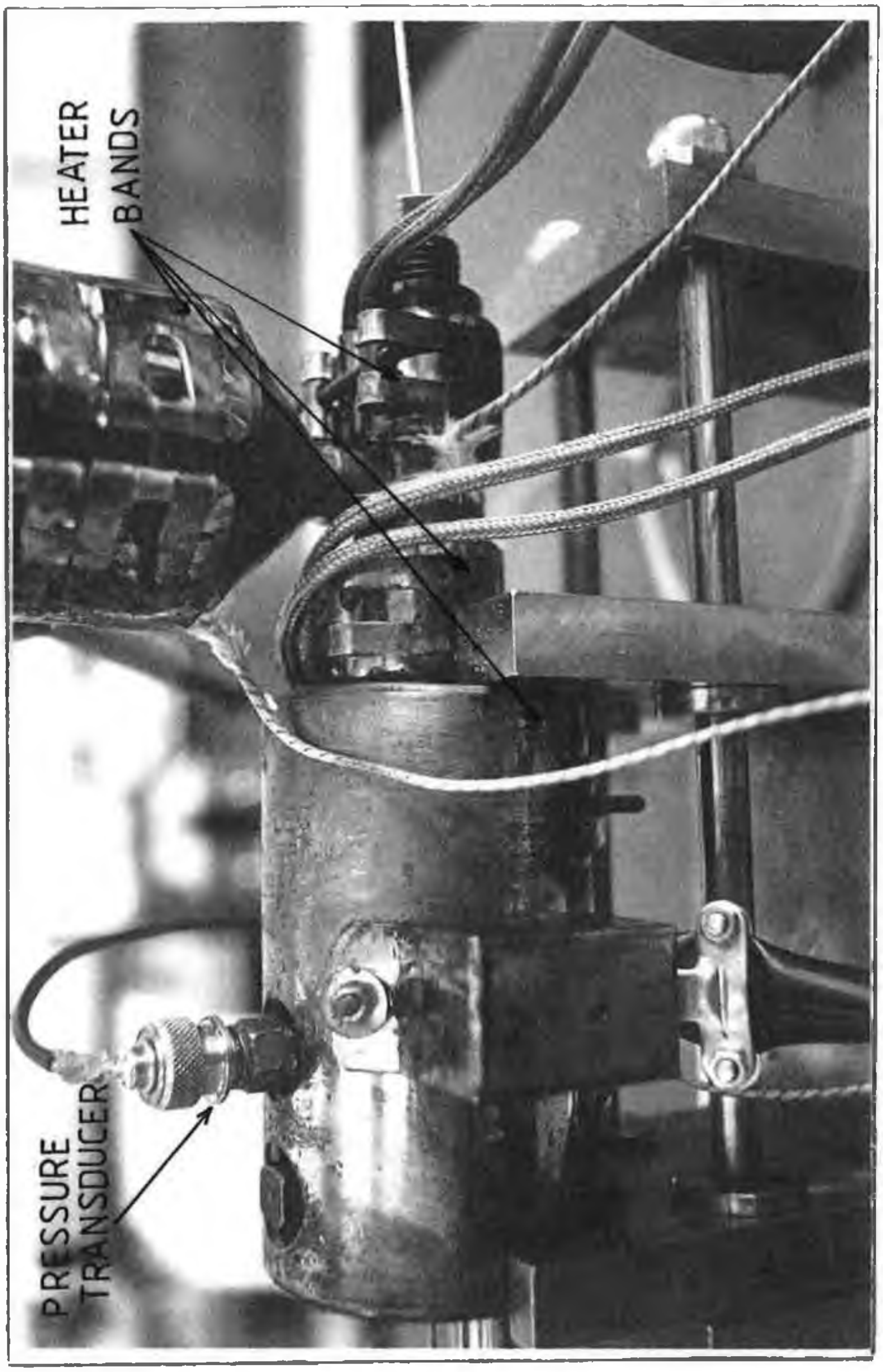

PLATE 3

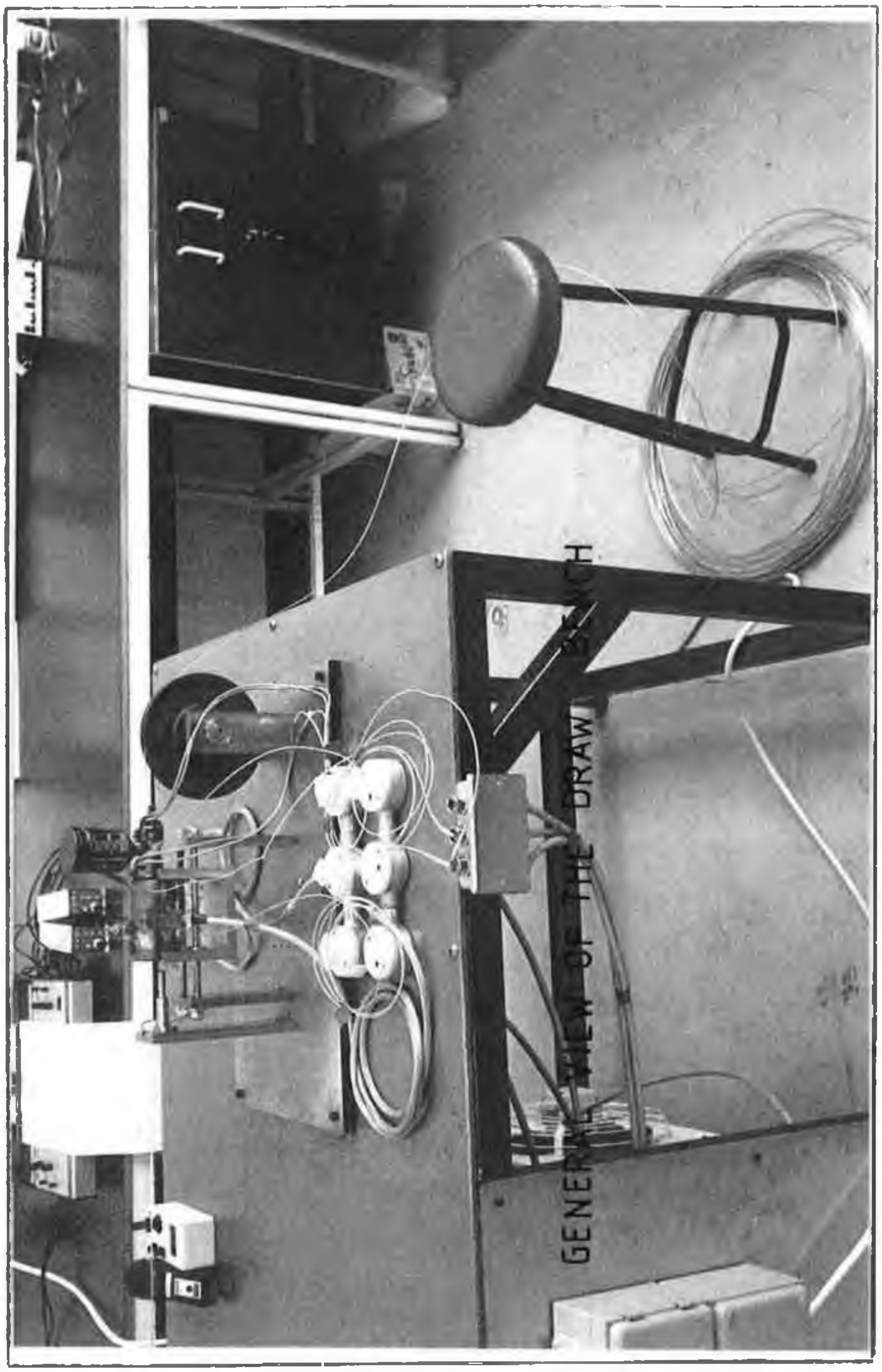

GENERAL VIEW OF THE DRAW BENCH

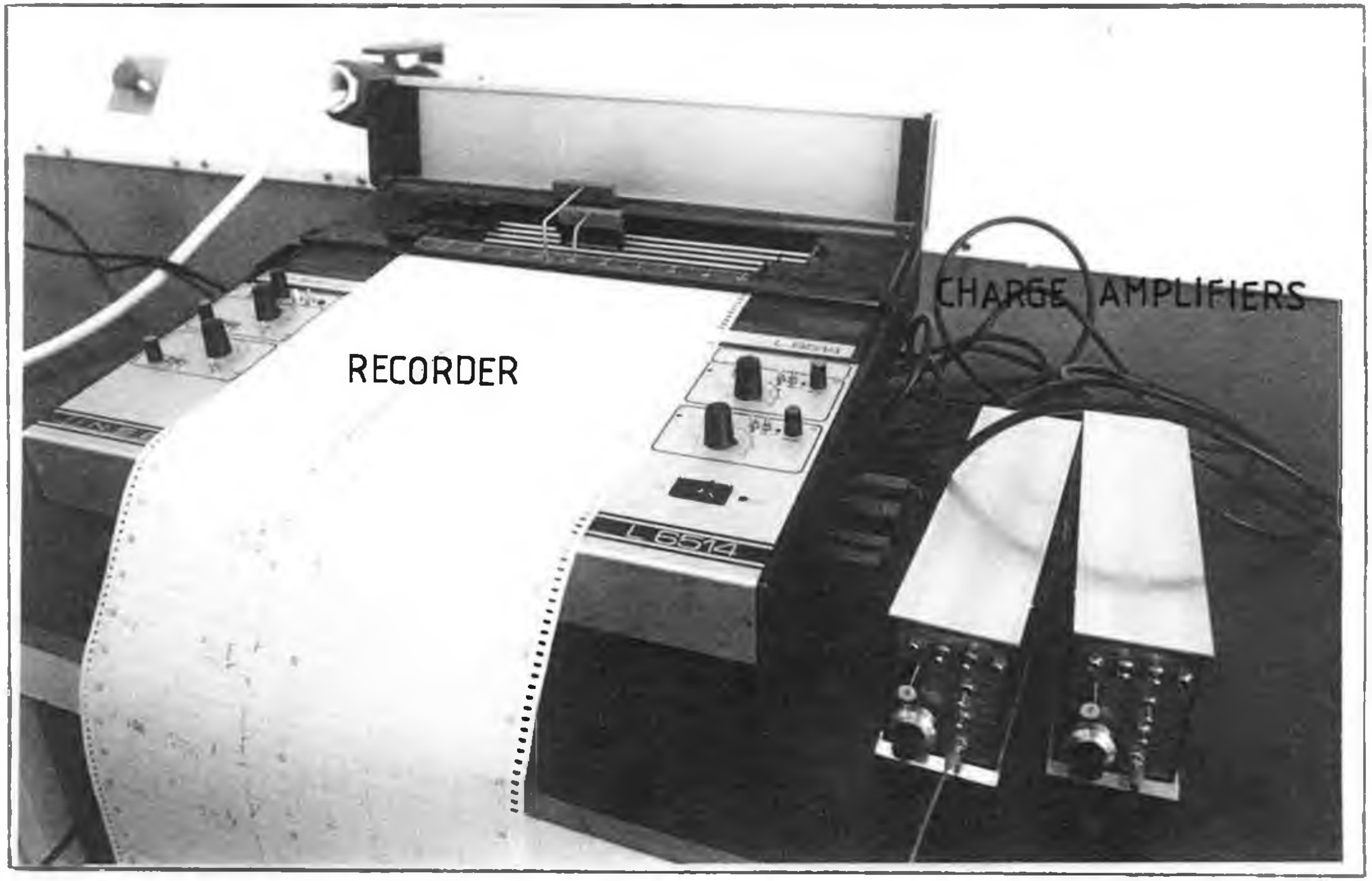

PLATE 4

PLATE 5

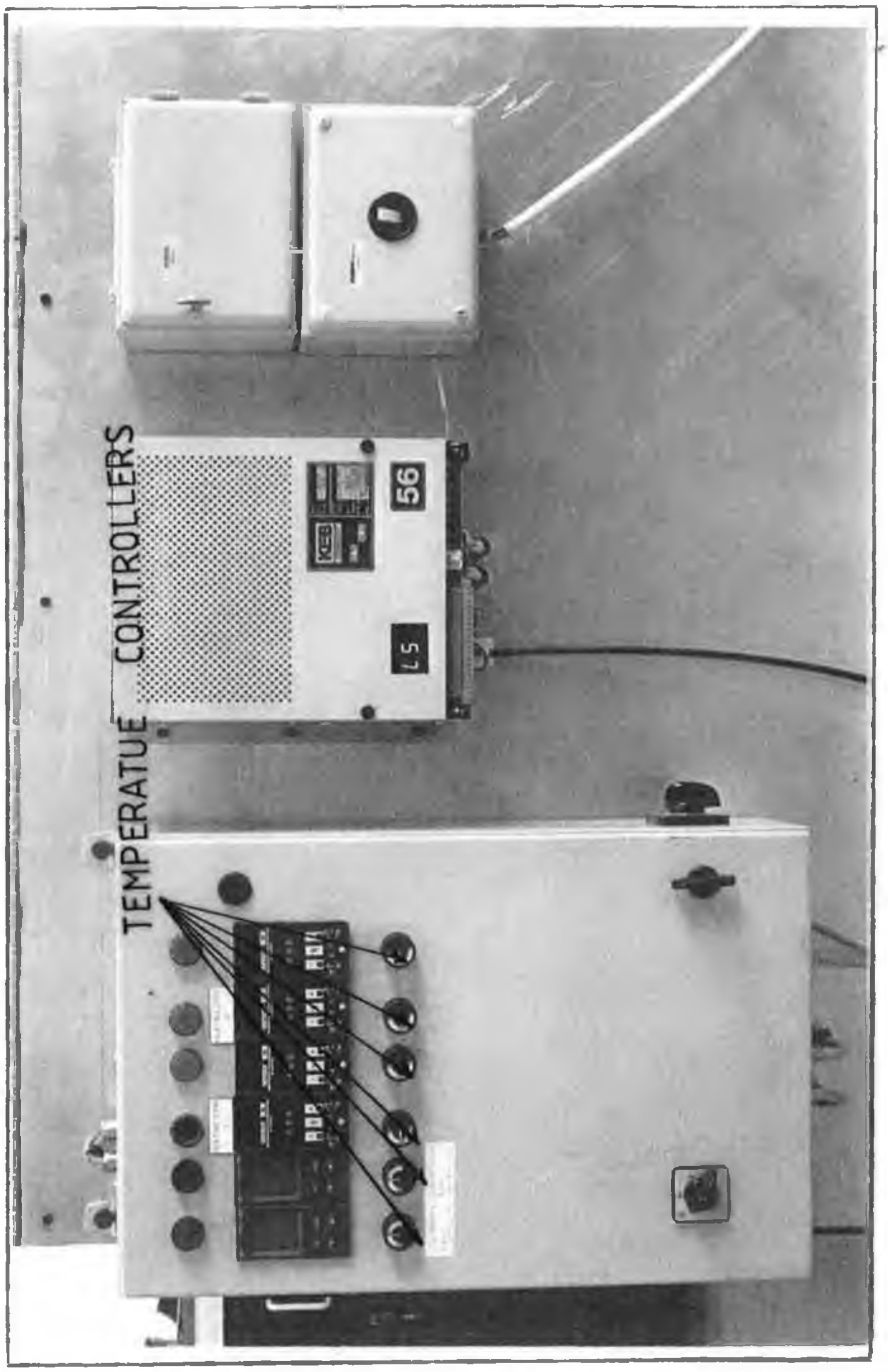

PLATE 6

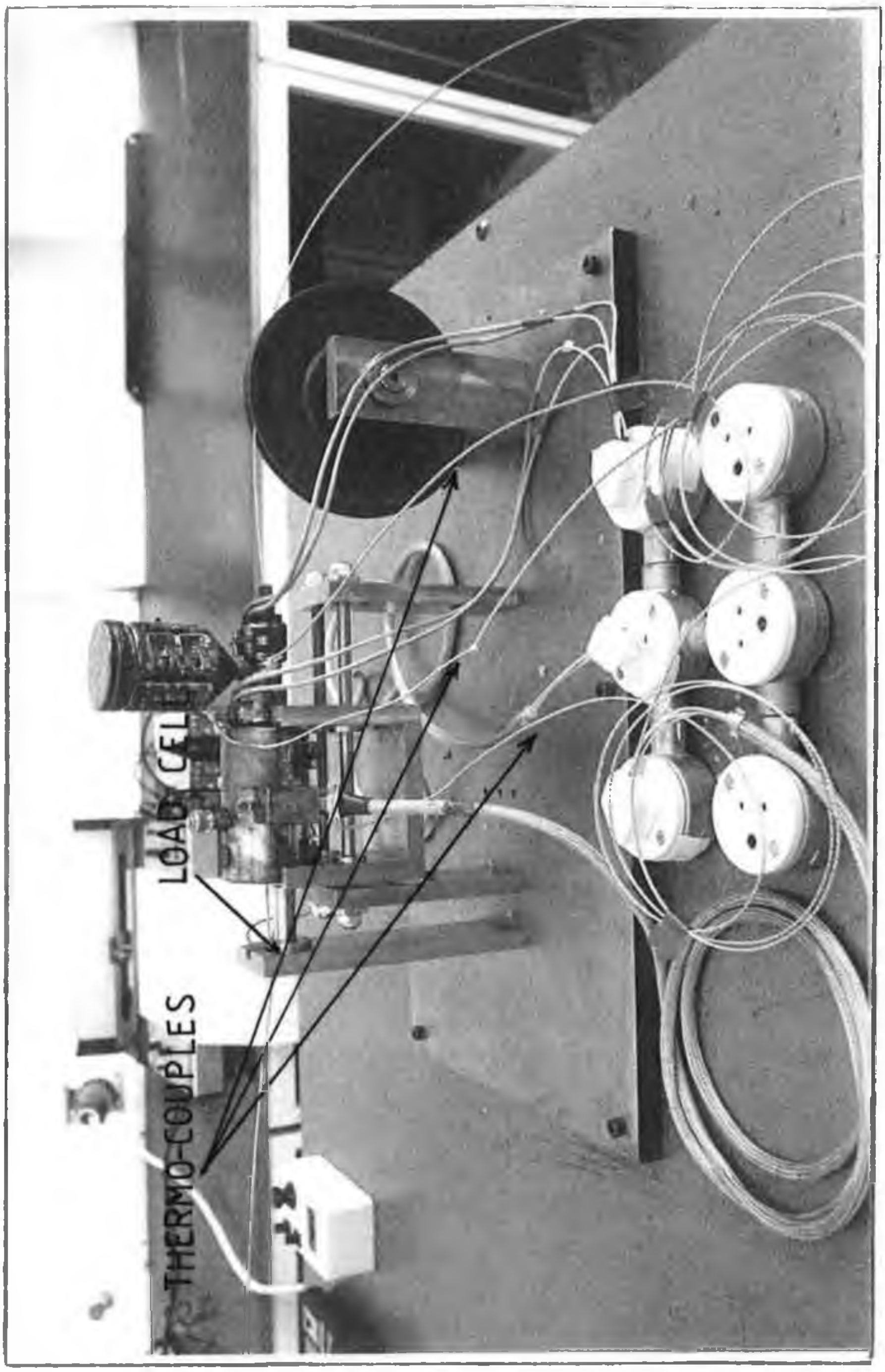

PLATE 7

CHAPTER-4

EXPERIMENTAL WORK AND RESULTS

4.1 Experimental Procedure

The following procedure was followed before carrying out any test. The heater bands were first switched on and were controlled thermostatically to maintain the temperature at the pre-set level. The hopper and melt chamber were filled with polymer in granulated form. The other instruments were also switched on. The pressure unit was left for one hour to reach the steady state temperature level. Wire from the coil was placed on the ground of the laboratory next to the drawing bench was passed over the pulley before being inserted through the unit. The wire was then attached to the bull-block The electric motor was started and set running at the desired speed. The build-up of speed was determined by the accelerator time set on the frequency inverter which varies the motor speed settings. The charge amplifier for the pressure transducer was switched to the static position which gave a steady and uniform reading through out the run. The electric motor, the recorder and the charge amplifier were switched back to their original positions. The test number was recorded on the data sheet for subsequent collection and analysis. While the wire was being drawn, the rotational speed of the bull block was measured using a hand held digital tachometer. When analysing the experimental results the traces for pressures on the recorder paper were measured and recorded on the data sheet for each test. A typical paper trace is shown in Fig. 22

4.2 Experimental Results

Experimental results obtained using the combined stepped and taper bore pressure unit are presented in graphical form in this section. Dimensional details of the pressure unit used for the tests are shown in schematic form in the diagram in Fig. 23 and are as follows :

Pressure Unit 1	Pressure Unit 2
L_1=60 mm	L_1=60 mm
L_2=20 mm	L_2=20 mm
h_1=3.48 mm	h_1=3.48 mm
h_2=0.68 mm	h_2=0.18 mm
h_3=0.025 mm	h_3=0.025 mm
h_1/h_3= 139.2	h_1/h_3=139.2
h_2/h_3=27.2	h_2/h_3=7.2

Pressure Unit 3

L_1=60 m.m

L_2=20 m.m

h_1=3.505 m.m

h_2=0.705 m.m

h_3=0.05 m.m

h_1/h_3=70.1

h_2/h_3=14.1

Pressure Unit 4

L_1=60 mm

L_2=20 mm

h_1=3.54 mm

h_2=0.74 mm

h_3=0.085 mm

h_1/h_3=41.6

h_2/h_3=8.7

Pressure Unit 5

L_1=60 mm

L_2=20 mm

h_1=3.54 mm

h_2=0.24 mm

h_3= 0.085 mm

h_1/h_3=41.6

h_2/h_3=2.8

Pressure Unit 6

L_1=60 mm

L_2=20 mm

h_1=3.54 mm

h_2= 0.085 mm

h_1/h_2=41.6

Pressure Unit 7

h_1=1.54 mm

h_2=0.74 mm

h_3=0.085 mm

h_1/h_3=18.1

h_2/h_3=8.7

4.2.1 Results Of Pressure

The generated hydrodynamic pressures in the pressure unit were measured by means of the pressure transducer mounted on the unit.The results of the pressures are divided into two sections i) the pressure variations versus drawing speed and ii) the pressure distribution in the pressure unit. Numbers on each figure refers to the locations of the pressure transducers as shown in Fig. 18

i) Results of Pressure Versus Speed

Fig. 24 shows the measured pressures for brass wire versus speed with lupolen polymer at 170 °C. The measured pressures at position 3 and 4 increased as drawing speed was increased. Higher pressures were recorded at position 4 for drawing speeds of up to 0.184 m/s. The measured pressures at positions 1 and 2 remained fairly constant with speed.

Fig. 25 shows the measured pressures for brass wire versus speed with lupolen polymer at 170 °C but at gap ratio of $h_2/h_3=7.2$. The measured pressures increased as drawing speed was increased at position 4. While the measured pressures were constant at position 2. It was observed that the measured pressures at gap ratio $h_2/h_3=7.2$ is much higher compared to those shown in Fig. 24 for gap ratio $h_2/h_3=27.2$.

Figure 26 gives the pressure variations versus speed for copper wire with polyethylene at 125 °C. For drawing speeds in excess of about 0.12 m/s the pressure readings were found to be approximately constant for position 2 while the measured pressures increased at position 3 as the drawing speed was increased. Higher pressures were recorded with this polymer at position 4 and the maximum pressure was observed at 0.12 m/s.

Figure 27 shows the measured pressures for copper wire with polyethylene at 150 °C. The general trends were found to change compared to those in Fig 26. For drawing speed in excess of about 0.12 m/s the pressure readings were found to be approximately constant at position 2 but the pressure was found to increase as drawing speed was increased at position 3 The maximum pressures were recorded at positions 3 and 4 at speed of 0.08 m/s.

Fig. 28 is showing the measured pressures for mild steel wire with lupolen polymer at melt temperature of 170 °C. When this polymer was used as the pressure medium the results were found to be similar to those in Fig. 24. Higher pressures were recorded at higher drawing speeds for positions 3 and 4. For drawing speed in excess of about 0.08 m/s the pressure readings were found to be approximately constant at positions 1 and 2.

Figure 29 shows the pressure variations versus speed for mild steel wire when lupolen polymer was used as the pressure medium at 150 °C. The general trends of the results were found to be similar to those in Fig. 28. Higher pressures were recorded at higher drawing speeds for position 4 while for a drawing speed in excess of 0.16 m/s the pressure readings were found to be approximately constant at positions 2 and 3.

Figure 30 gives the measured pressures for mild steel wire with polyethylene at 114 °C. The magnitudes of the generated pressures at lower drawing speeds were different from those in Fig. 26. At position 4 the pressure reduced as speed was increased. The pressure was found to be approximately constant at position 3. For drawing speeds in excess of 0.2 m/s approximately the pressures decreased as the drawing speed was increased. at position 3. Figure 31 gives the measured pressures for mild steel wire with polyethylene at 125 °C. The pressure curves at positions 2 and 4 were found to be similar to those in Fig. 26.

Figure 32 is showing the pressure variations with speed for mild steel wire with polyethylene at 140 °C. The general trend of the results were found to be similar to those in Fig. 31. The maximum pressure was at position 4. for all speeds of up to 0.18 m/s. Figure 33 shows the measured pressures versus speed for mild steel wire with polyethylene at 140 °C but at gap ratio of $h_1/h_3=18.11$. It was observed that the pressure magnitudes at positions 1, 2 and 3 remained approximately constant. The pressure curve at position 4 was found to be different from that in Fig. 28 at same position. Pressure decreased as drawing speed was decreased. Higher pressures were recorded with the gap ratio $h_1/h_3=18.11$ as compared to those in Fig. 32

Figure 34 gives the variations of pressure versus speed for mild steel wire with polyethylene at 140°C and gap ratio $h_2/h_3=2.8$. The measured pressure at position 2 was found to be approximately constant. For drawing speed in excess of 0.14 m/s the pressures were found to be constant at position 3. The magnitudes of the generated pressures at higher drawing speeds increased significantly at position 4. Higher pressures were recorded with changing gap ratio h_2/h_3 compared to those in Fig. 32.

<u>ii) The Pressure Distribution In The Pressure Unit</u>

Figures 35 and 36 show the pressure distribution when brass wire was drawn using lupolen polymer at different gap ratios of h_2/h_3 but same temperatures. In all cases the measured pressure was found to be the maximum at the position 4 . The maximum pressure was found to vary between 90 and 225 MN/m^2 Fig. 37 shows effect of gap ratio h_2/h_3 on pressure distribution for brass wire with lupolen at 170 °C and at the speed of 0.12 m/s. Higher pressures were recorded for gap ratio $h_2/h_3=7.2$ compared to the gap ratio h_2/h_3=27.2.

Figures 38 and 39 show the pressure distribution for the copper wire with polyethylene polymer at different melt temperatures but the same gap ratio. The measured pressures were found to be maximum at position 4. Figure 38 shows that the measured pressure increased as the drawing speed was increased while Fig. 39 shows the measured pressures decreased slightly as the drawing speed increased. Little changes were observed in the pressure profiles in positions 1 and 2 at different drawing speeds.

Figure 40 shows the effect of temperature on pressure distribution for copper wire with polyethylene at drawing speed of 0.12 m/s. Figures 41 and 42 show the pressure distribution for mild steel wire with lupolen polyethylene at 170 °C, 150 °C respectively. In all cases the measured pressures were found to be maximum at position 4. The pressure readings were found to increase with speed and was found to vary between 20-90 MN/m^2

Figure 43 shows effect of temperature on pressure distribution for mild steel wire with lupolen at drawing speed of 0.08 m/s at the same gap ratio. The pressure decreased as melt temperature was increased. Figures 44 and 45 show the pressure distribution for mild steel wire with polyethylene polymer at two different melt temperatures but same gap ratio. In all cases the measured pressure was found to be the maximum at the position 4 at all drawing speeds. The measured pressure was found to be little changed at position 1 and 2 at all drawing speed. Figure 46 shows the pressure distribution for mild steel wire with polyethylene at 140 °C and a gap ratio of $h_2/h_3=2.8$ The maximum pressure was found to be much higher compared to those in Fig. 44 with a gap ratio of $h_2/h_3=8.7$ Figure 47 shows the pressure distribution for mild steel wire with polyethylene at 140 C and gap ratio of $h_1/h_3=18.1$. The maximum pressure in position 4 did not change for two different drawing speeds of 0.2 m/s. and 0.09 m/s respectively. In all cases the measured pressure was found to be maximum at position 4. Higher pressures were recorded with gap ratio of $h_1/h_3=18.1$ compared to those in Fig. 44 with a gap ratio of $h_1/h_3=41.6$. Figures 48 and 49 show the effect of gap ratio h_1/h_3 and h_2/h_3 on pressure distribution for mild steel wire with polyethylene at 140°C and drawing speed of 0.14m/s.In all cases the maximum pressures increased with the decrease of gap ratio h_1/h_3 and h_2/h_3.

Figure 50 shows the effect of temperatures on pressure distribution for mild steel wire with polyethylene a drawing speed of 0.17 m/s. Figure 51 shows the pressure distribution for mild steel wire with polyethylene at 140 C using a stepped bore unit and a combined stepped and tapered pressure unit.

The maximum pressure is much higher with the combined geometry unit than the stepped bore unit at the same final gap of 0.085 mm.

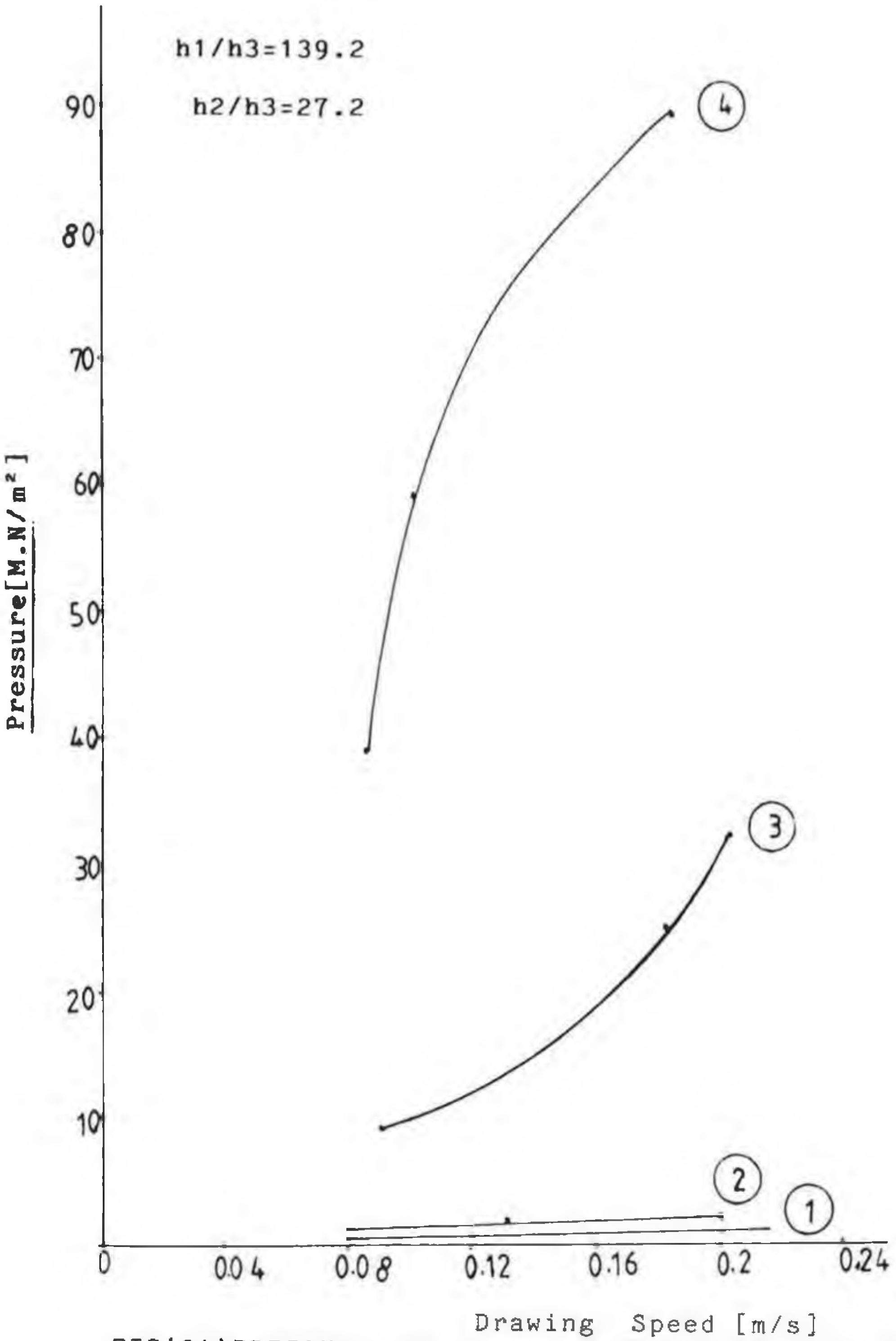

FIG(24)PRESSURE VERSUS SPEED FOR BRASS WIRE WITH LUPOLEN AT 170°C

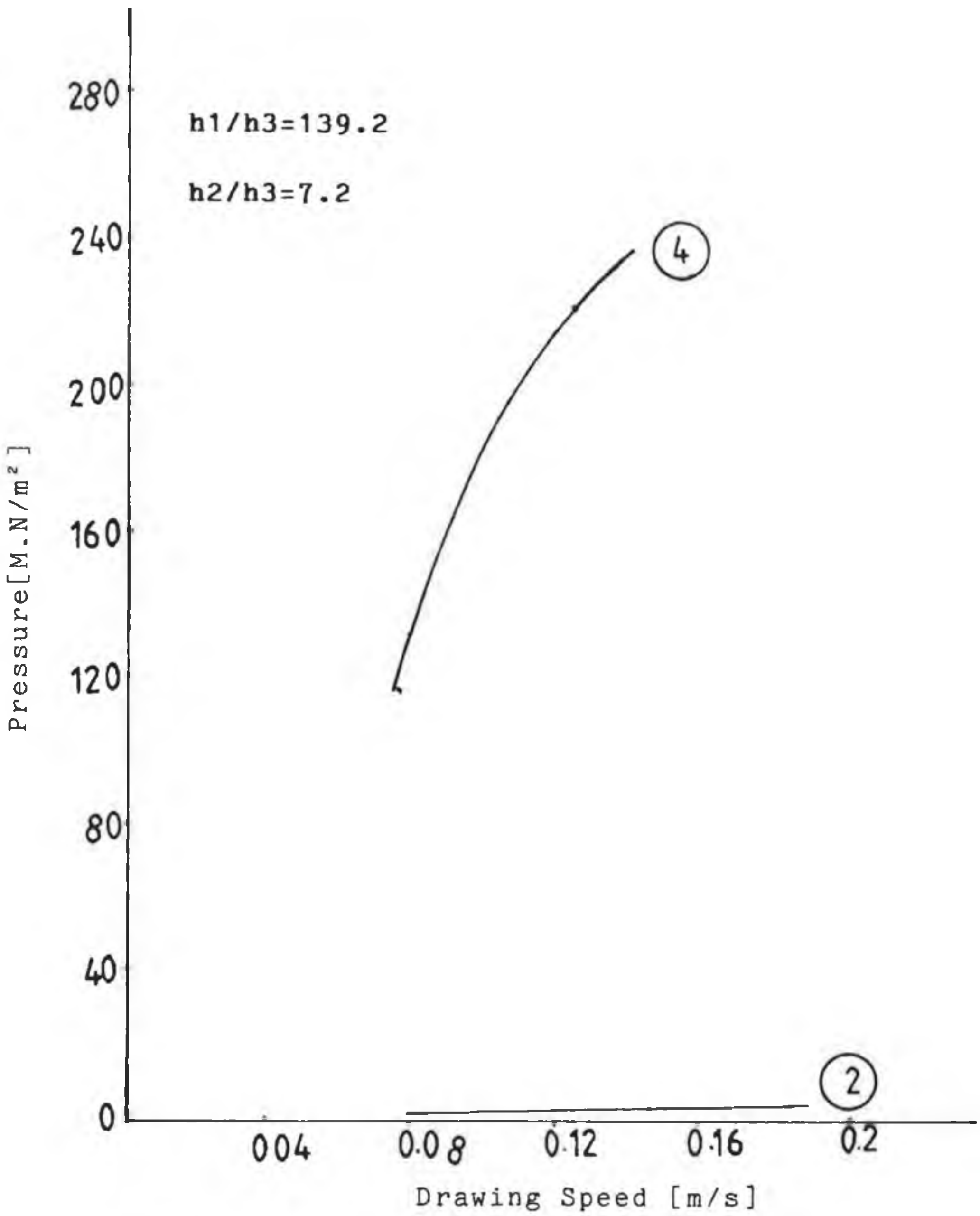

FIG(25) PRESSURE VERSUS SPEED FOR BRASS WIRE WITH LUPOLEN AT 170 °C

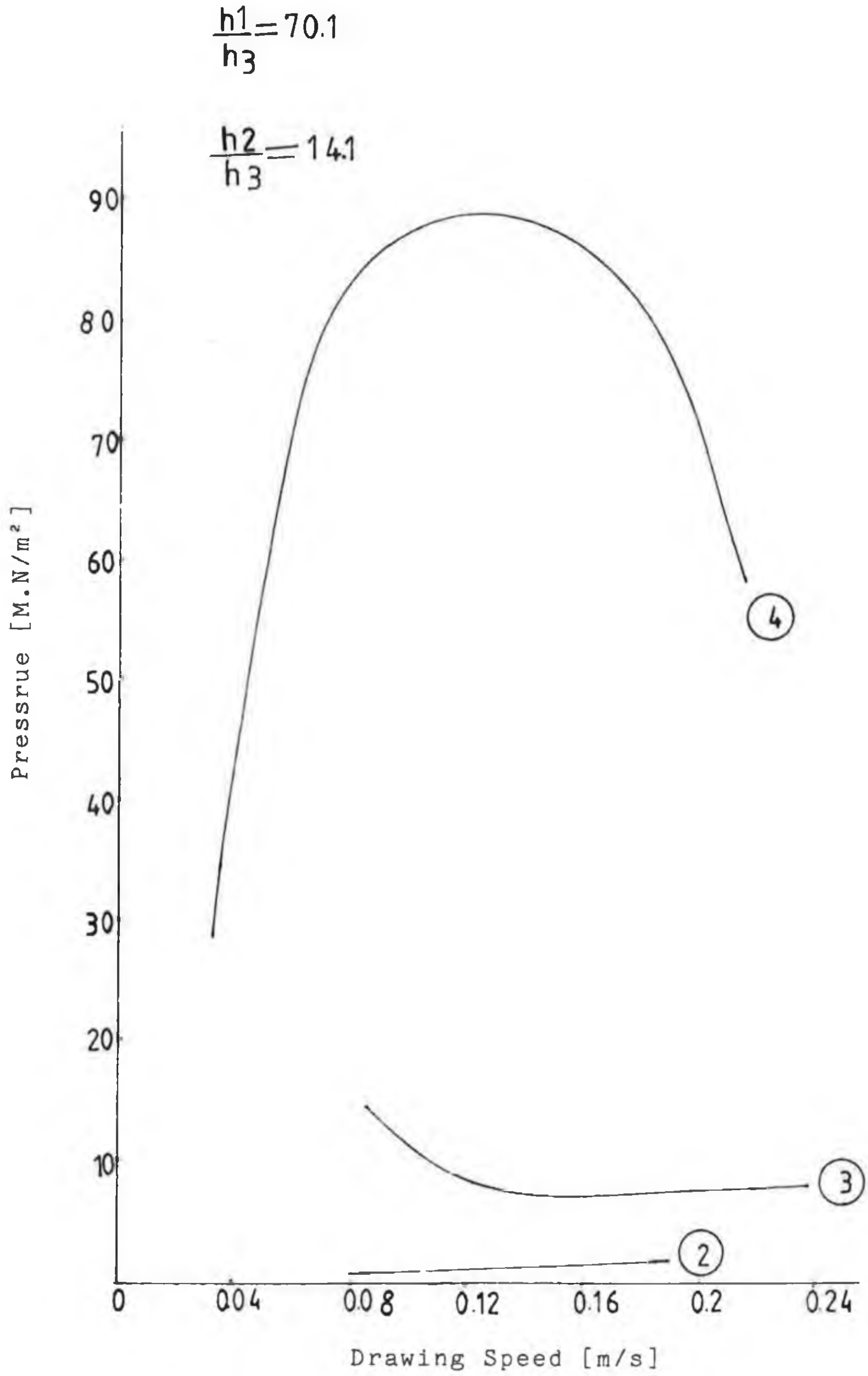

FIG(26) PRESSURE VERSUS SPEED FOR COPPER WIRE WITH POLYETHYLENE (ESCORENE) AT 125 °C

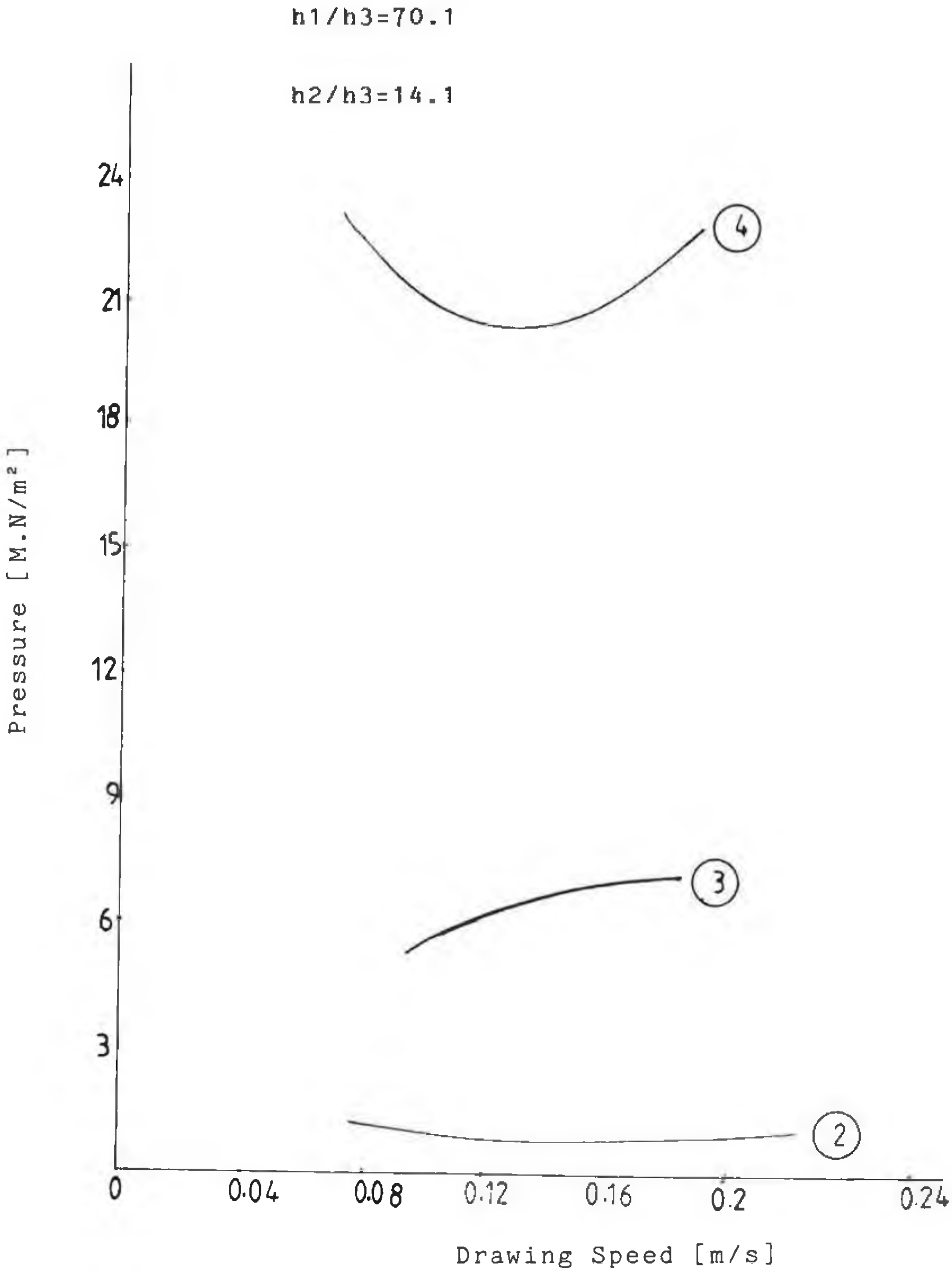

FIG(27) PRESSURE VERSUS SPEED FOR COPPER WIRE WITH POLYETHYLENE (ESCORENE) AT 150 °C

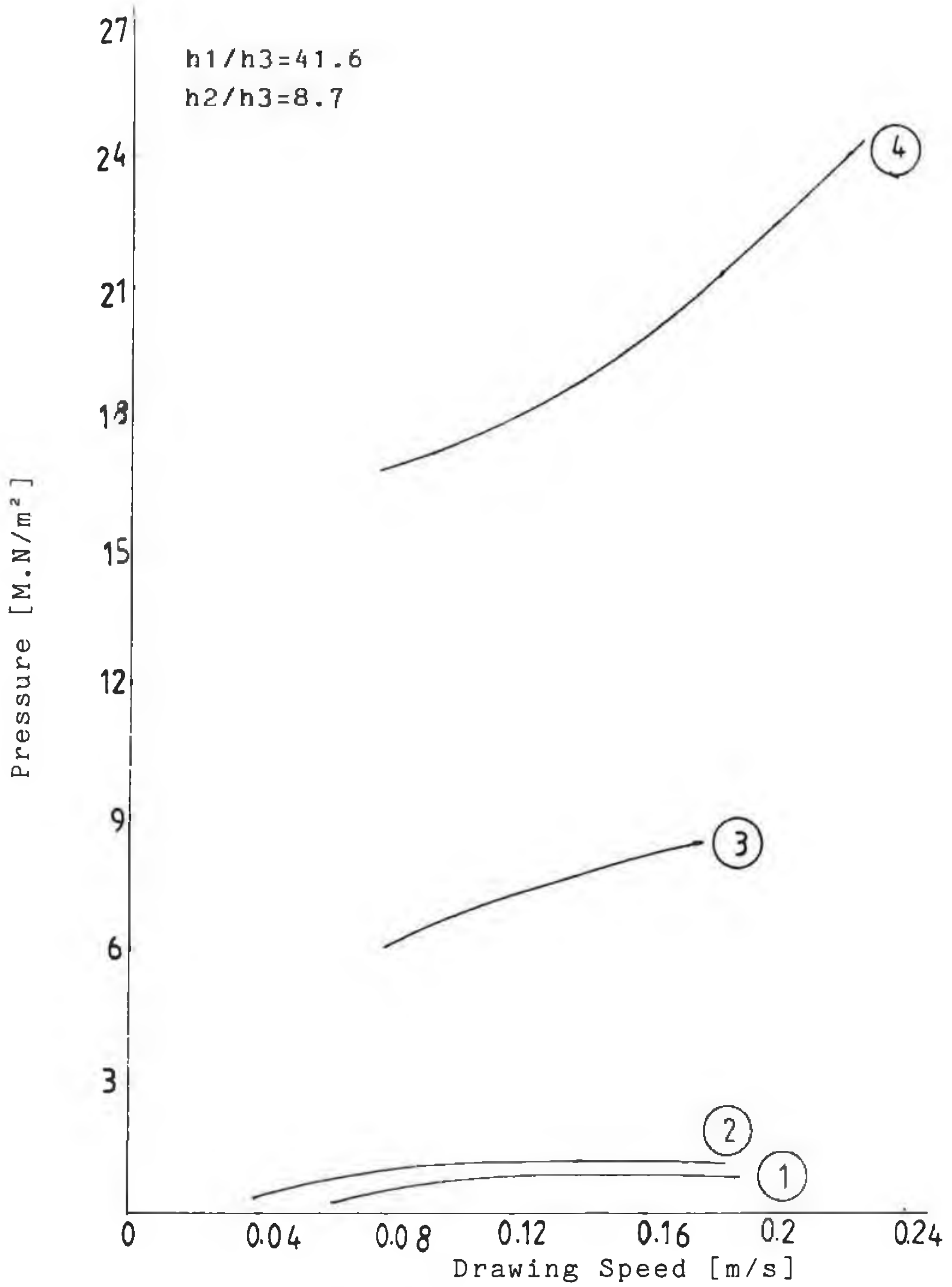

FIG (28) PRESSURE VERSUS DRAWING SPEED FOR MILD STEEL WIRE WITH LUPOLEN AT 170 °C

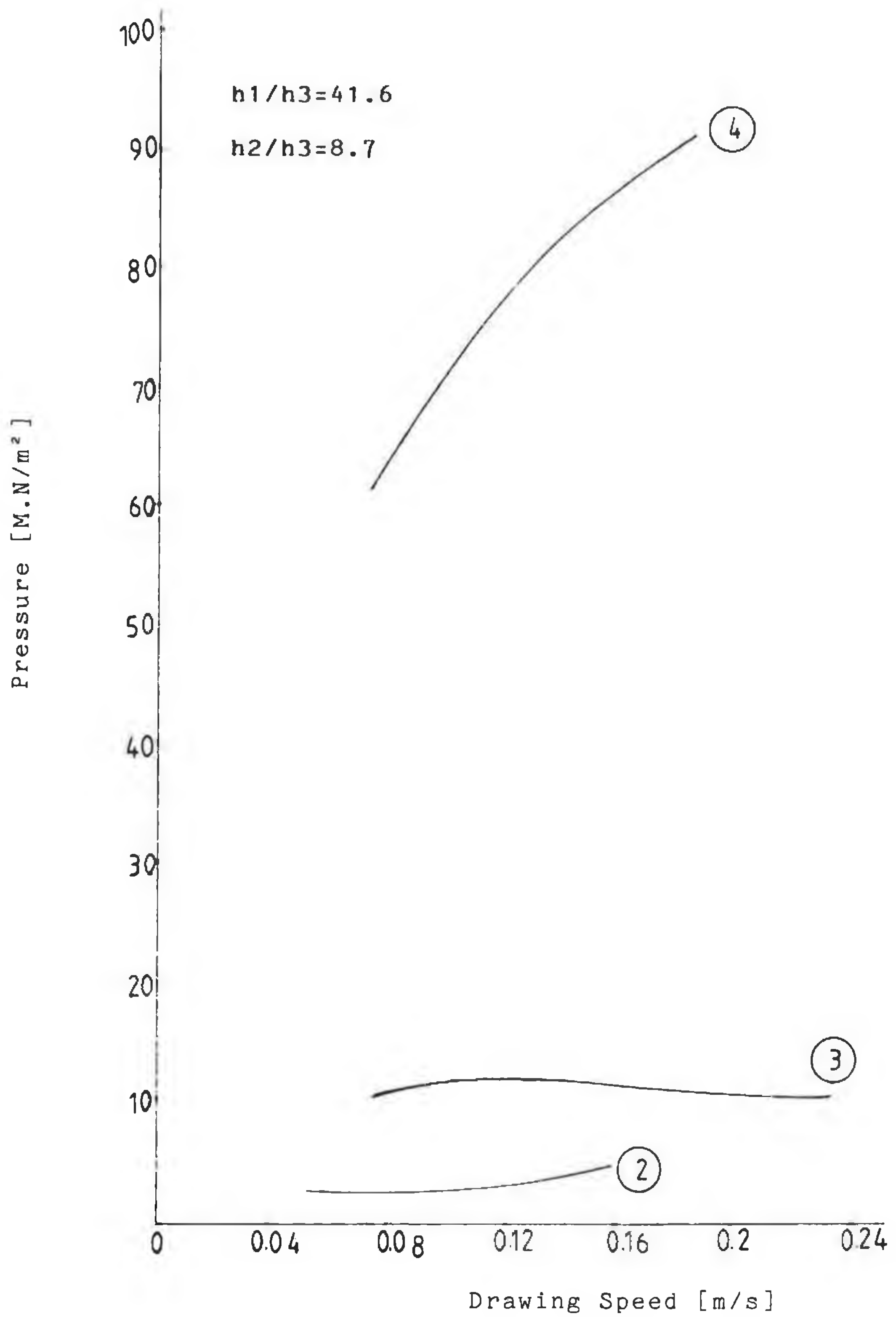

<u>**FIG (29) PRESSURE VERSUS SPEED FOR MILD STEEL WIRE WITH LUPOLEN AT 150 °C**</u>

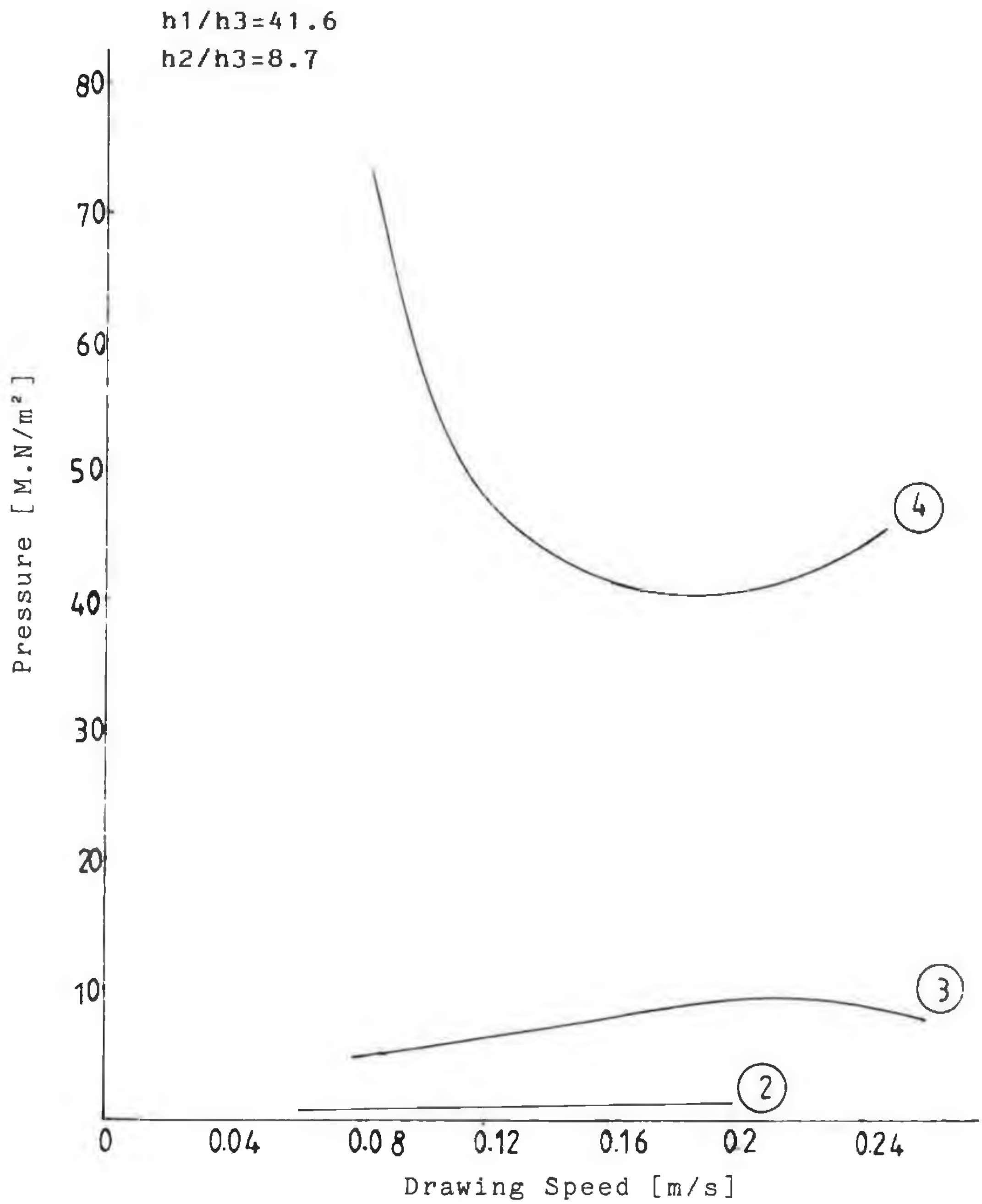

FIG (30) PRESSURE VERSUS SPEED FOR MILD STEEL WIRE WITH POLYETHYLENE(ESCORENE) AT 114 °C

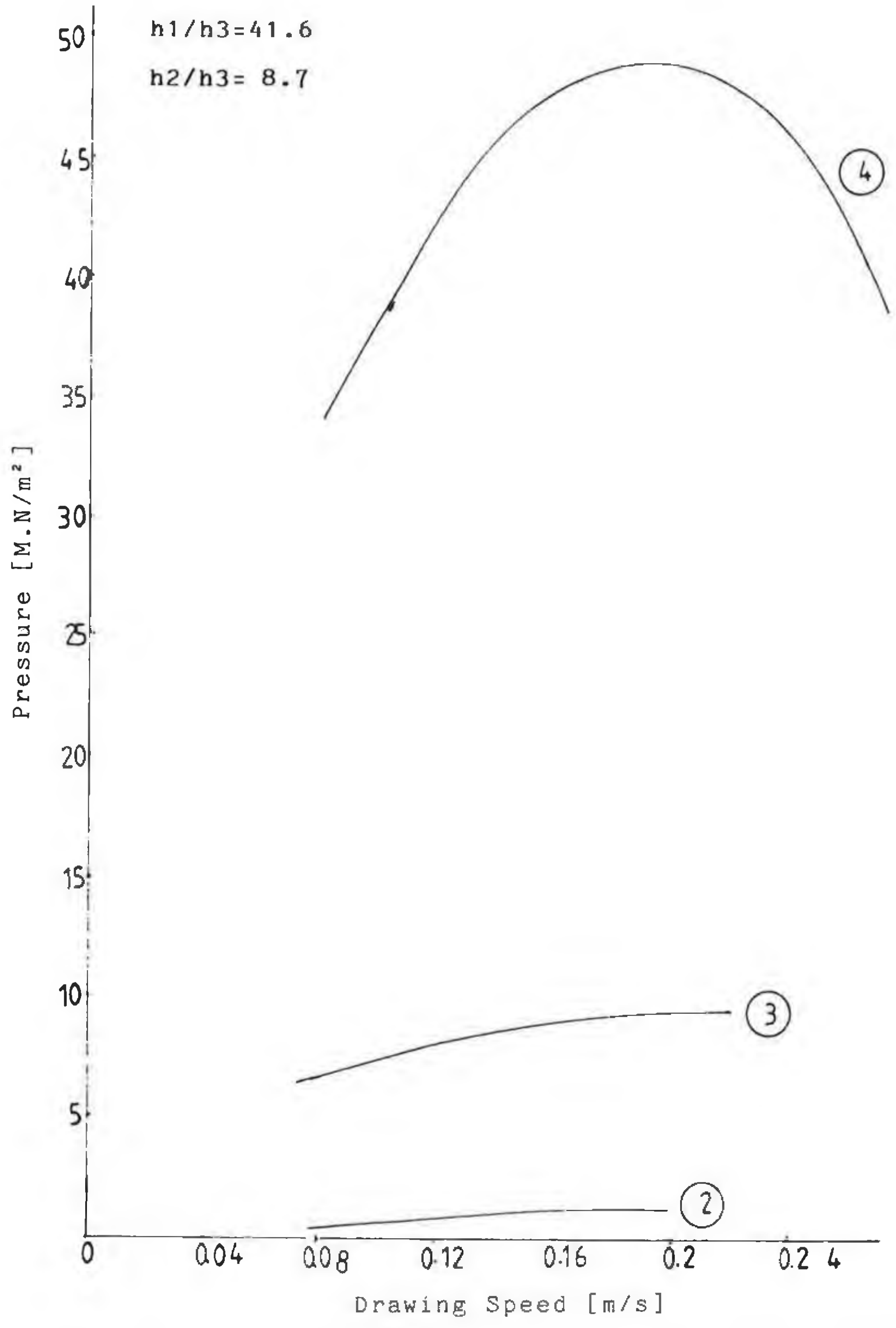

FIG(31) PRESSURE VERSUS SPEED FOR MILD STEEL WIRE WITH POLYETHYLENE(ESCORENE) AT 125 °C

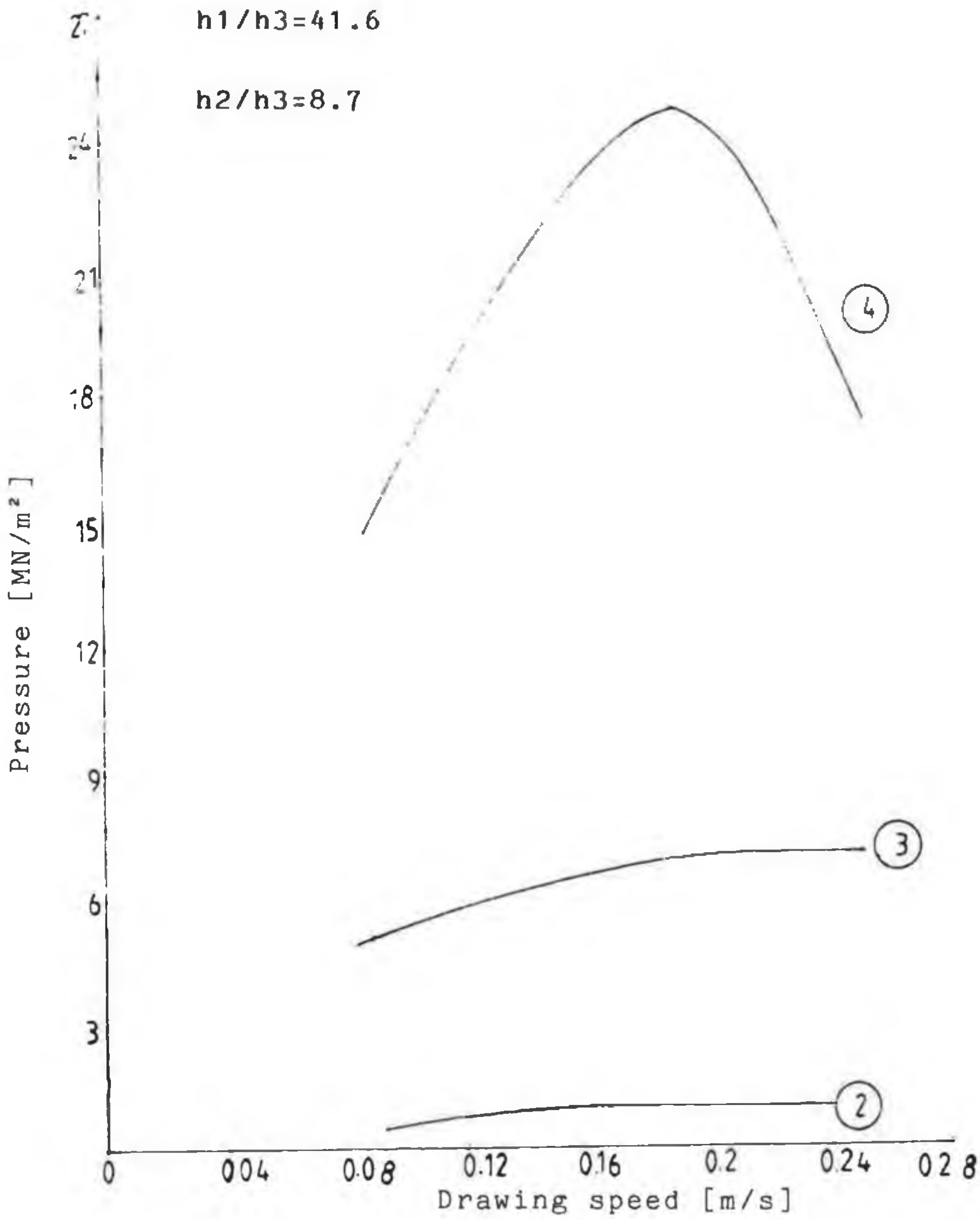

FIG (32) PRESSURE VERSUS SPEED FOR MILD STEEL WIRE WITH POLYETHYLENE (ESCORENE) AT 140 °C

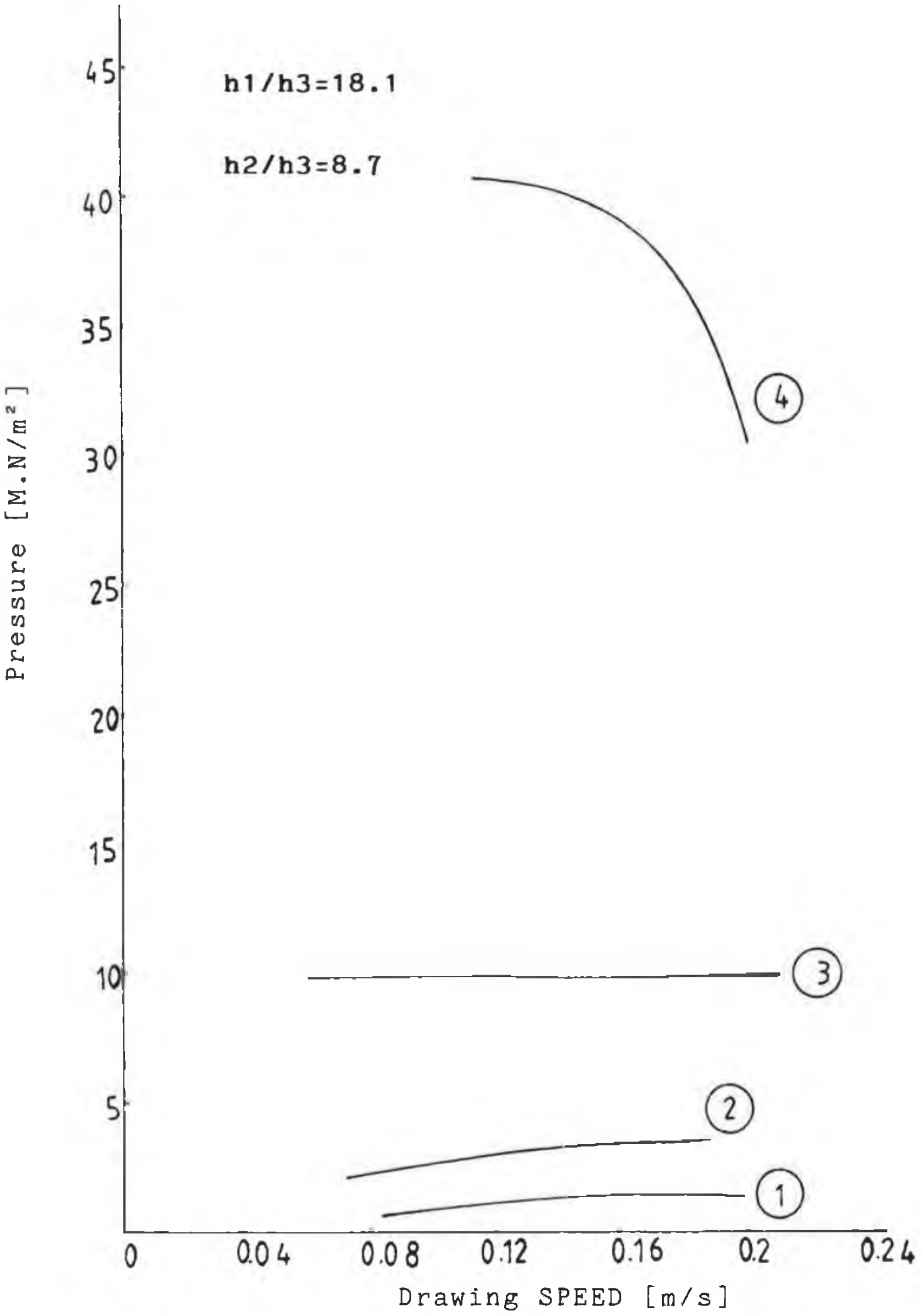

FIG (33) PRESSSURE VERSUS SPEED FOR MILD STEEL WIRE WITH POLYETHYLENE(ESCORENE) AT 140 °C

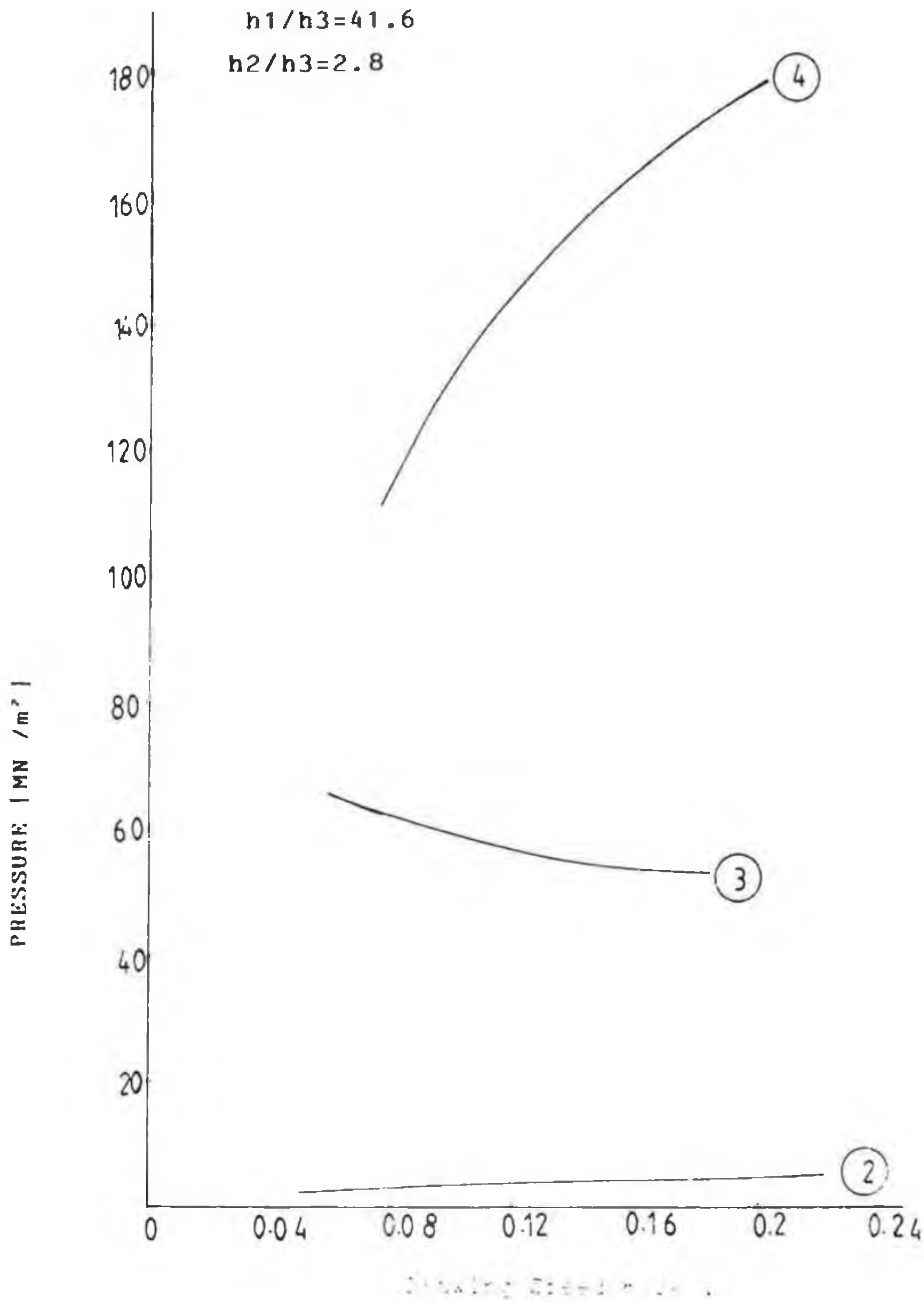

FIG 34 PRESSURE VERSUS SPEED FOR MILD STEEL WIRE WITH POLYETHYLENE AT 140°C

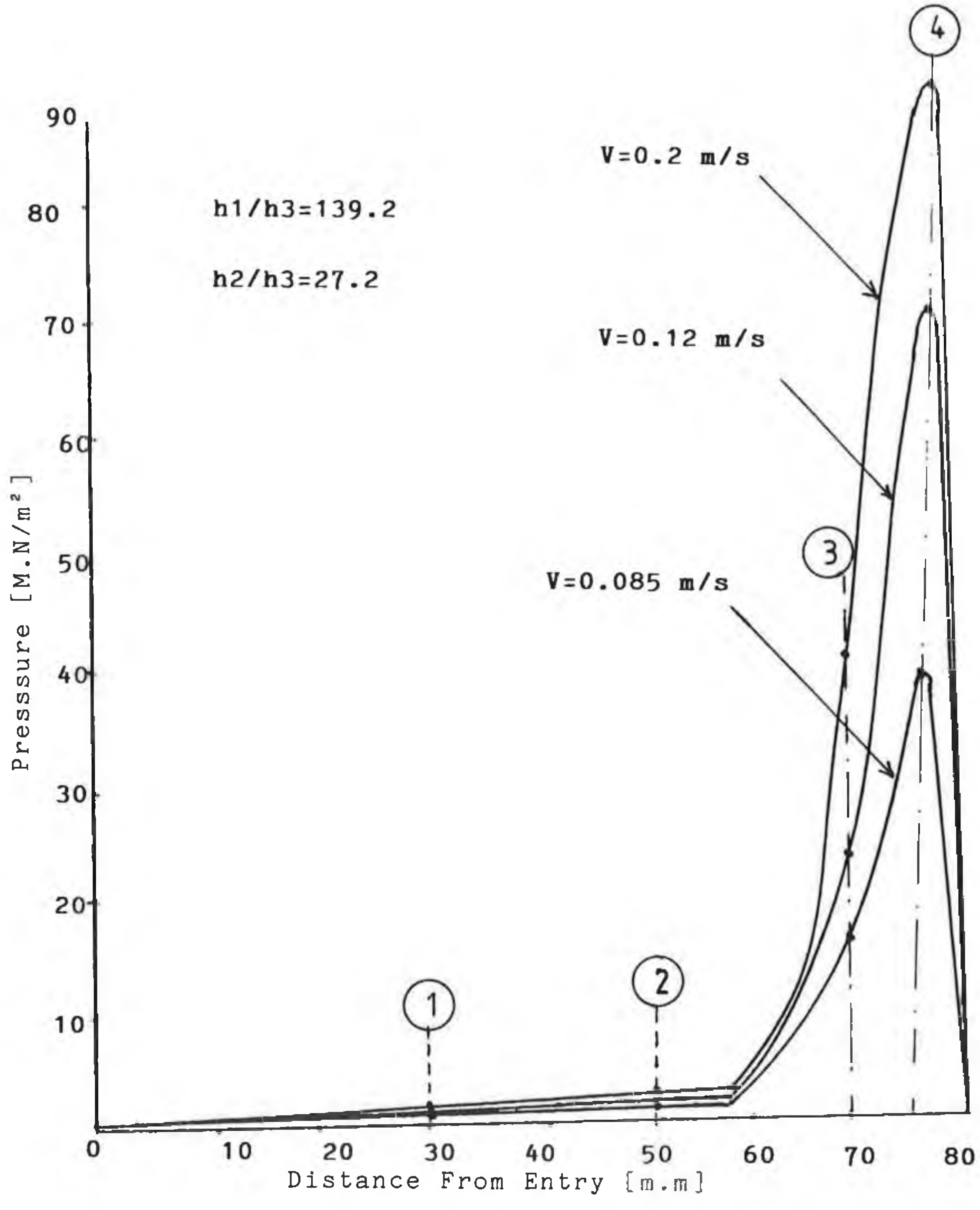

FIG (35) PRESSURE DISTRIBUTION FOR BRASS WIRE WITH LUPOLEN AT 170 °C

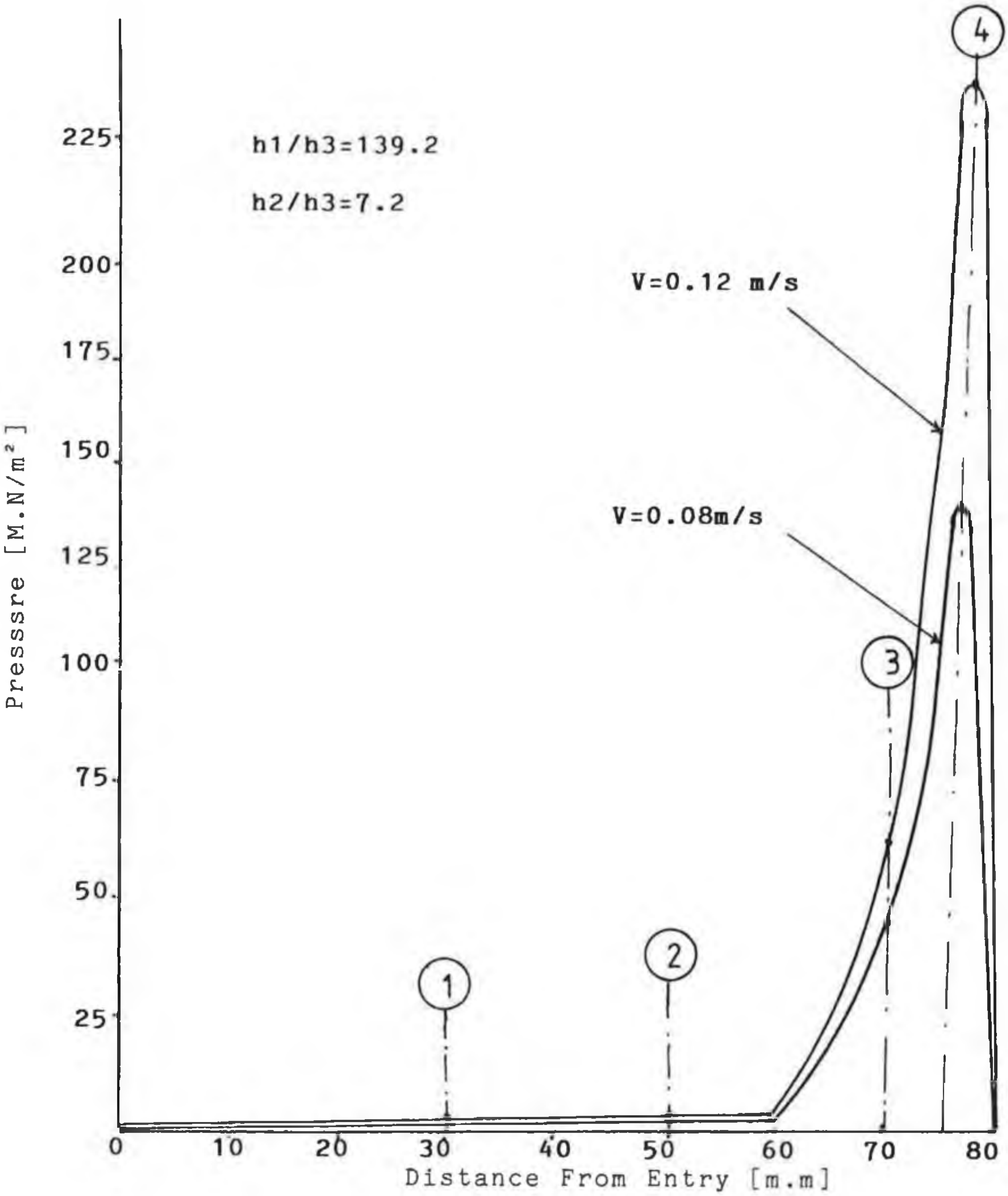

FIG (36) PRESSURE DISTRIBUTION FOR BRASS WIRE WIT LUPOLEN AT 170 °C

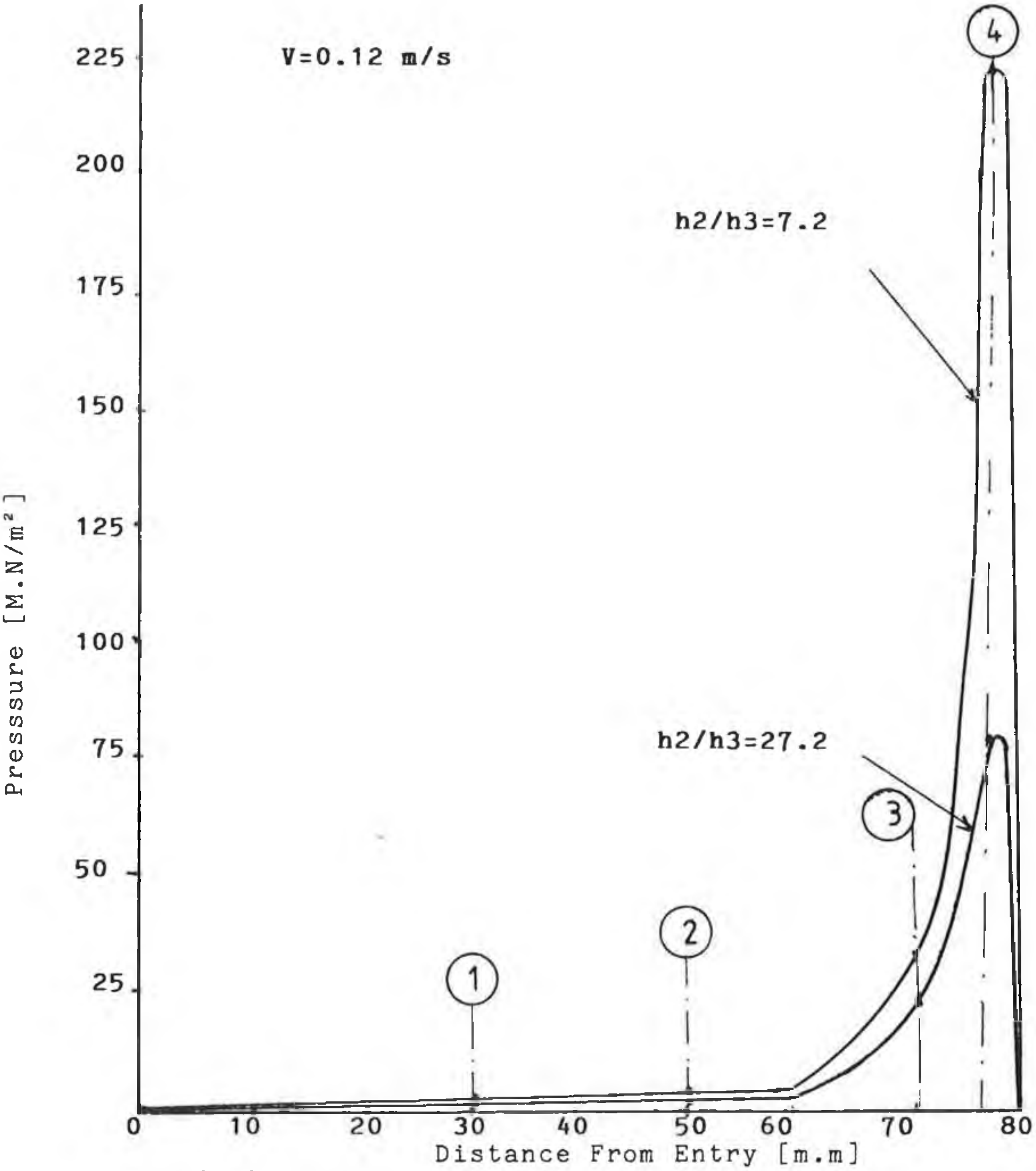

FIG(37) EFFECT OF GAP RATIO h2/h3 ON PRESSURE DISTRIBUTION FOR BRASS WIRE WITH LUPOLEN AT 170 °C

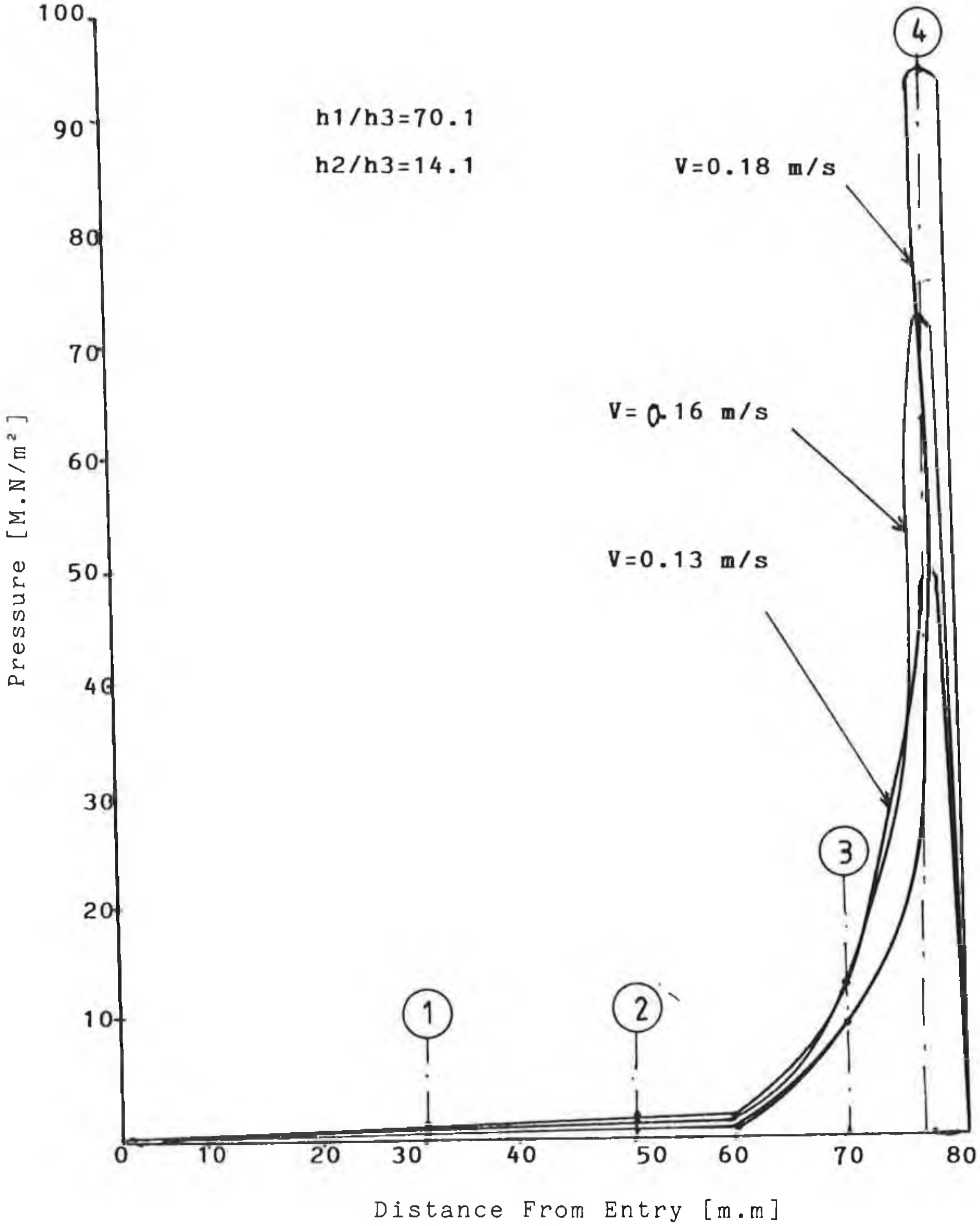

FIG (38) PRESSURE DISTRIBUTION FOR COPPER WIRE WITH POLYETHYLENE (ESCORENE) AT 125 °C

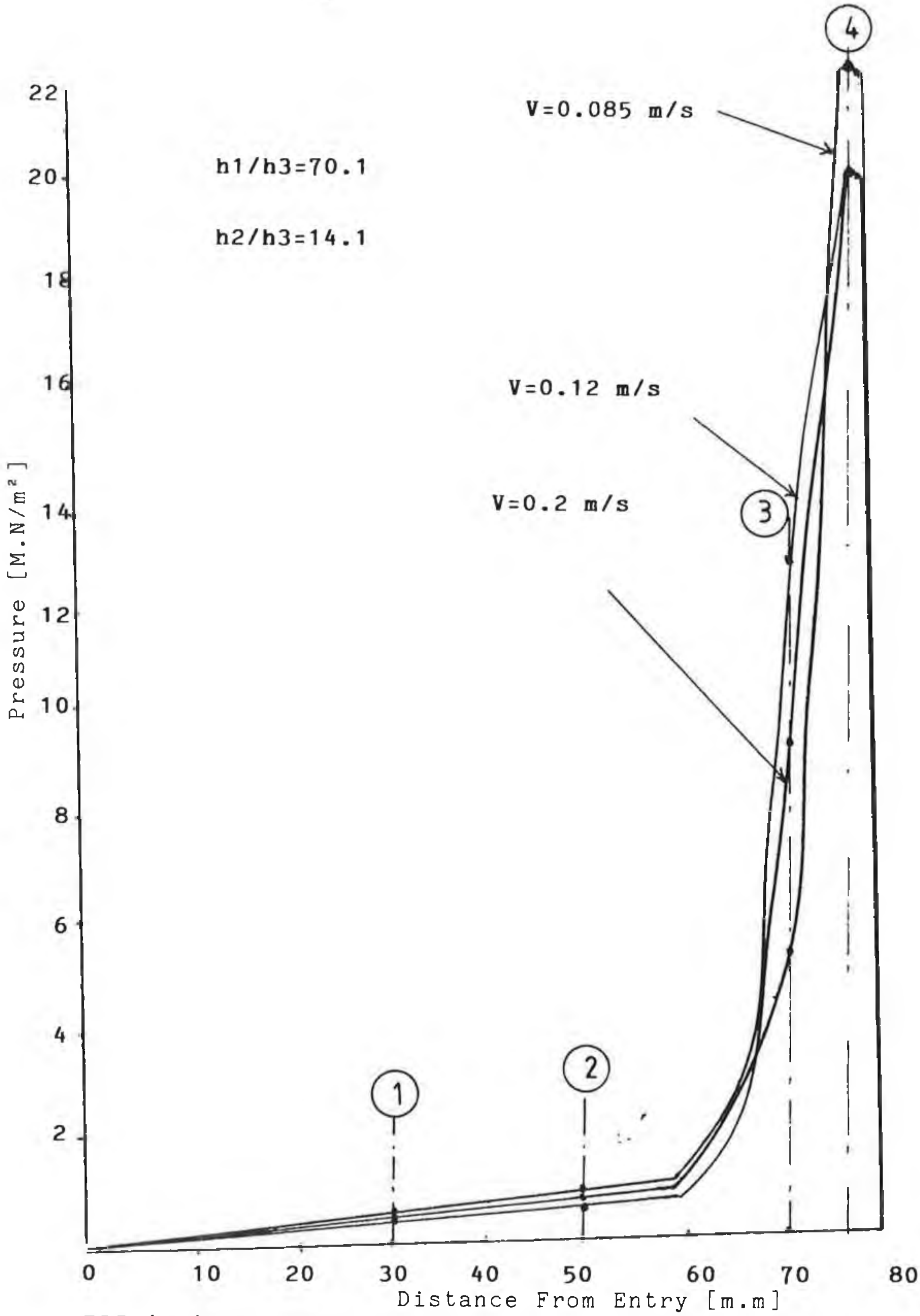

FIG (39) PRESSURE DISTRIBUTION FOR COPPER WIRE WITH POLYETHYLENE (ESCORENE) AT 150 °C

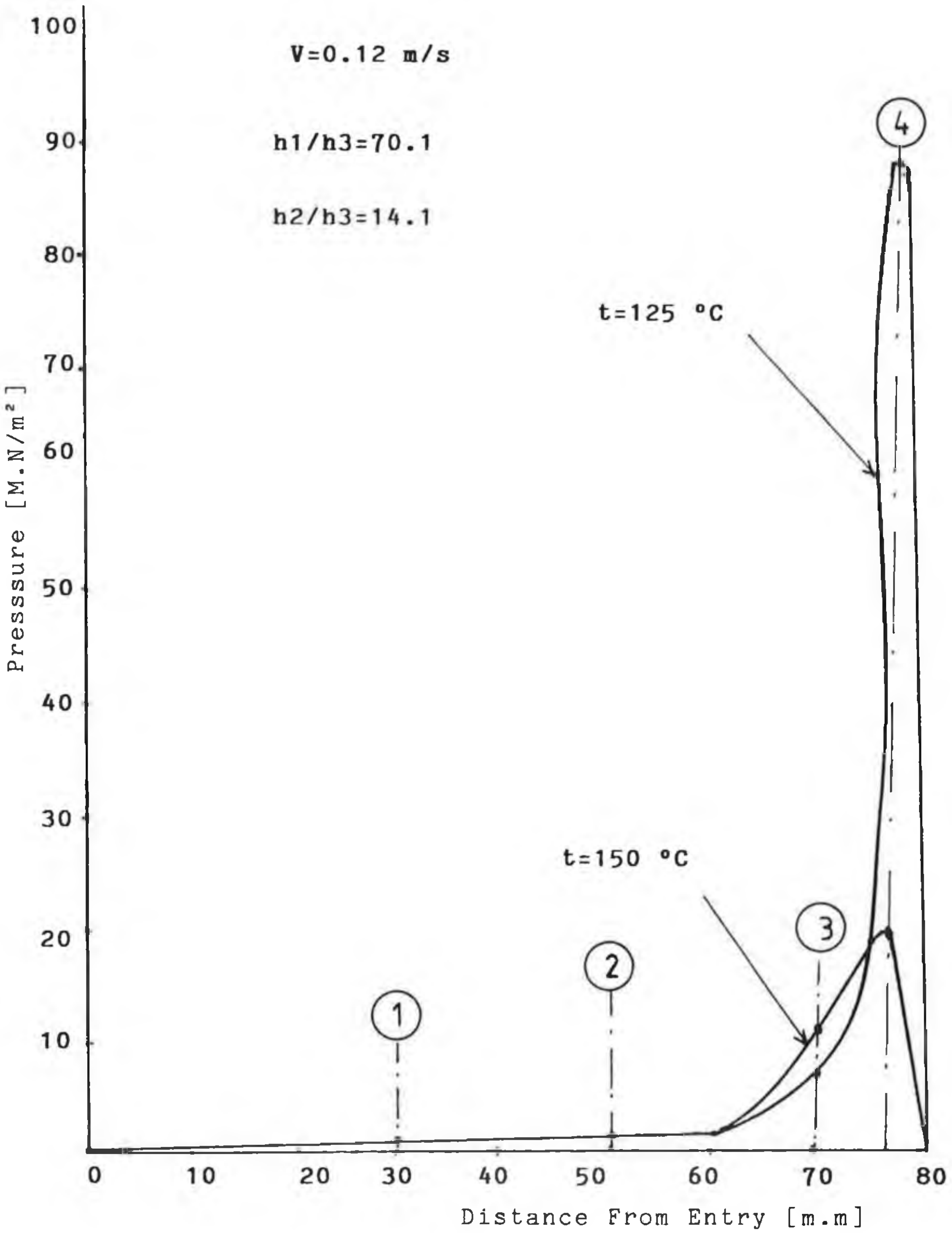

FIG (40) EFFECT OF TEMPERATURE ON PRESSSURE DISTRIBUTION FOR COPPER WIRE WITH POLYETHYLENE (ESCORENE)

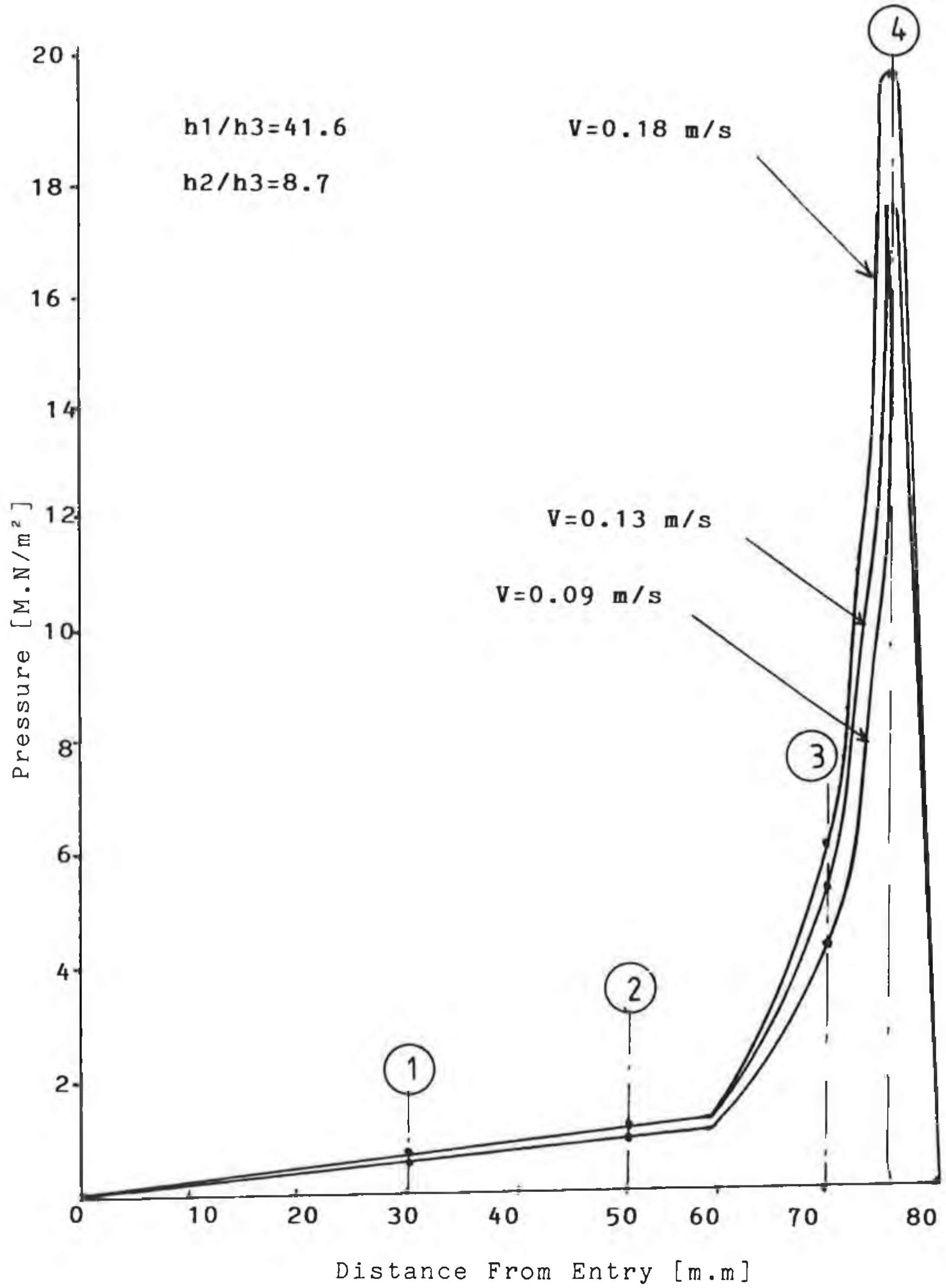

FIG (41) PRESSURE DISTRIBUTION FOR MILD STEEL WIRE WITH LUPOLEN AT 170 °C

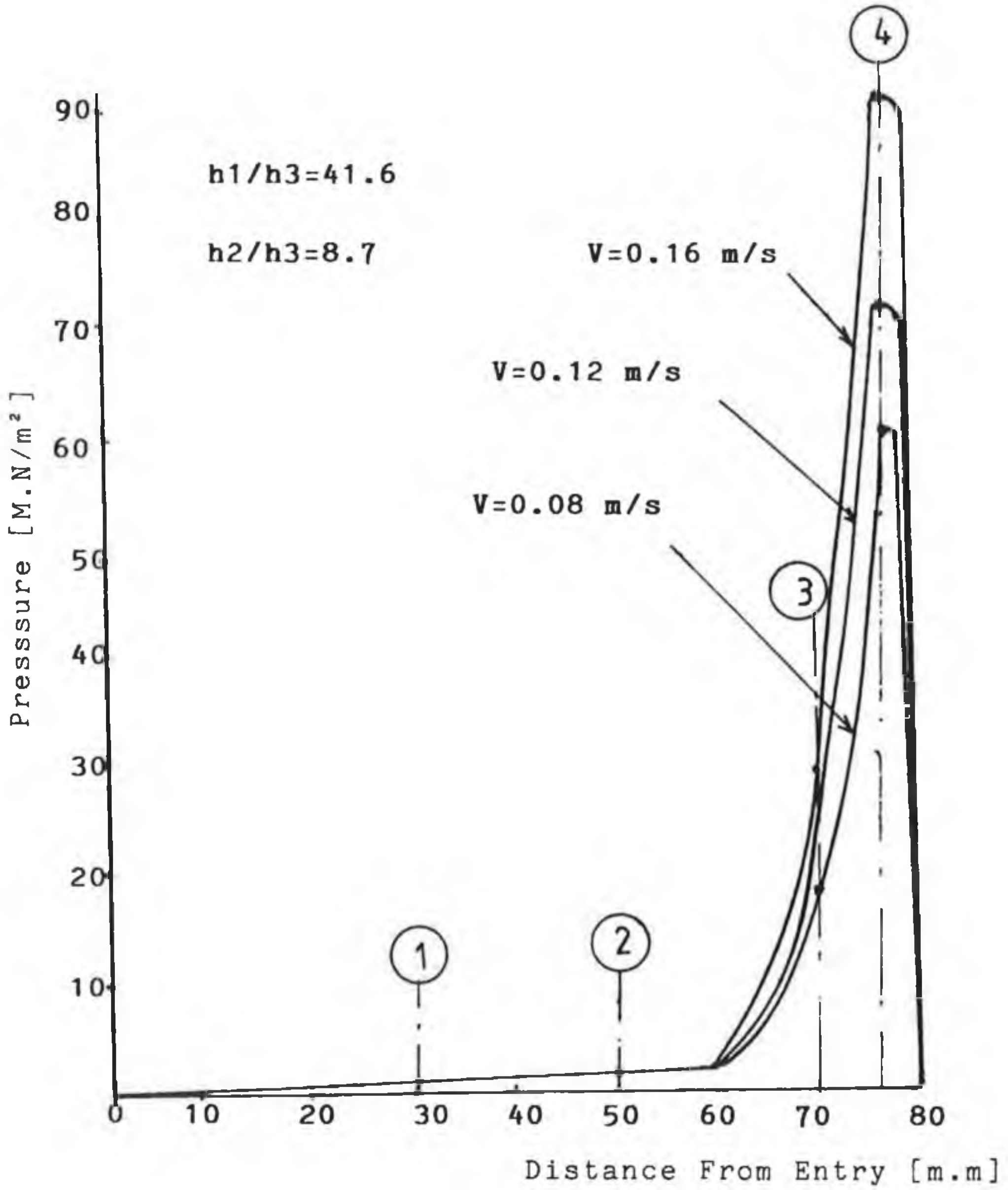

FIG (42) PRESSURE DISTRIBUTION FOR MILD STEEL WIRE WITH LUPOLEN AT 150 °C

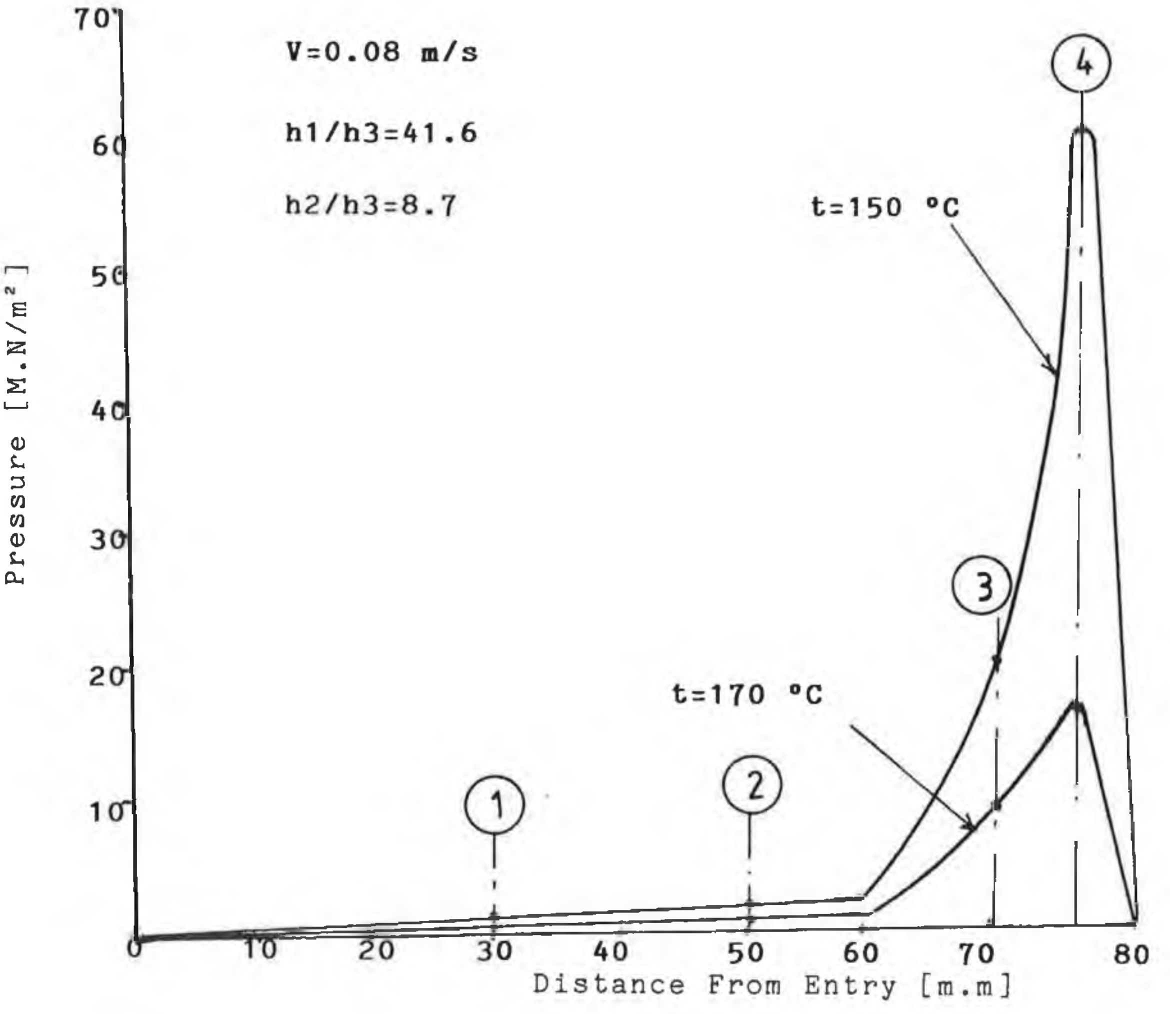

FIG (43)EFFECT OF TEMPERATURE ON PRESSURE DISTRIBUTION FOR MILD STEEL WIRE WITH LUPOLEN

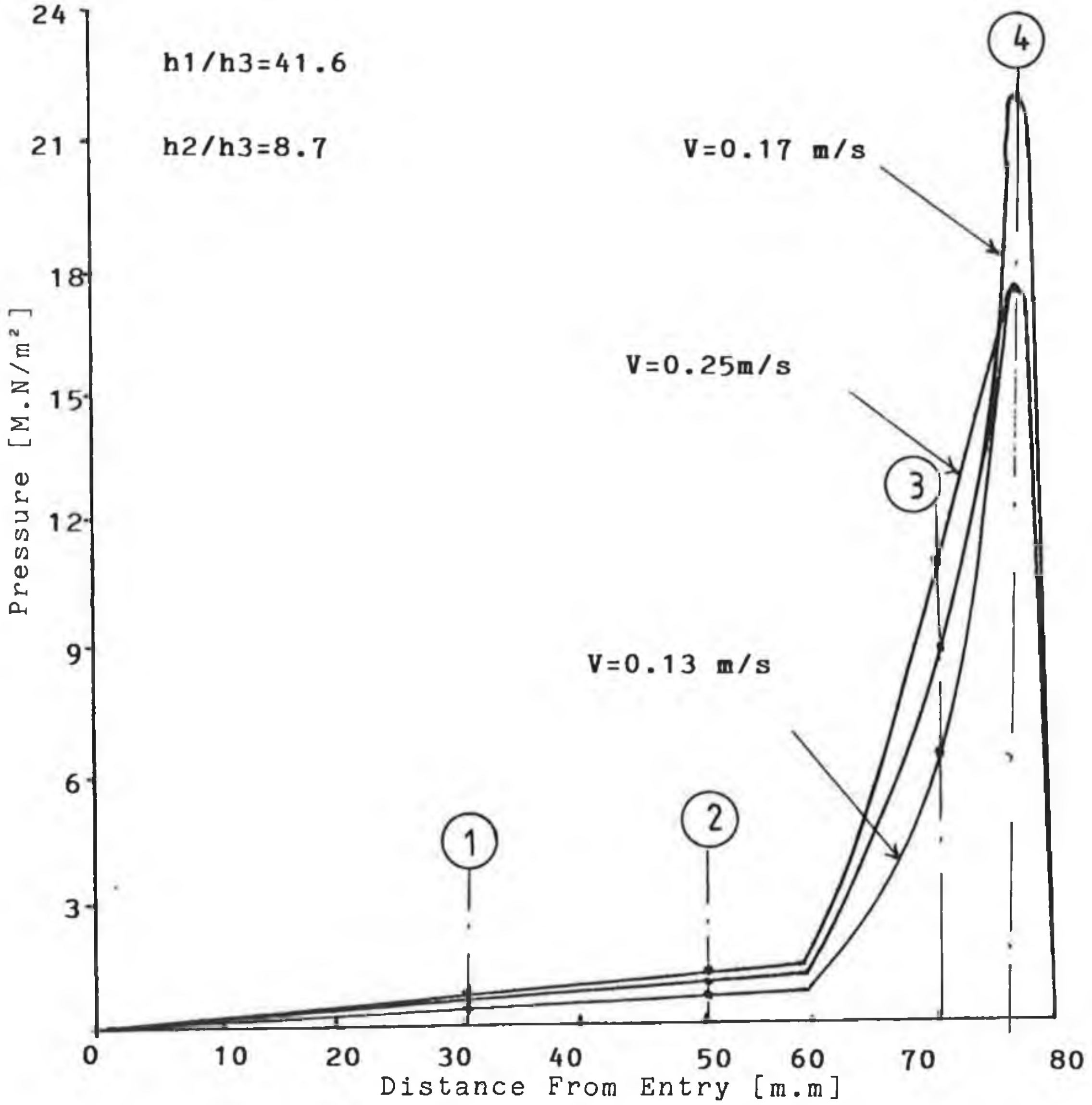

FIG (44) PRESSURE DISTRIBUTION FOR MILD STEEL WITH POLYETHYLENE (ESCORENE) AT 140 °C

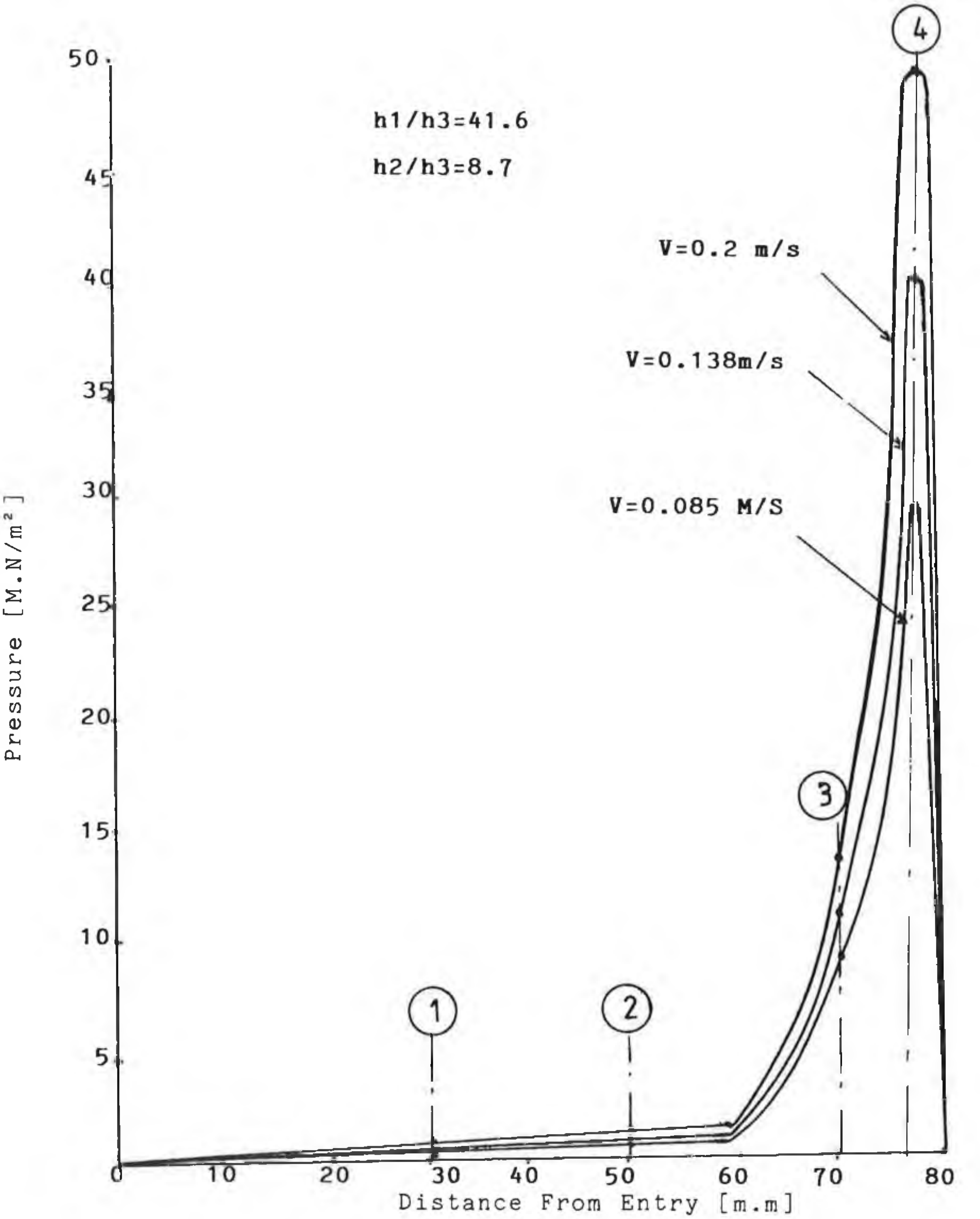

FIG (45) PRESSURE DISTRIBUTION FOR MILD STEEL WIRE WITH POLYETHYLENE (ESCORENE) AT 125 °C

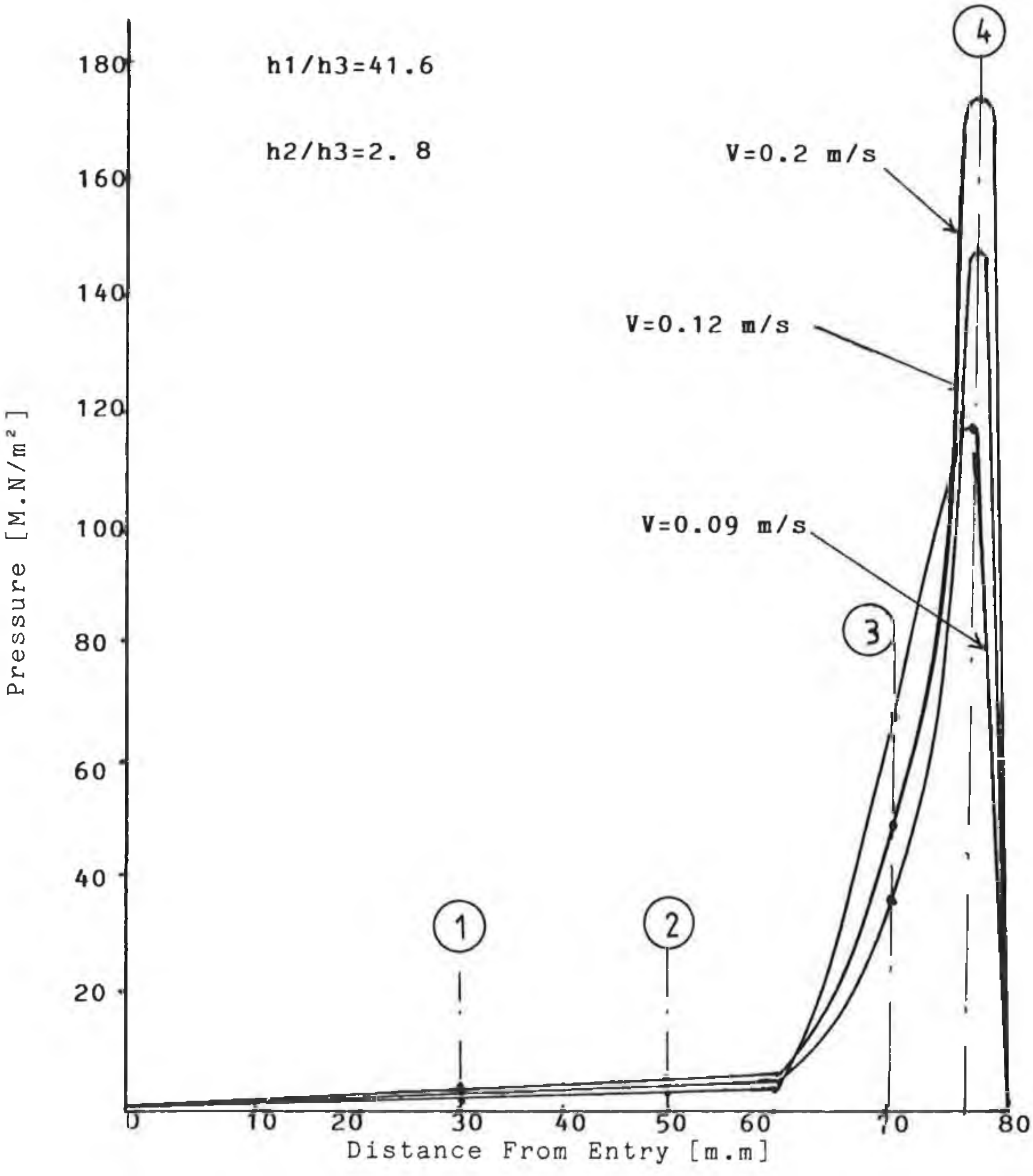

FIG (46) PRESSURE DISTRIBUTION FOR MILD STEEL WIRE WITH POLYETHYLENE (ESCORENE) AT 140 °C

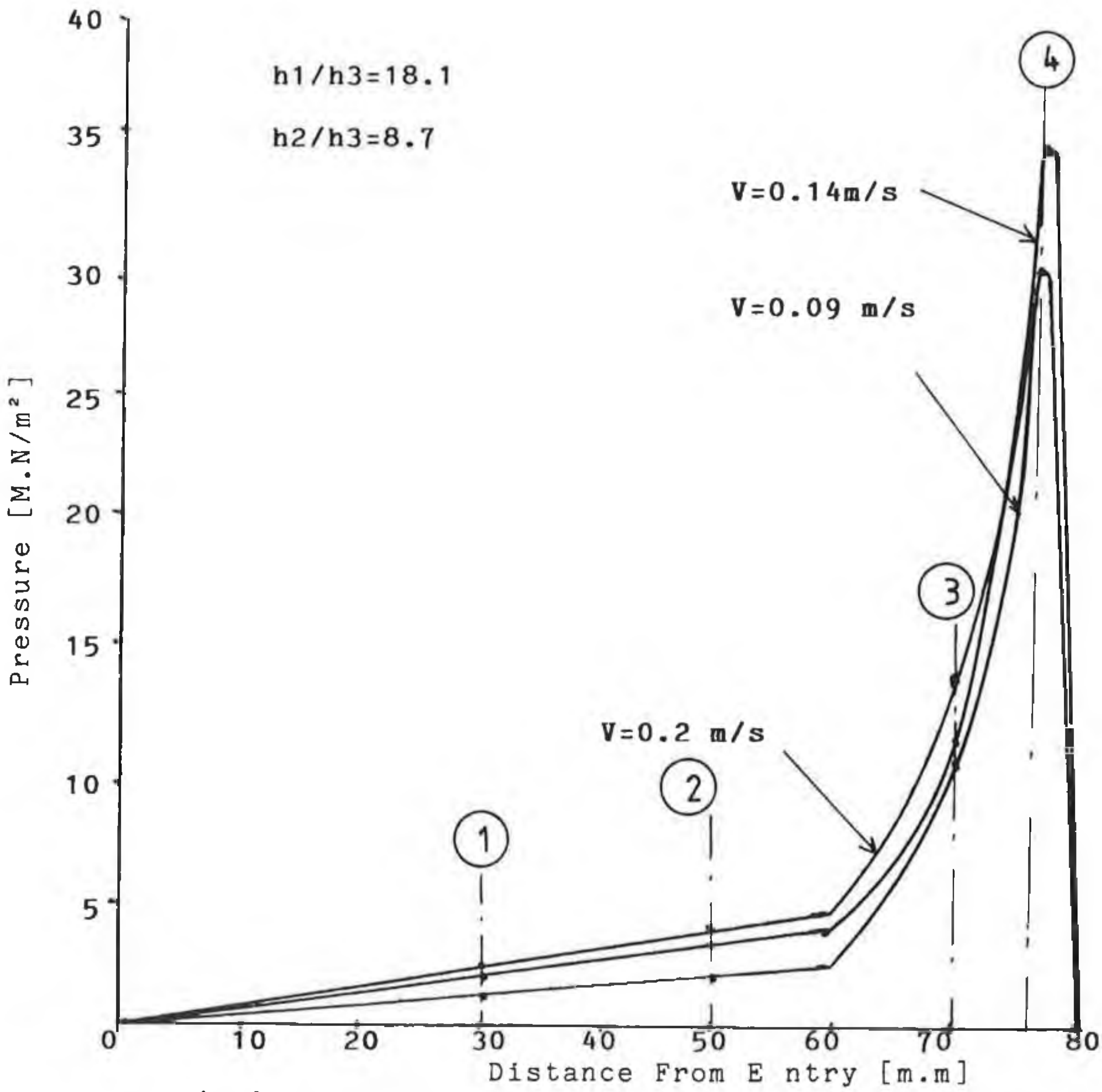

FIG (47) PRESSURE DISTRIBUTION FOR MILD STEEL WIRE WITH POLYETHYLENE (ESCORENE) AT 140 °C

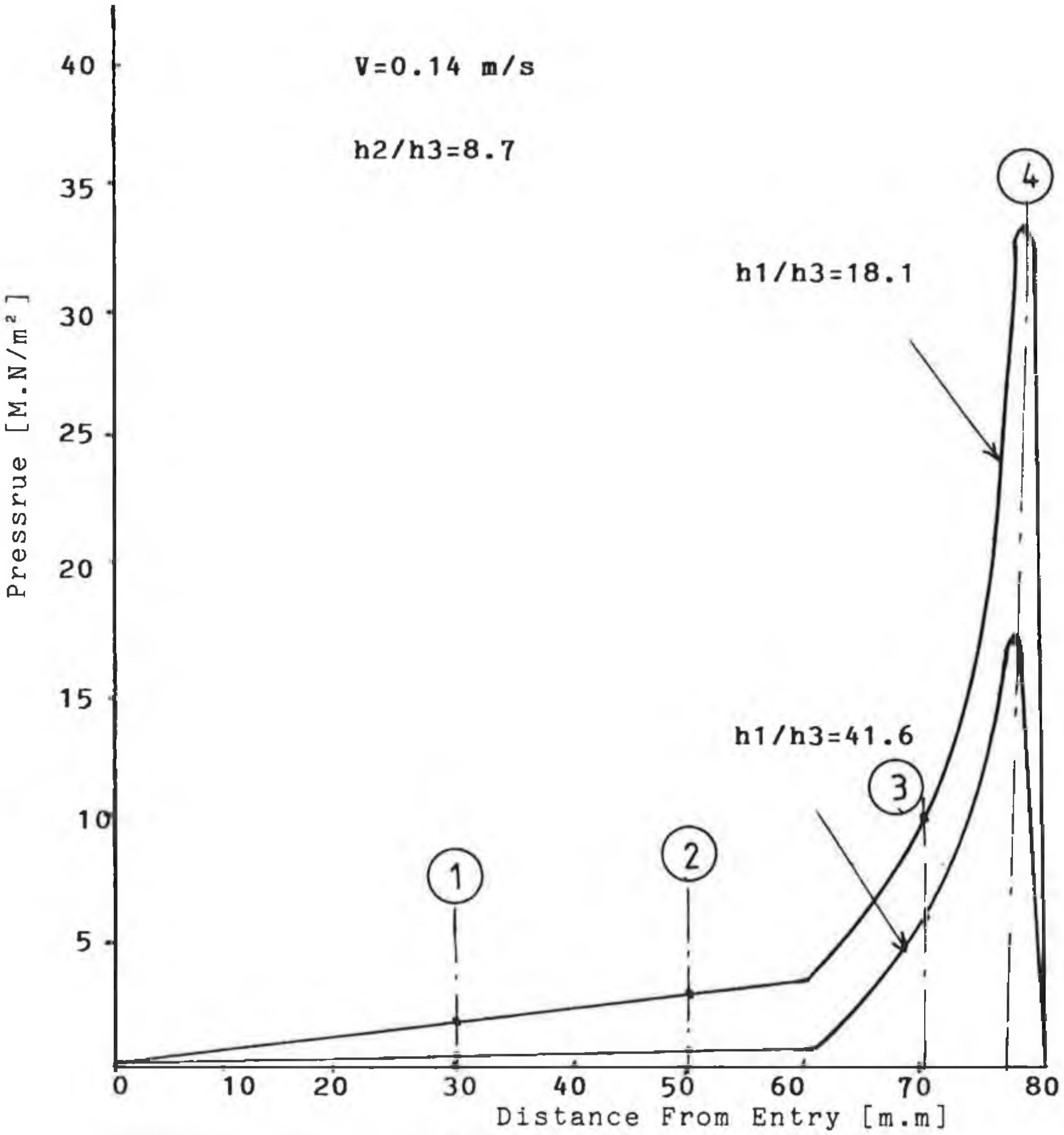

FIG(48) EFFECT OF GAP RATIO h1/h3 ON PRESSURE DISTRIBUTION FOR MILD STEEL WIRE WITH POLYETHYLENE (ESCORENE) AT 140 °C

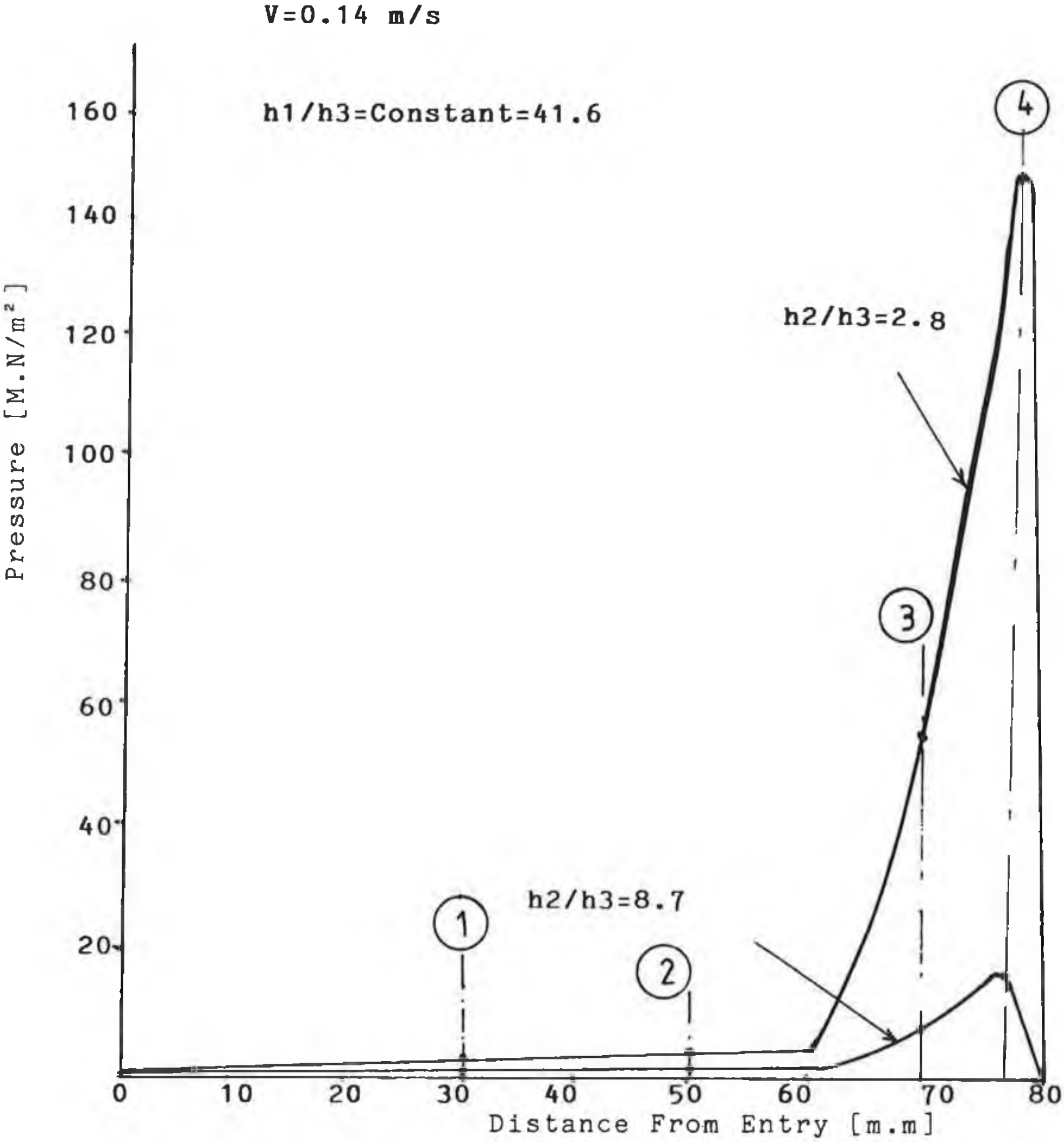

FIG (49)EFFECT OF GAP RATIO h2/h3 ON PRESSURE DISTRIBUTION FOR MILD STEEL WIRE WITH POLYETHELENE (ESCORENE) AT 140 °C

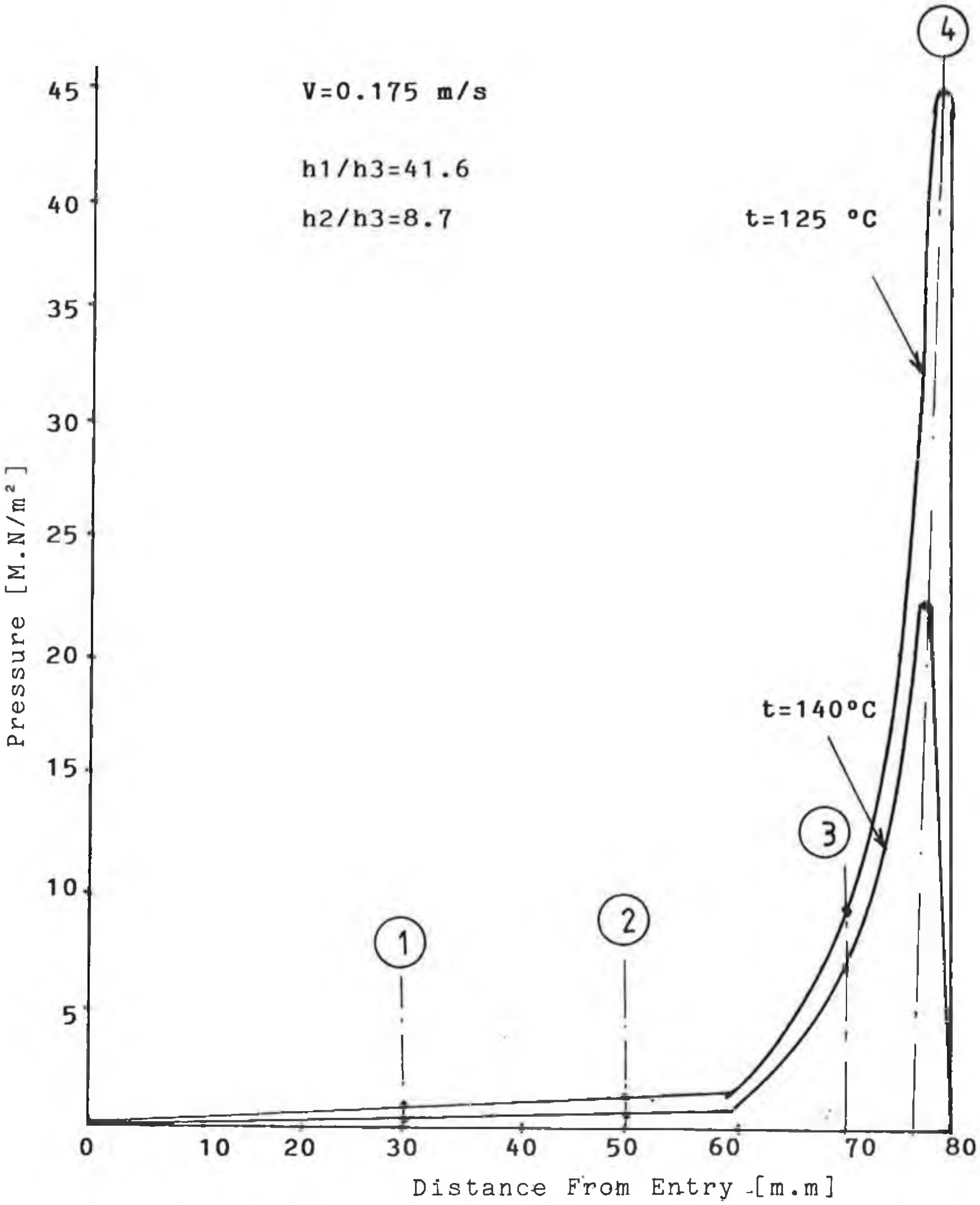

FIG(50) EFFECT OF TEMPERATURE ON PRESSURE DISTRIBUTION MILD STEEL WIRE WITH POLYETHYLENE(ESCORENE)

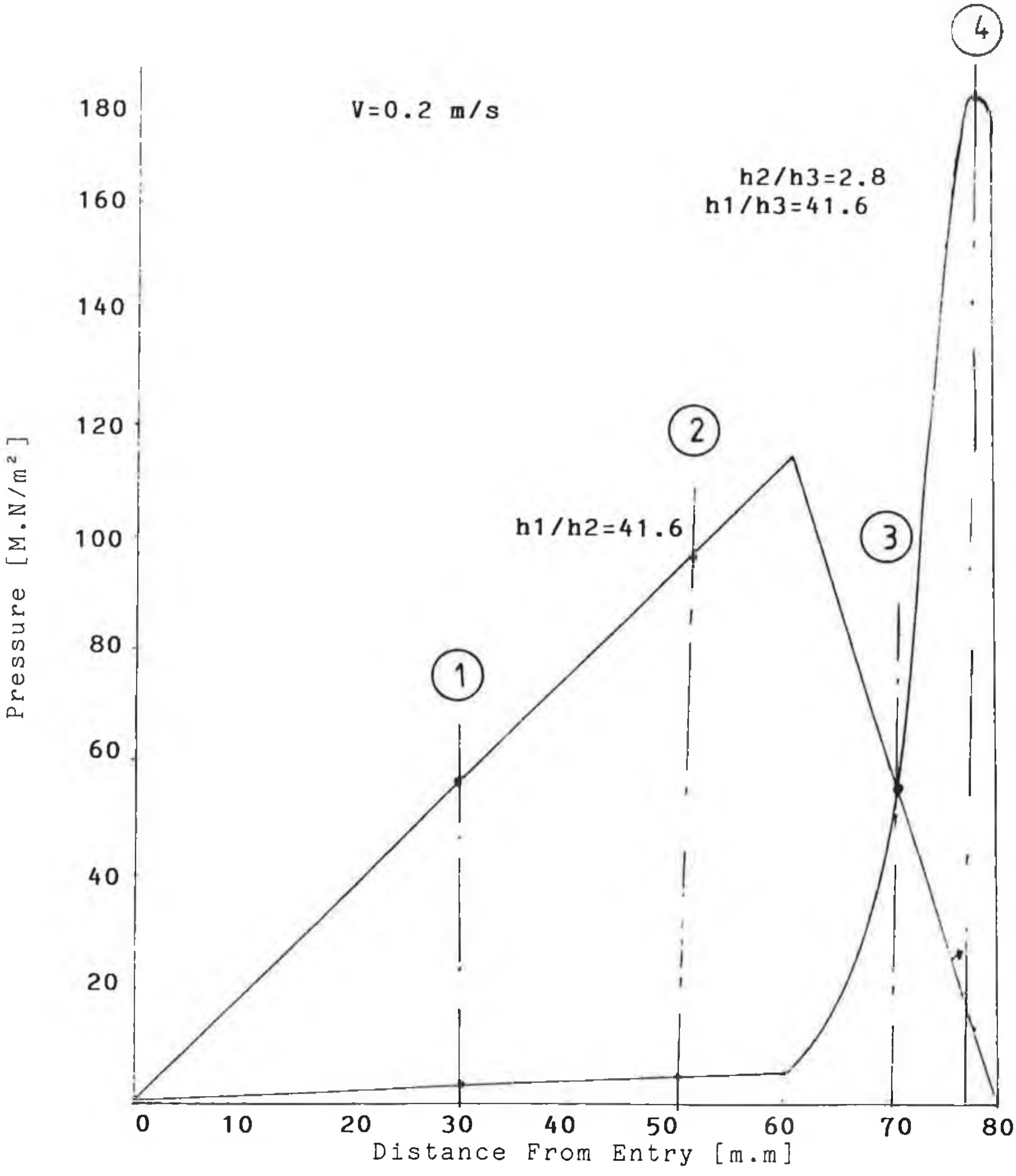

FIG(51) PRESSURE DISTRIBUTION FOR MILD STEEL WIRE WITH POLYETHYLENE(ESCORENE) AT 140 °C USING STEPPED UNIT AND COMBINE, STEPPED AND TAPERED PRESSURE UNIT

CHAPTER-5

THEORETICAL MODEL BASED ON NEWTONIAN FLUID CHARACTERISTICS

5.1 INTRODUCTION

In order to study and verify the mechanics of the process of hydrodynamic pressure development within the unit, it is important to develop a suitable mathematical model.

As a first step, such a model has been developed based on the assumption that the pressure medium demonstrates ideal Newtonian characteristics.

5.2 ANALYSIS

The geometrical configuration of the pressure unit and the wire during drawing are shown in Fig. 23. To formulate The analysis the following reasonable assumptions are made:

(i) The fluid has the characteristics of a Newtonian fluid,namely, the viscosity remains constant with shear rate and pressure.

(II) The flow of the fluid is purely axial and laminar

(III) the thickness of the fluid layer is small compared to the bore of the pressure unit.

(IV) The pressure in the fluid is uniform in the thickness direction at any point along the length of the pressure unit. (V) The flow of fluid is isothermal

(VII) The material of the wire is rigid.

The analysis of flow is carried out in plane flow rather than in cylindrical co-ordinates.

In the first part of the unit,the relationship between the pressure and shear stress gradient between the outer surface of the wire and the inner surface of the pressure unit is given by

$$(\partial P/\partial X)_1=(\partial u/\partial Y)_1 , \qquad (5.1)$$

The relationship between the shear stress and the rate of shear for the Newtonian fluid is given by

$$\tau_1=\mu(\partial u_1/\partial Y)_1 \qquad (5.2)$$

Where μ is the viscosity and u_1 is the fluid velocity at a distance Y from the surface of the wire. Integrating equation (5.1) with respect to Y and noting that $(\partial P/\partial X)$ is constant with Y, we have

$$\tau_1 = P'_1 Y + \tau_{c1} \,, \tag{5.3}$$

Where $P' = (\partial P/\partial X)$ and τ_{c1} is the shear stress on the wire surface at Y=0 Substituting for τ_1 from equation (5.3) into equation (5.2) we have

$$\mu(\partial u_1/\partial Y) = P'_1 Y + \tau_{c1} \,,$$

Which after integration becomes

$$\mu u_1 = \tfrac{1}{2} P'_1 Y^2 + \tau_{c1} Y + C_1 \,. \tag{5.4}$$

Applying the boundary condition that at Y=0 (at the surface of the wire) $u_1 = v_1$, we have

$C_1 = \mu v_1$

So that

$$u_1 = P'_1 Y^2/2\mu + \tau_{c1} Y/\mu + v_1 \,. \tag{5.5}$$

Applying the boundary condition that at $Y = h_1$ (at the surface of the unit) $u_1 = 0$ in equation(5.5) and rearranging we have

$$\tau_{c1} = -P'_1 h_1/2 - v_1 \mu/h_1 \,. \tag{5.6}$$

The flow of the pressure medium in the first part of the unit Q_1, is given by

$$Q_1 = \int_0^{h_1} u_1 dY,$$

Which upon substituting for u_1 from equation (5.5) we get

$$Q_1 = \int_0^{h_1} (P'Y^2/2\mu + \tau_{c_1} Y/\mu + v_1)dY.$$

The above, after integrating becomes

$$Q_1 = P'_1 h^3{}_1/6\mu + v_1 h_1 + \tau_{c_1} h^2{}_1/2\mu .$$

Substituting for τ_{c_1} from equation (5.6) into the above equation we get

$$Q_1 = -h^3{}_1/12\mu(\partial P/\partial X)_1 + v_1 h_1/2, \qquad (5.7)$$

The continuity of fluid flow gives

$$(\partial Q/\partial X) + (\partial Q/\partial Y) + (\partial Q/\partial Z) = 0,$$

but $\partial Q/\partial Y = \partial Q/\partial Z = 0$, and

hence $\partial Q/\partial X = 0$

Therefore, for given h1,h2, and v_1

$\partial P/\partial X$ in equation (5.7) must be constant.

Therefore $\partial P/\partial X = P'_1 = Pms/L_1 = \text{Constant}$

Pms is the pressure at the step and L_1 is the length of the first part of the unit. It is shown that the pressure profile in the first part of the pressure unit is linear.

The pressure at any point $X_1<L_1$ is given by

$$P= \int_0^{X_1} P'_1 \, dx = Pms/L_1 \; X_1 . \tag{5.8}$$

The axial stress on the wire at any point distance X_1 from the entry can be obtained by considering the shear force action on the surface of the wire

Thus,

$\sigma x_1 = \tau c1 X_1/D$.

Substituting τc_1 from equation (5.6), we get ,

$$\sigma x_1 = (-X_1/D)(Pms.h_1/2L_1 + v_1 \mu/h_1). \tag{5.9}$$

From the geometrical configuration as shown in Fig. 23 the gap between the second part of the unit and the surface of the wire is given by

$$h=h_2-BX_2 , \tag{5.10}$$

where $B=(h_2-h_3)/L_2$.

For the Newtonian fluid the pressure gradient is given by

$$(\partial P/\partial X)_2=(\partial \tau/\partial Y)_2 , \tag{5.11}$$

and the shear stress is expressed by

$$\tau_2=\mu(\partial u_2/\partial Y) , \tag{5.12}$$

Where u_2 is the velocity in the second part of the unit.

Differentiating equation (5.12) with respect to Y we obtain

$$(\partial \tau/\partial Y) =\mu(\partial^2 u_2/\partial Y^2).$$

Substituting the above in equation (5.11) we obtain:

$$\partial^2 u_2/\partial Y^2=(1/\mu)(\partial P/\partial X), \tag{5.13}$$

Integrating and noting that $\partial P/\partial X$ is assumed to be constant with Y we get

$$(\partial u_2/\partial Y)=(1/\mu)(\partial P/\partial X)Y + C_2 . \tag{5.14}$$

Integrating again,

$$u_2=(1/2\mu)(\partial P/\partial X)Y^2+ C_2Y + C_3 , \tag{5.15}$$

where C_2 and C_3 are constants.

Using the boundary condition that $u_2=0$ at $Y=h$ (at the surface of the unit),

and $u_2=v_2$ at $Y=0$ (at the surface of the wire) we obtain

$C_2=(-1/2\mu)(\partial P/\partial X)h - v_2/h$ and
$C_3= v_2$
So that:

$$u_2=1/2\mu(\partial P/\partial X)(Y^2- hY) +v_2(1-Y/h) \qquad (5.16)$$

The flow of the fluid in axial direction is given by

$$Q_x = \int_0^h u_2 \, dY ,$$

which upon substituting for u_2 from equation (5.16) and integrating becomes

$$Q_x=(-h^3/12\mu)(\partial P/\partial X) + v_2 \, h/2 \, . \qquad (6.17)$$

The continuity of the polymer melt flow shows that

$$\partial Qx/\partial X + \partial Qy/\partial Y + \partial Qz/\partial Z = 0$$

but $\partial Qy/\partial Y=\partial Qz/\partial Z=0$

hence $\partial Qx/\partial X=0$.

Differentiating equation (5.17) with respect to X and equating to zero and then integrating we obtain :

$$h^3/6\mu(\partial P/\partial X)=v_2h + C_4 .$$

Using the boundary condition that maximum pressure $(\partial P/\partial X=0)$ occurs at a point where $h=\bar{h}$ We have $C_4=-v_2\ \bar{h}$ So that

$$(\partial P/\partial X)=6\mu v_2(1/h^2-\bar{h}/h^3), \qquad (5.18)$$

which upon substitution for h from equation (5.10) gives

$$(\partial P/\partial X)_2=6\mu v_2/(h_2-BX_2)^2- 6\mu v_2\bar{h}/(h_2-BX_2)^3.$$

Integrating the above equation we have

$$P=(6\mu v_2/B)[1/(h_2-BX_2)-\bar{h}/2(h_2-BX_2)^2]+C_5 , \qquad (5.19)$$

but $P=0$ at $X_2=L_2$ where $(h_2-BX_2)=h_3$ and hence $C_5 = (-6\mu v_3/B)[1/h_3 - \bar{h}/2h^2_3]$.

Substituting for C5 in equation (5.19) we get

$$P=(6\mu v_2/B)[1/h_2-BX_2 - \bar{h}/2(h_2-Bx_2)^2 -$$

$$(6\mu v_2/B)[1/h_3-\bar{h}/2h^2_3\ ]. \qquad (5.20)$$

Applying the boundary condition that at $X_2=0$ $(h=h_2)$, $P=Pms$, we have

$$Pms=6\mu v_2/B[1/h_2-\bar{h}/2h^2_2]-6\mu v_2/B[1/h_3-\bar{h}/2h^2_3] \qquad (5.21)$$

For continuity of the flow we have $Qx_1=Qx_2$ and hence from equation (5.17) we obtain,

$$-h^3_1/12\mu(\partial P/\partial X)_1+v_1h_1/2 =-h^3/12\mu(\partial P/\partial X)_2+v_2h/2\ ;$$

but $v_1=v_2=v$ and $(\partial P/\partial X)=Pms/L_1=P'_1$ and herefore,

$$(\partial P/\partial X)_2=h^3_1/h^3(Pms/L_1)-6\mu v(h_1/h^3-1/h^2\ ). \qquad (5.22)$$

We have the boundary condition that the maximum pressure occurs at a point where $h=\bar{h}$ $(\partial P/\partial X=0)$ which after substituting in equation (5.22) becomes

$$\bar{h} = h_1 - h^3{}_1 \, Pms/(6\mu v L_1) \qquad (5.23)$$

After solving equations (5.23) and (5.21) we obtain:

$$Pms = \{(6\mu v h_1/2B)[1/h^2{}_3 - 1/h^2{}_2] + (6\mu v/B)[1/h_2 - 1/h_3]\} / [1 + (h^3 1/2B\ L1)(1/h^2{}_3 - 1/h^2{}_2)]. \qquad (5.24)$$

The maximum pressure occurs where $h=\bar{h}$ and $h=h_2-BX_2$ which after substituting in equation (5.19) gives

$$Pmax = (6\mu v/B)[1/2\bar{h} - 1/h_3 + \bar{h}/2h^2{}_3]. \qquad (5.25)$$

The expression for the shear stress may be obtained by differentiating equation (5.16) with respect to Y , Thus

$$(\partial u/\partial Y) = (1/2\mu)(\partial P/\partial X)(2Y-h) - \mu v/h \qquad (5.26)$$

shear stress $\tau_2 = \mu(\partial u/\partial Y)$, so that the at any depth in the polymer melt in the second part of the unit,

$$\tau_2 = (\partial P/\partial X)(2Y-h) - \mu v/h, \qquad (5.27)$$

At the surface of the wire , Y=0 and

ence,
$$\tau_{x_2}=(-h/2)(\partial P/\partial X)-\mu v/h$$

which after substituting for $(\partial P/\partial X)_2$ from equation (5.18) and for h from equation (5.10) becomes

$$\tau_2=\mu v[3\bar{h}/(h_2-BX_2)^2-4/(h_2-BX_2)] \tag{5.28}$$

The drag force on the wire inside the unit is given by

$$Fd=-\int_0^{X_2}\pi D\tau_x\, dx$$

Substituting for τ_2 from equation (5.28)

$$=-\int_0^{X_2}\pi D\mu v[\ 3\bar{h}/(h2-BX_2)^2-4/(h_2-BX_2)]dx$$

$$=-D\pi\mu v[\ \int_0^{X_2}3\bar{h}/(h_2-BX_2)^2dx-\int_0^{X_2}4\ dx/h_2-BX_2\ ]$$

$$=\pi D\mu v[3\bar{h}/B(h_2-BX_2) + 4/B\, \ell n(h_2-BX_2)]_0^{X_2}$$

$$=(-\pi D\mu v/B)[3\bar{h}\{1/(h_2-BX_2)-1/h_2\}+4\ell n\{h_2-BX_2)/h_2\}] \qquad (5.29)$$

The axial stress on the wire at any point distance X_2 from the second part of the unit can be obtained by

$$\sigma x_2=Fd/A=4Fd/\pi D^2,$$

$$\sigma x_2=(-4\mu v/DB)[3\bar{h}\{1/h_2-BX_2-1/h_2\}+4\ell n\{(h_2-BX_2)/h_2\}]$$

5.3 <u>SOLUTION PROCEDURE</u>

Pms can be calculated by substituting the values of V,μ,h_1, h_2, h_3, B and L1 into equation (5.24), $\tau c1$ can be calculated by substituting the values of P', V, h_1 and h_2 into equation (5.6). At any point distance X_1 from the entry, σx_1 can be calculated from equation (5.9) by substituting for Pms, D, L_1, V and h_1. Pressure distribution at any point in the first part of the unit can be calculated from equation (5.8) by substituting for Pms and L_1. $\bar{h}$ can be calculated from equation (5.23) by substituting for h1, μ , V,

L_1, and Pms. The maximum pressure can be calculated from equation (5.25) by substituting for v, B, h3. The pressure distribution in the second part of the unit can be calculated by substituting the values of μ , V, B, h_2, h_3 and $\bar{h}$ into equation (5.20). the magnitude of τx_2 at any point in the second part of the unit can be calculated from equation (5.28) by substituting for μ, V, h_2, h and B. The drag force in the second part of the unit at any point can be calculated from equation (5.29). Finally σx_2 at any point can be calculated from equation (5.30) by substituting for μ , V, D, $\bar{h}$, h_2 and B.

5.4 THEORETICAL RESULTS

Theoretical results were obtained using the equations derived in the theoretical analysis section. The following are the magnitudes of the known parameters which were used to solve the equations and were varied to show their effect on the pressure distribution in the unit.

Dimensions of the pressure unit:

Total length, 95 mm

Position of step from inlet, L_1=60 mm

Position of step from outlet, L_2=20 mm

Inlet gap, h_1=1 mm

Middle gap, h_2=0.5 mm

Outlet gap, h_3=0.05 mm

Viscosity= 100 N.s/m^2

Data for wires:

Diameter, D=2 mm

5.4.1 THEORETICAL RESULTS OF MAXIMUM PRESSURE

Fig 52 to 54 show the effect of h_1, h_2 and h_3 respectively on maximum pressure These figures indicate that for smaller values of h_1, h_2 and h_3 the maximum pressure is increased for a given drawing speed. In addition, these figures show that changes in the values of h_3 have comparatively greater effect than those of h_1 and h_2 on the maximum pressure. The effect of the lengths L_1 and L_2 of the unit on the maximum pressure are illustrated in Fig. 55 and Fig. 56 respectively. Fig. 55 suggests that the increase in the first length, L_1,of the unit does not significantly affect the maximum pressure, but Fig. 56 shows that for higher values of L_2 the maximum pressure should increase at all drawing speeds. The effect of viscosity on maximum pressure is demonstrated in Fig. 57 which indicates that the maximum pressure is increased when the viscosity of polymer is increased for a given drawing speeds.

5.4.2 THE THEORETICAL PRESSURE DISTRIBUTION

Figures 58 and 59 show the theoretical pressure distribution for two different gap ratios. Figure 58 shows the pressure distribution for gap ratio of $h_2/h_3=10$ at three different drawing speeds. This figure suggests that the pressure increases from zero at the entry of the unit to maximum value just before the end of the unit as the drawing speed is increased. Figure 59 shows the results for the gap ratio of $h_2/h_3=14$ which shows a similar trend to that in Fig. 58. Figure 60 shows the effect of gap ratio on pressure distribution for three different gap ratios, h_2/h_3, at the drawing speed of 0.1 m/s. This figure suggests that the maximum pressure increases as the gap ratio is decreased. Also this figure shows that this changing of the gap ratio, h_2/h_3, does not affect on the pressure distribution in the first part of the unit.

Figure 61 shows the predicted pressure distribution for different gap ratios, h_2/h_3 at a drawing speed of 0.1 m/s. This figure suggests that there exists a gap ratio $h_2/h_3=2$ (optimum) for which the pressure is maximum, everything else being the same. This maximum pressure occurs towards the exit end of the tapered part of the pressure unit. For greater or smaller values of the gap ratio than the optimum value, a decreased magnitude for the maximum pressure is predicted. For a gap ratio of unity(stepped bore) the maximum pressure occurs at the step.

The effect of length ratio on pressure

distribution is illustrated in Figures 62 and 63. Figure 62 shows the pressure distribution for two different length ratios at the drawing speed of 0.1 m/s where L2 is constant. This figure suggests that the change of the length ratio at the same velocity does not affect on the pressure distribution where the maximum value of the pressure is approximately the same at $L_1/L_2=3$ and 3.25. Figure 63 shows the pressure distribution for two different length ratios for constant L_1. This figure suggests that the maximum pressure increases as the length ratio is decreased for a given drawing speed.

The effect of viscosity of the fluid on pressure distribution is shown in Fig. 64 .This figure shows the pressure distribution for three different viscosity at the drawing speed of 0.1 m/sec and suggests that the pressure is increased with increasing of the viscosity of the fluid and the pressure reaches maximum value just before the end of the unit.

5.4.3 COMPARATIVE PERFORMANCE OF THE PRESENT UNIT WITH STEPPED BORE UNIT

Figure 65 shows the pressure distribution for the present unit (solid line) and the pressure distribution for stepped and parallel bore unit (dotted lines). This figure suggests that the maximum pressure for the present unit is greater by about three times than for the stepped bore unit at drawing speed of 0.1 m/s. This higher pressure generation should be very useful for drawing and/ or coating processes which use the hydrodynamic phenomenon.

5.4.4 THEORETICAL RESULTS BASED ON PSEUDO-NEWTONIAN SOLUTION

From the experimental results reported in reference (39) for similar type of polymers (low density polyethylene) the following relationship can be deduced:

$$\mu_a=(A + B\ Pe^2)/\dot{\gamma} \qquad (5.31)$$

here A and B are constants, Pe is the excess pressure (over atmospheric)and $\dot{\gamma}$ is the shear rate. For $A=1.7.10^6$ N/m^2, $B=5.66.10^{-10}$ m^2/N. This expression for the apparent viscosity gives very good representation for shear rates ranging from 200 to 1000 per second and for excess pressures of up to 150 MN/m^2. In order to determine the appropriate apparent viscosity corresponding to a given velocity, the maximum increase in pressure is estimated first using the maximum pressure from experiments. The excess pressure is then taken to be half this maximum and substituted in equation (5.31) to give the mean apparent viscosity.

Figs 66 and 67 show the experimental results of the effect of shear rate on viscosity for Polyethylene(Escorene) and (Lupolen) at same gap ratio of $h_2/h_3=8.7$ and at different melt temperatures.

Figures 68 and 69 show the pressure distribution with Lupolen polymer at 170 °C and Escorene at 140 °C respectively. These figures suggest that the maximum pressure decreases as the drawing speed is increased and at lower drawing speed the maximum pressure becomes greater.

Figure 70 shows the pressure distribution with Escorene at melt temperature of 140 °C and at gap ratio of $h_2/h_3=2.8$. This figure suggests that the maximum pressures decrease as the drawing speed is increased. However, the increasing of drawing speed does not affect the pressure distribution in the first part of the pressure unit.(However, see Figs. 58 and 59 for a Netonian fluid)

Figure 71 shows the pressure distribution for a gap ratio of $h_2/h_3=8.7$ and $h1/h3=41.6$ with Escorene polymer at melt temperature of 125 °C. This figure shows very little difference in the maximum pressure at speeds of 0.2 m/s and 0.25 m/s .However the maximum pressure increased slightly at a drawing speed of 0.1 m/s.

Figure 72 shows the pressure distribution for different gap ratios , h_2/h_3 at a drawing speed of 0.1 m/s and a melt temperature of 140 °C for Escorene polymer. This figure shows that there is a gap ratio of 2.8 (optimum) for which the maximum pressure is the greatest, everything else being the same. For greater or smaller values of the gap ratio than the optimum value, a decreased magnitude for the maximum pressure is predicted.

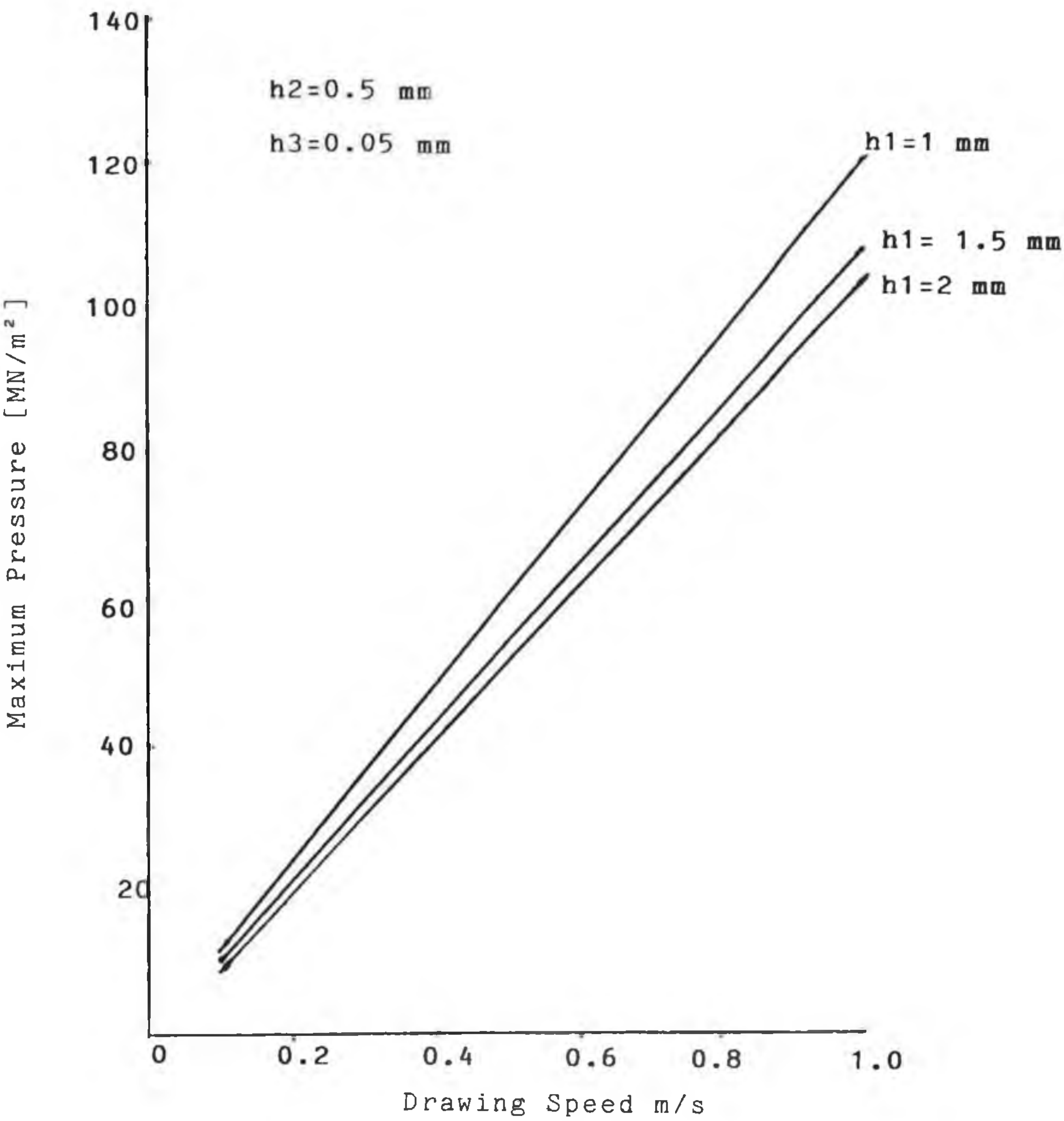

FIG (52) THEORETICAL EFFECT OF h1 ON MAXIMUM PRESSURE

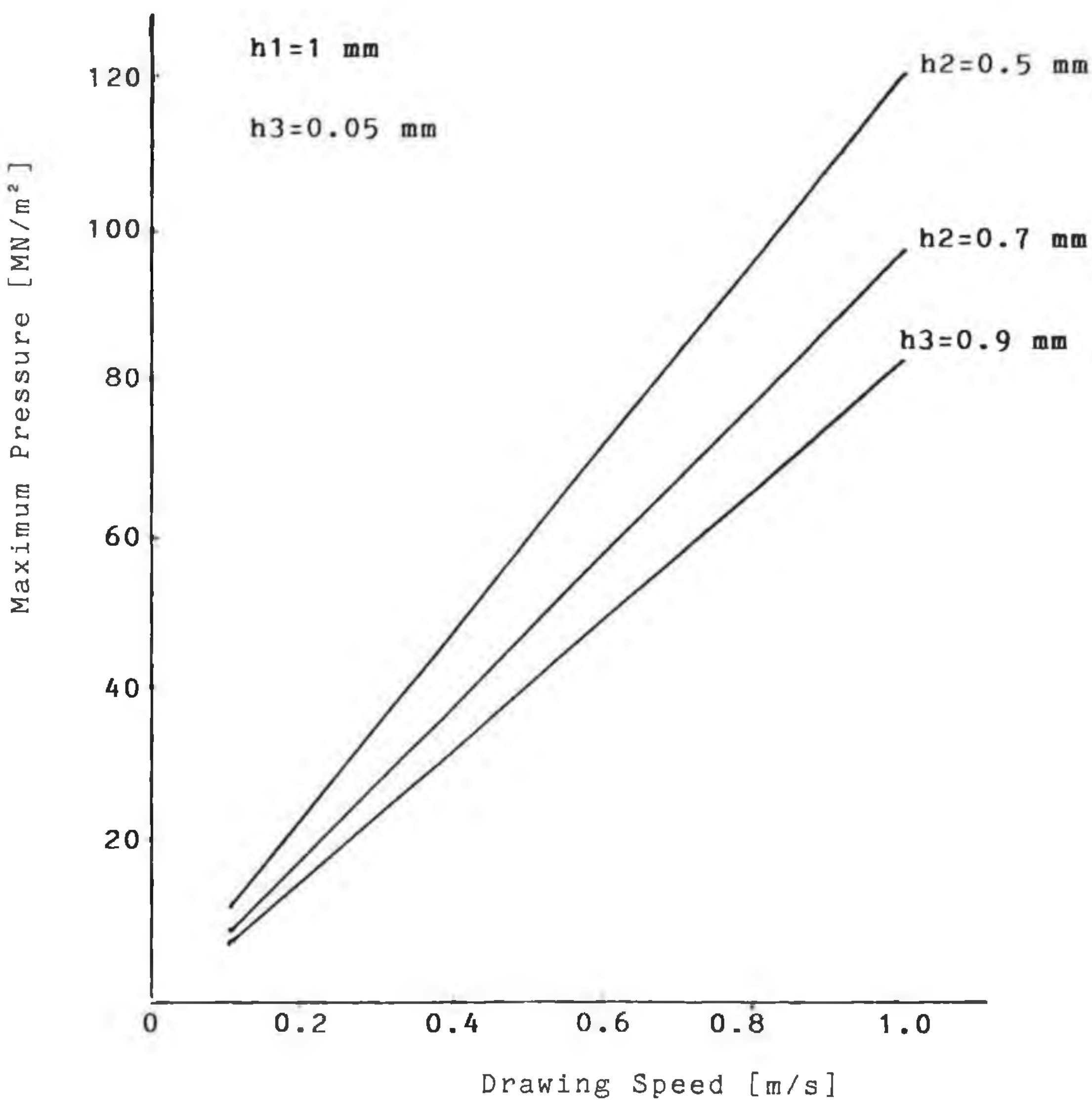

FIG (53) THEORETICAL EFFECT OF h2 ON MAXIMUM PRESSURE

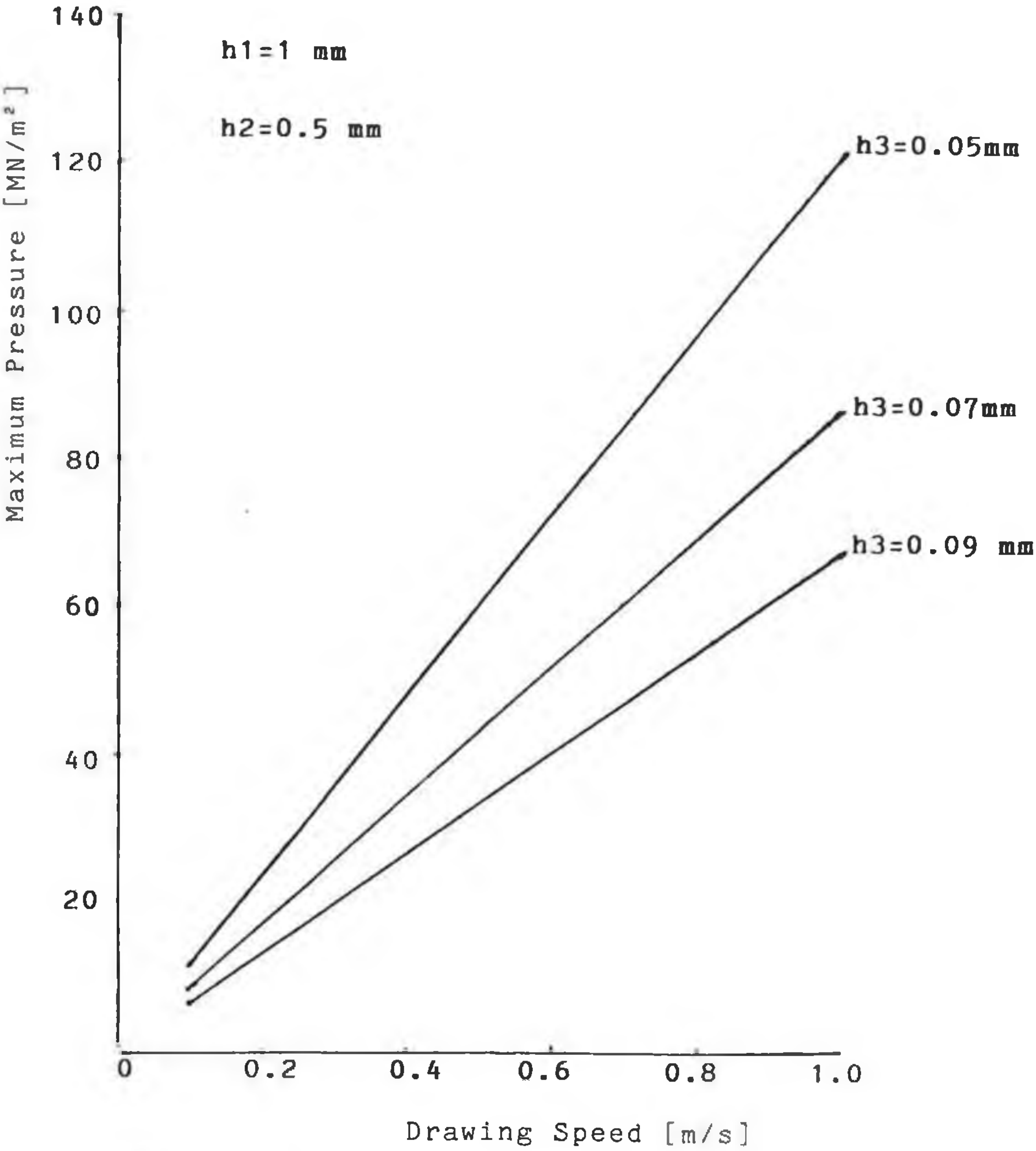

FIG(54) THEORETICAL EFFECT OF h3 ON MAXIMUM PRESSURE

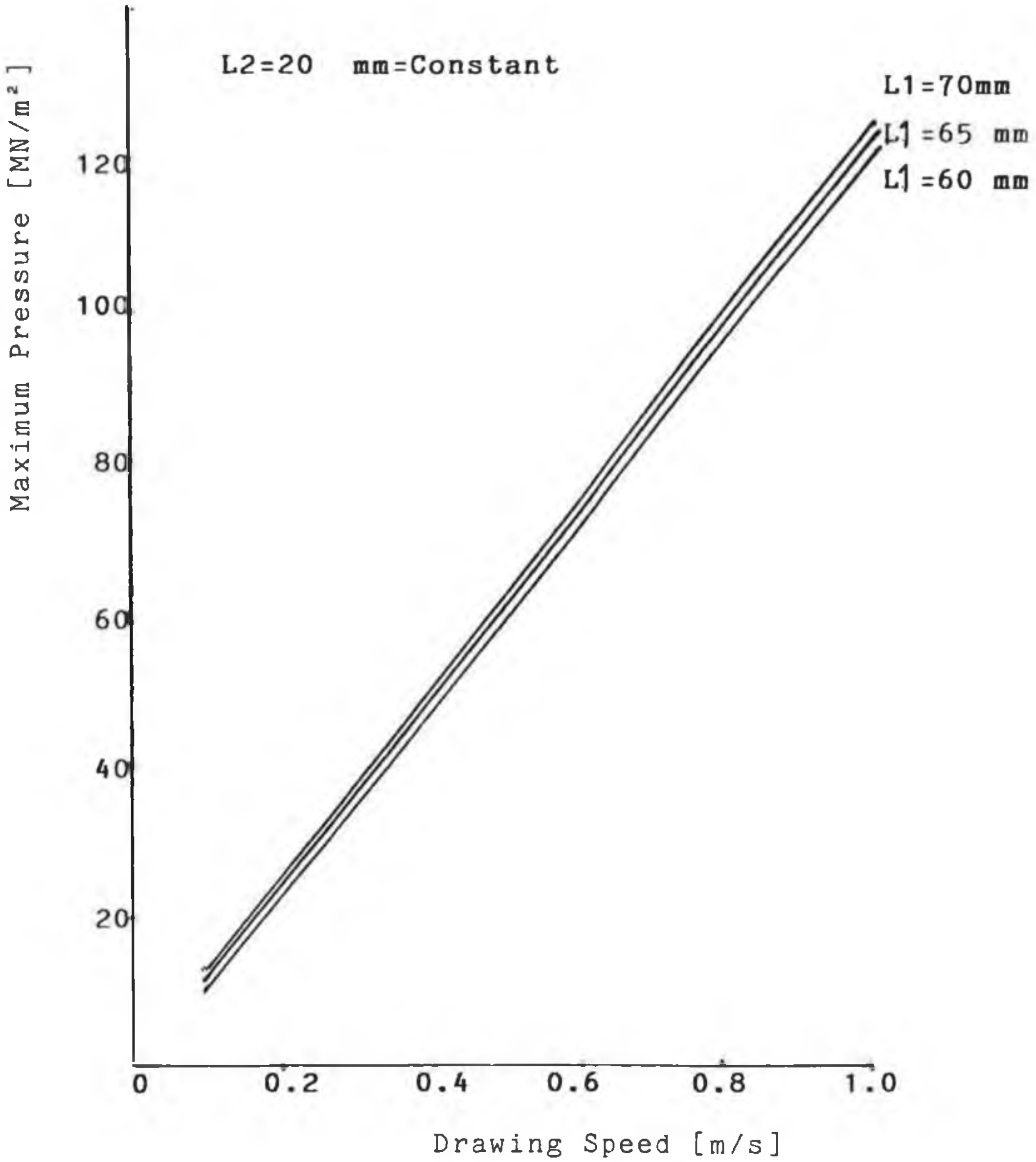

FIG (55) THEORETICAL EFFECT OF L1 ON MAXIMUM PRESSURE

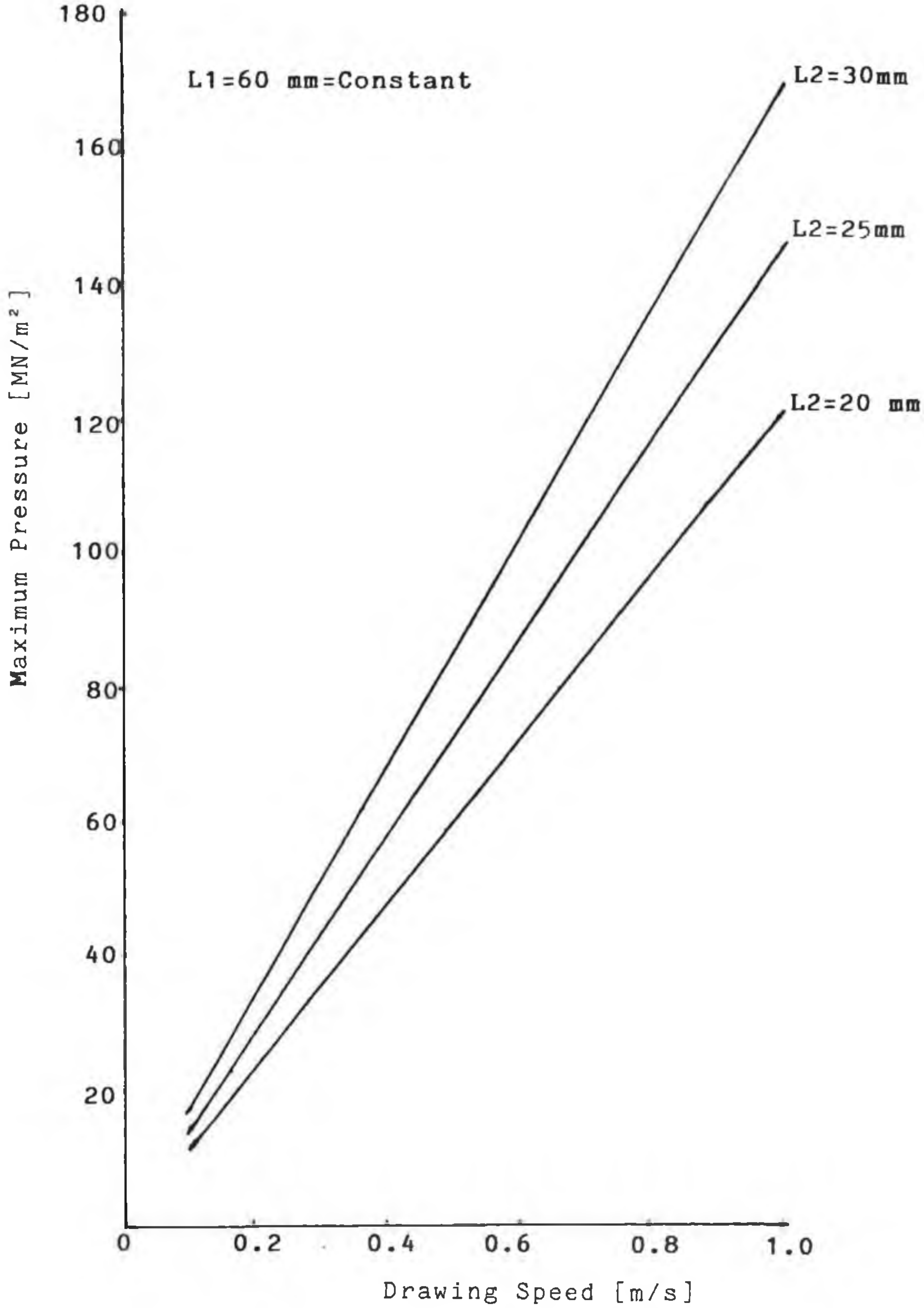

FIG (56) THEORETICAL EFFECT OF L2 ON MAXIMUM PRESSURE

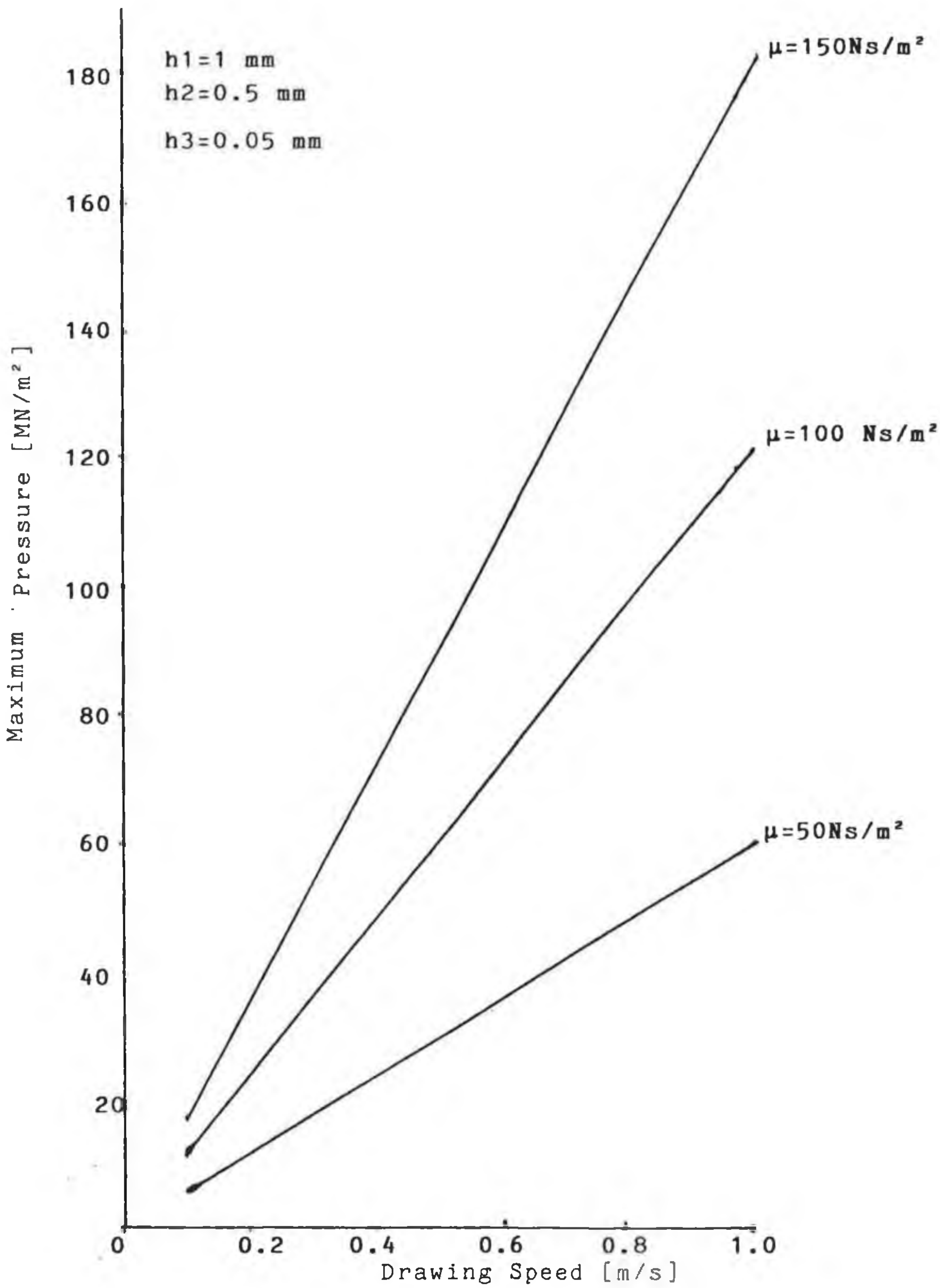

FIG (57) THEORETICAL EFFECT OF VISCOSITY ON MAXIMUM PRESSURE

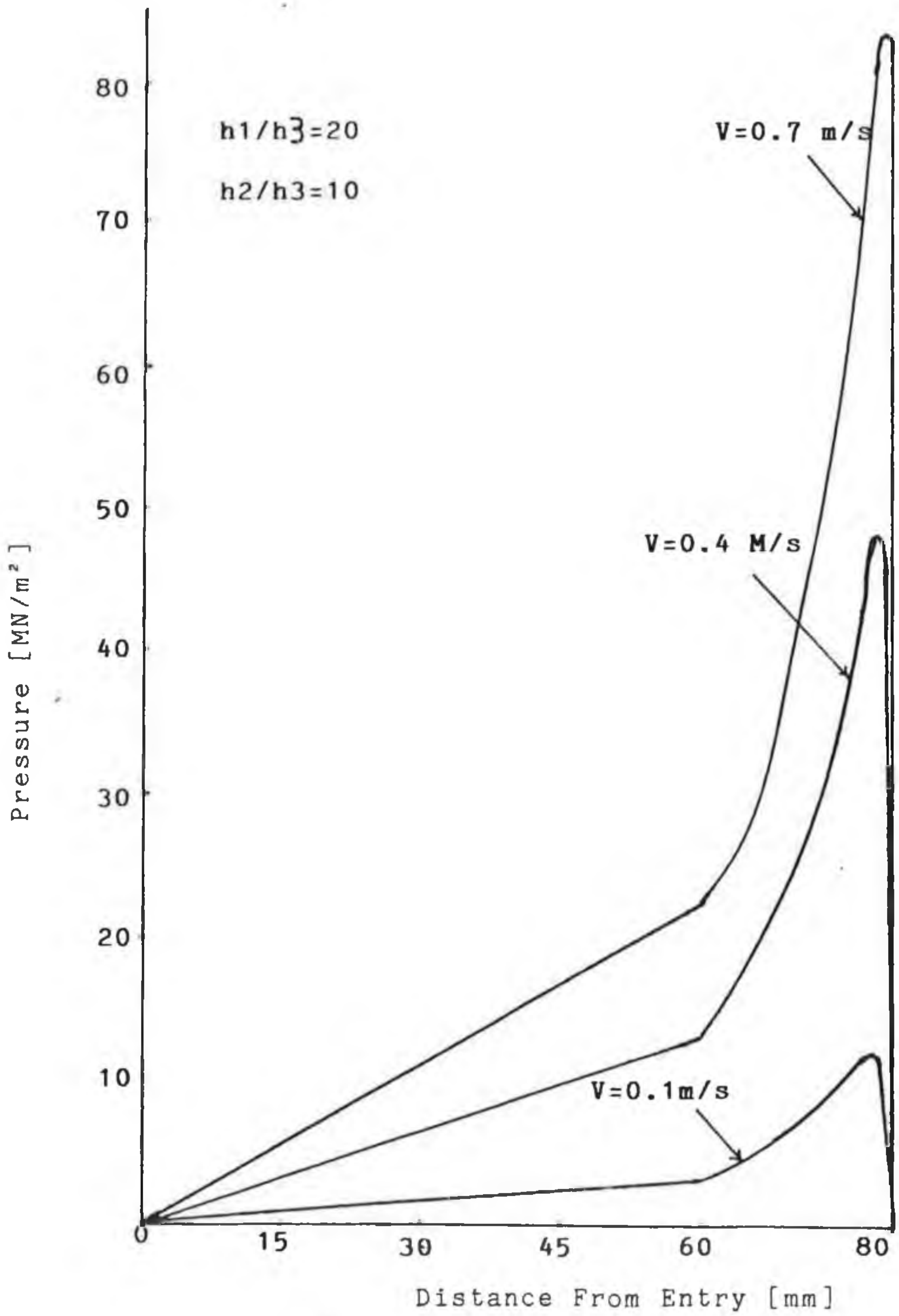

FIG (58) THEORETICAL RESULTS OF PRESSURE DISTRIBUTION

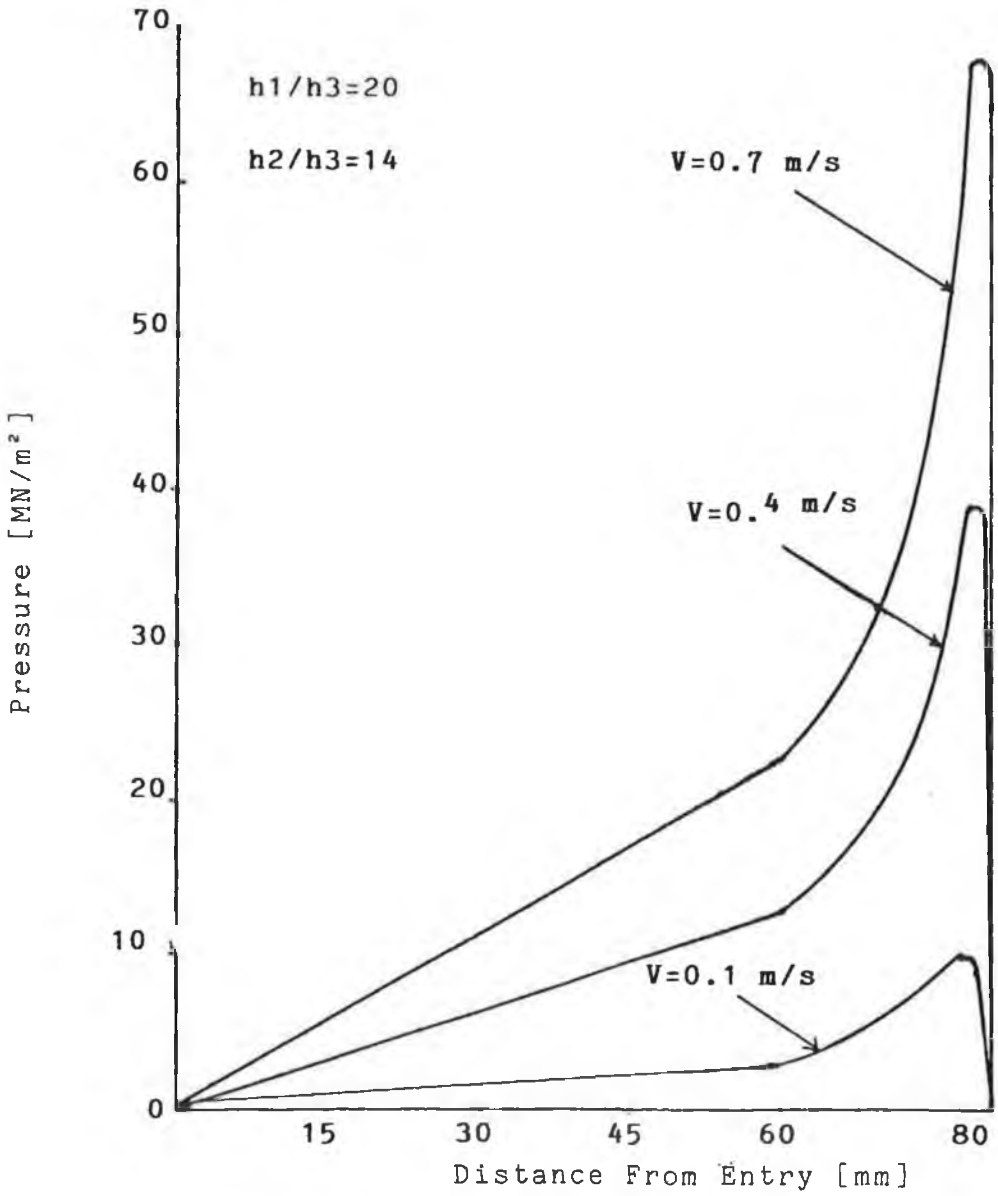

FIG(59) THEORETICAL RESULTS OF PRESSURE DISTRIBUTION

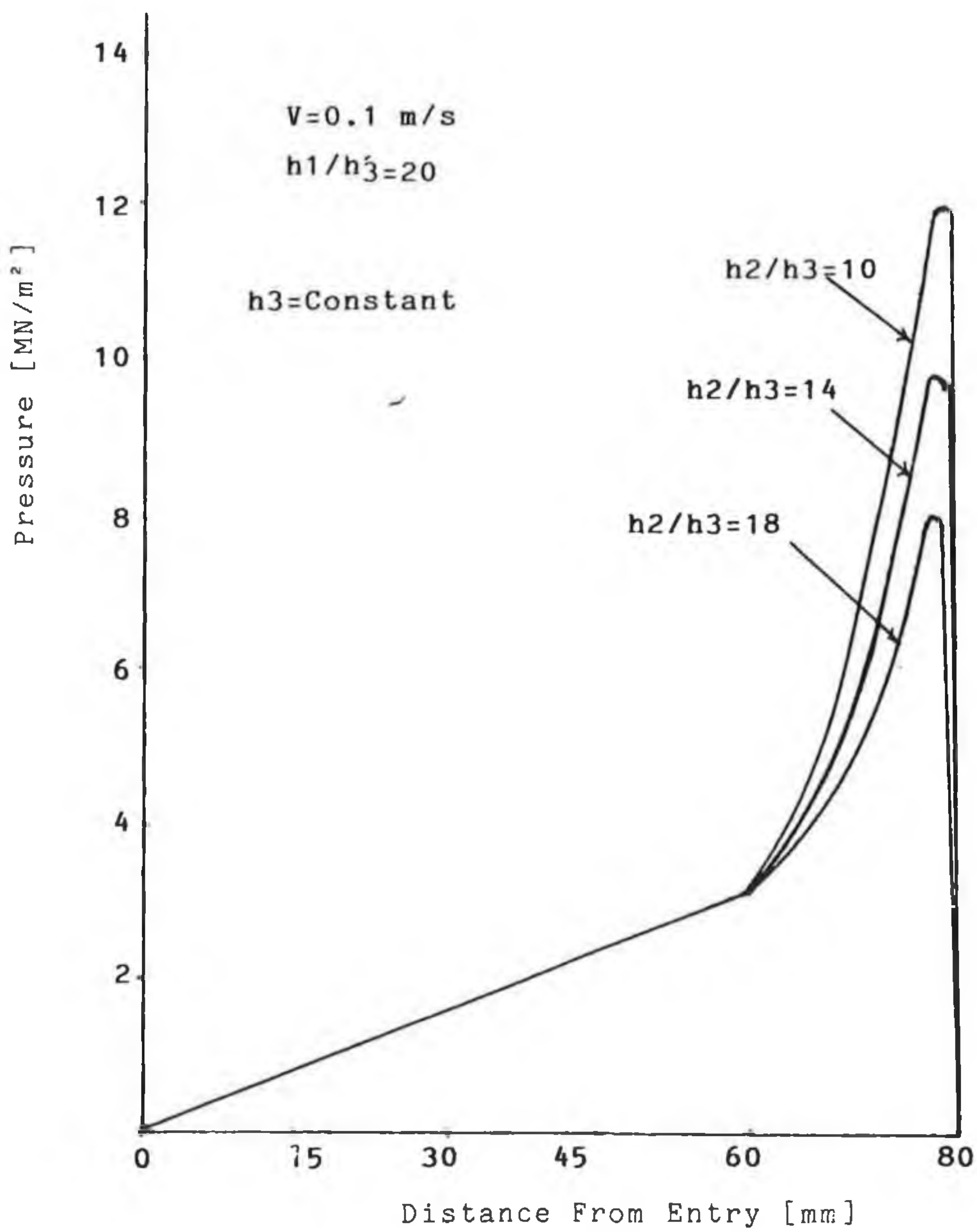

FIG (60) THEORETICAL EFFECT OF GAP RATIO h2/h3 ON PRESSURE DISTRIBUTION

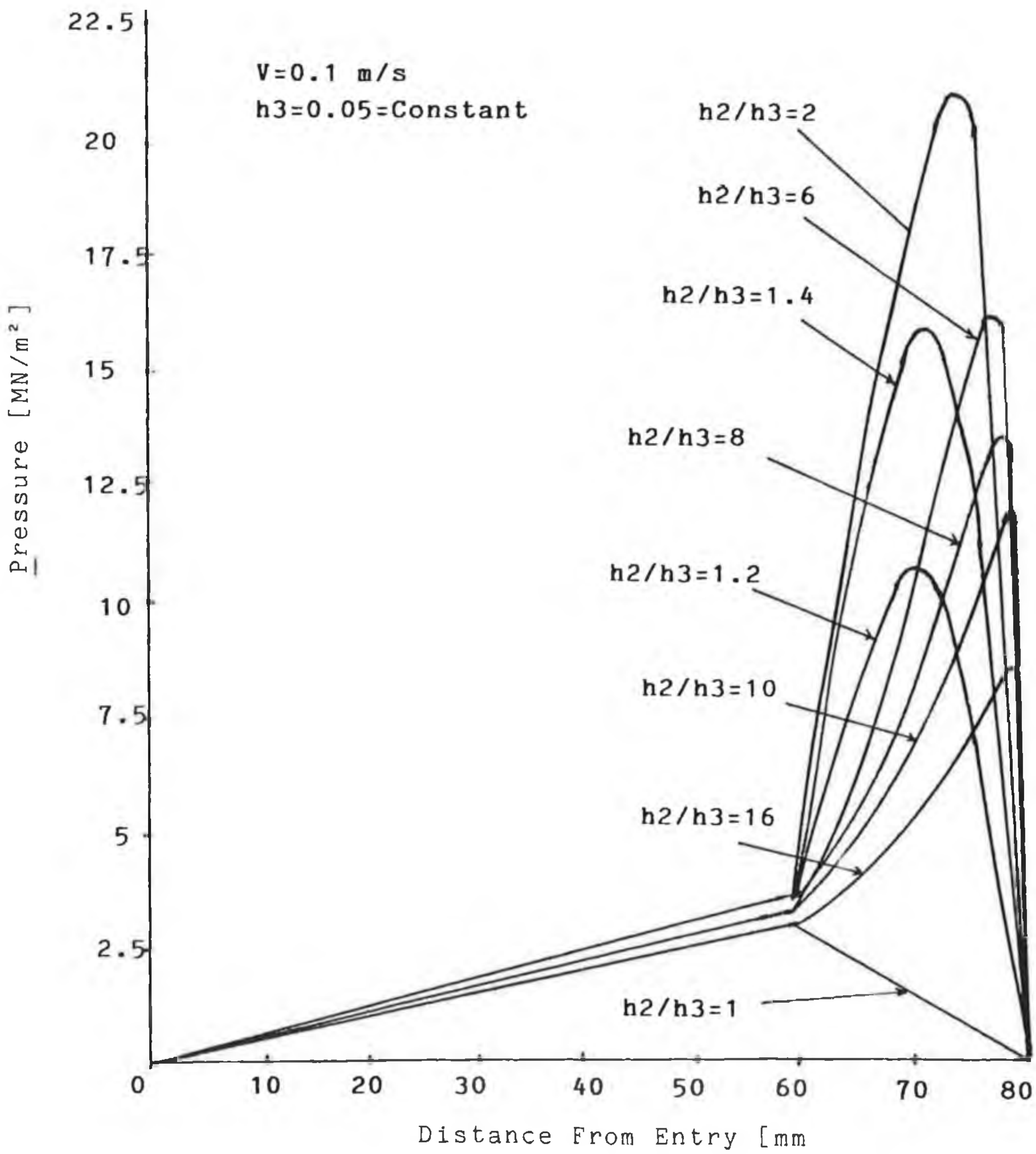

FIG(61) THEORETICAL EFFECT OF GAP RATIO h2/h3 ON PRESSURE DISTRIBUTION

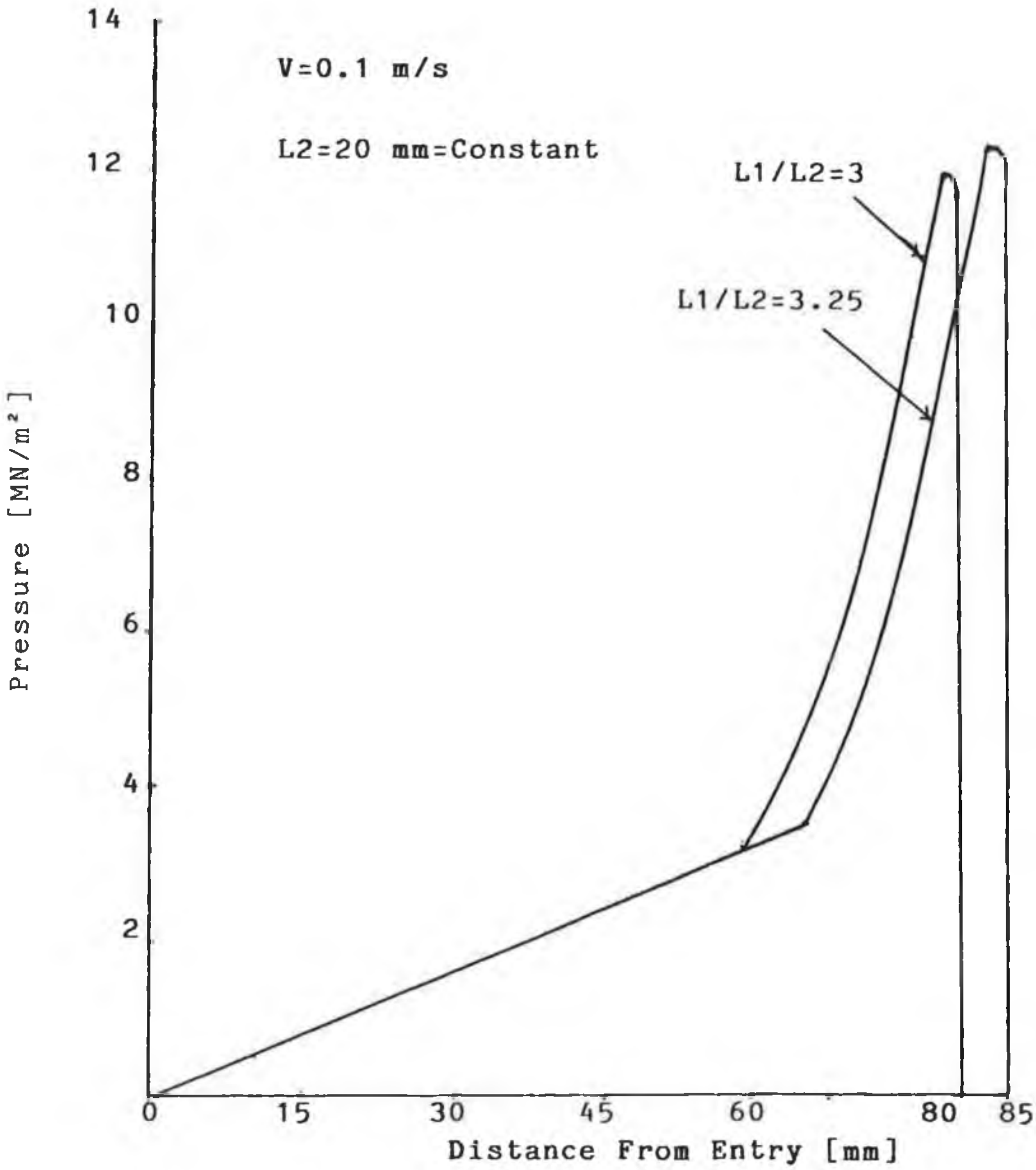

FIG(62) THEORETICAL EFFECT OF LENGTH RATIO L1/L2 ON PRESSURE DISTRIBUTION

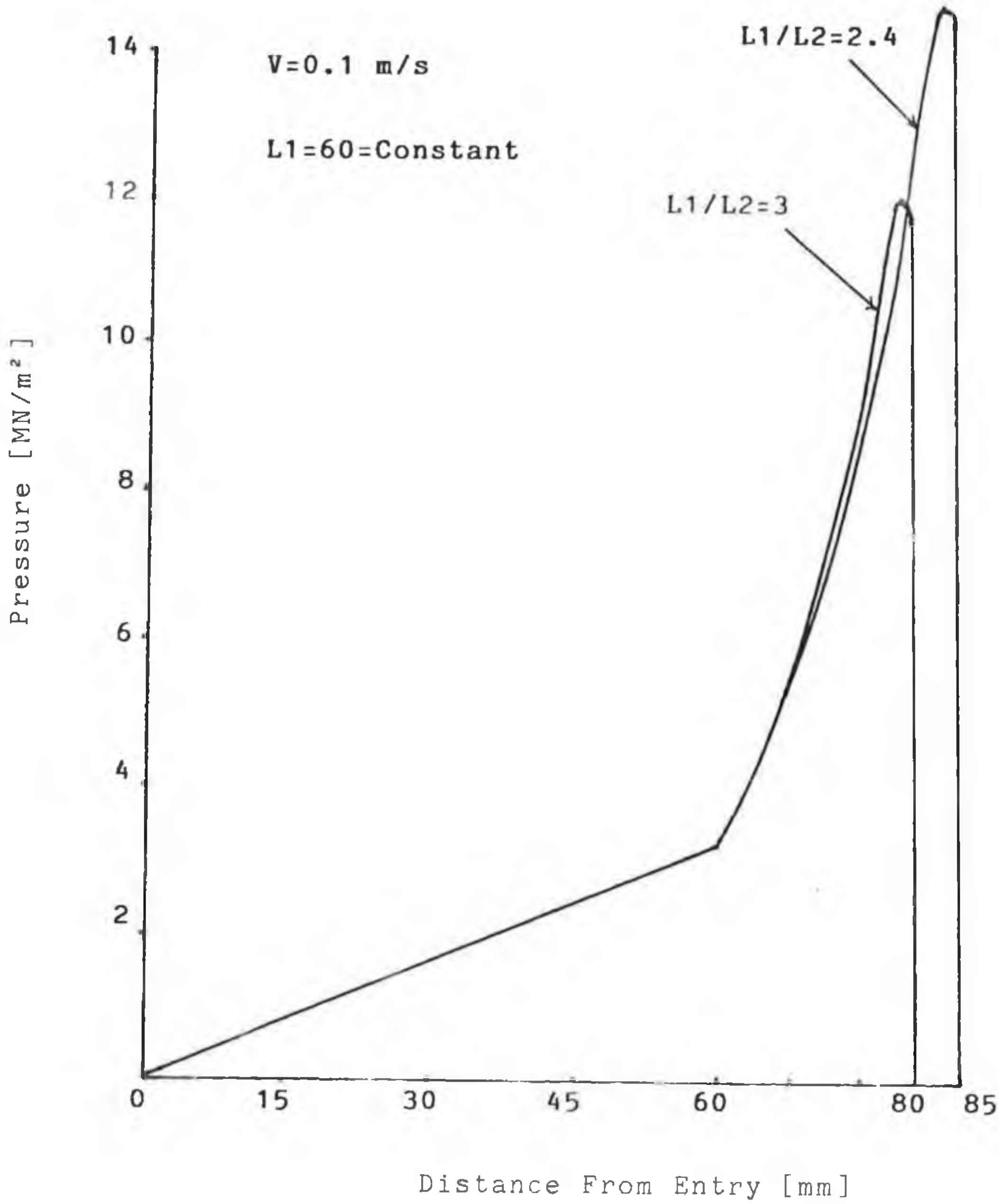

FIG(63) TEORETICAL EFFECT OF LENGTH RATIO L1/L2 ON PRESSURE DISTRIBUTION

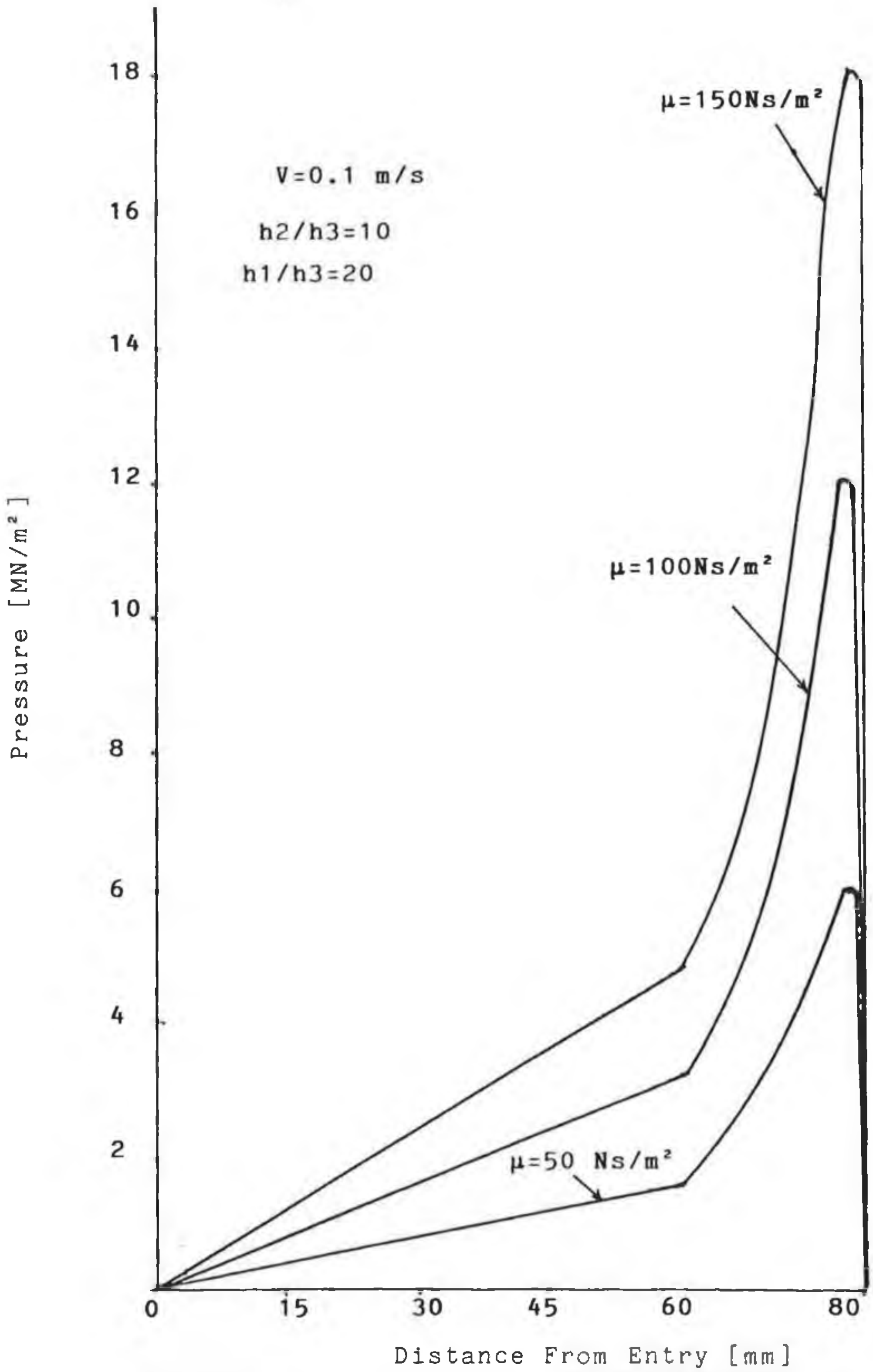

FIG(64) THEORETICAL EFFECT OF VISCOSITY ON PRESSURE DISTRIBUTION

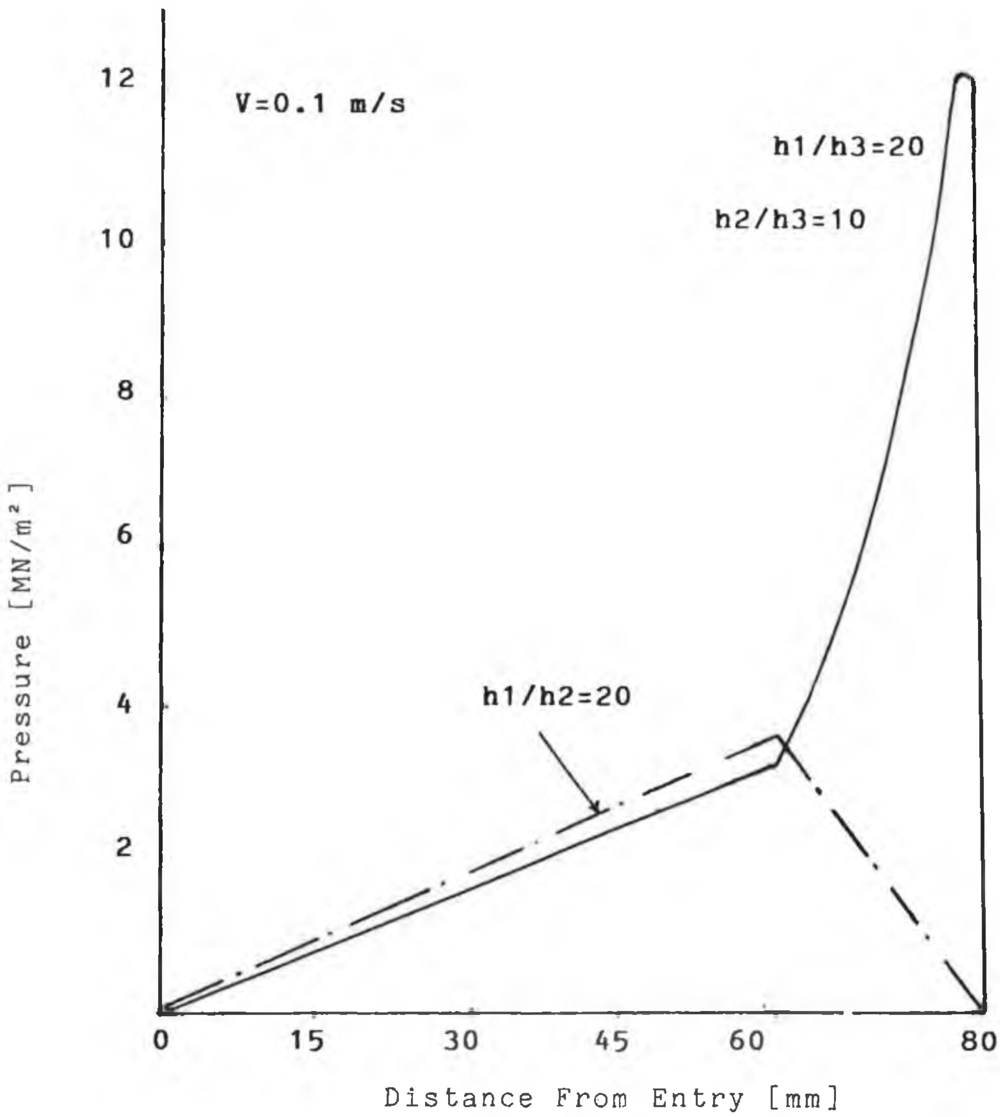

FIG(65) COMPARATIVE BETWEEN THE COMPLEX GEOMETRY PRESSURE UNIT WITH STEPPED BORE UNIT

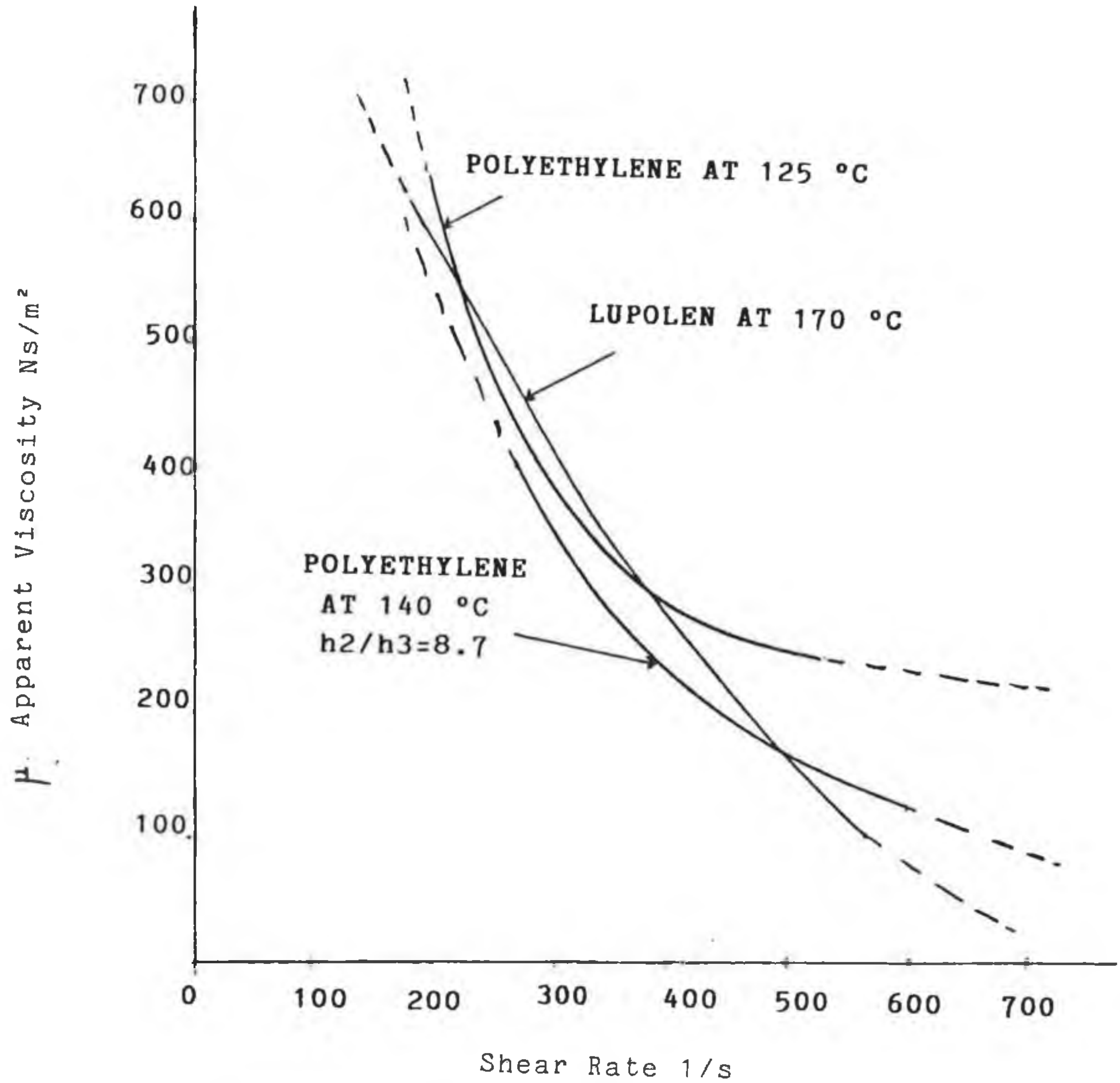

FIG(66) EFFECT OF SHEAR RATE ON VISCOSITY

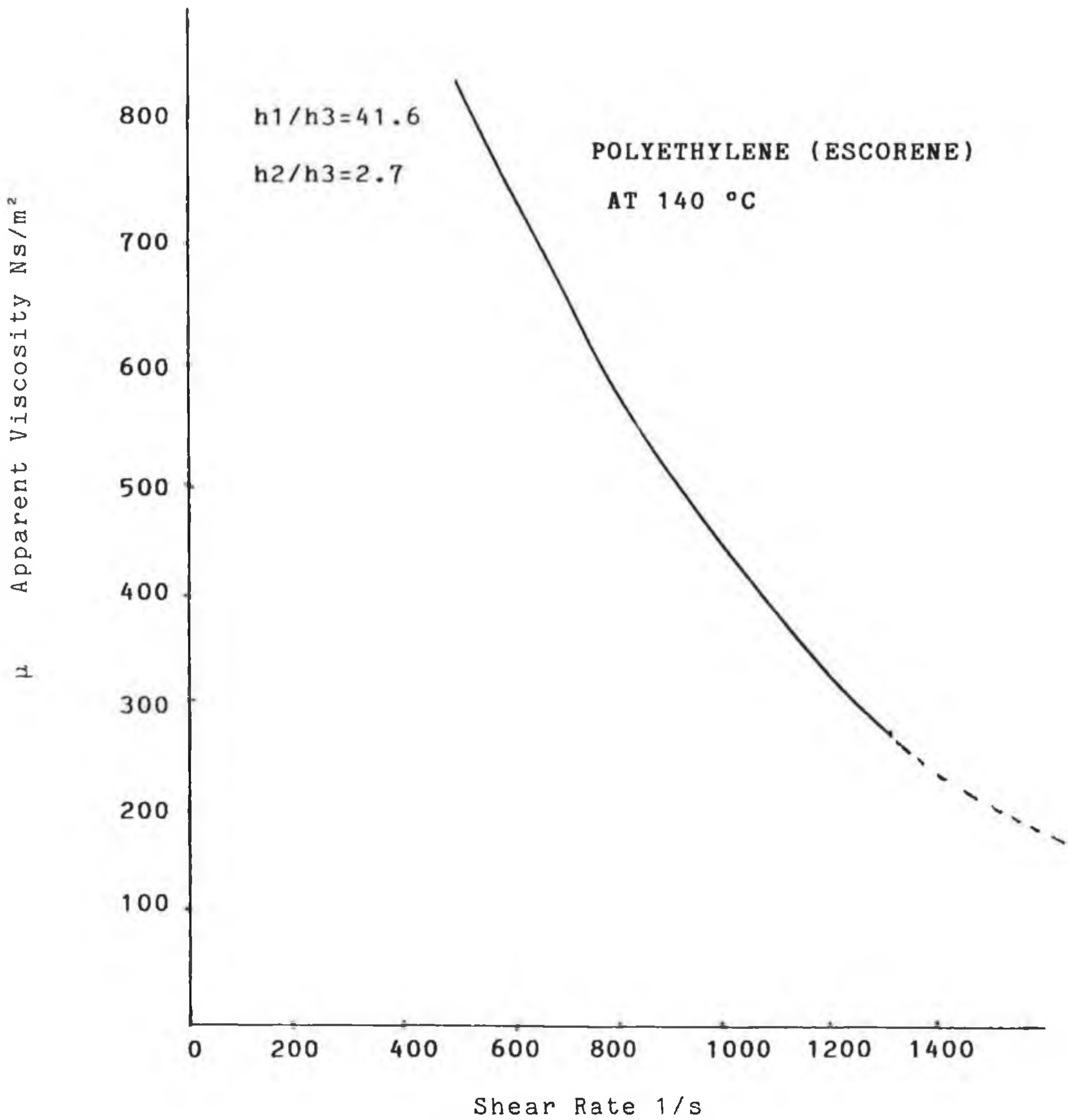

FIG (67) EFFECT OF SHEAR RATE ON VISCOSITY OF POLYETHYLENE (ESCORENE) AT 140 °C

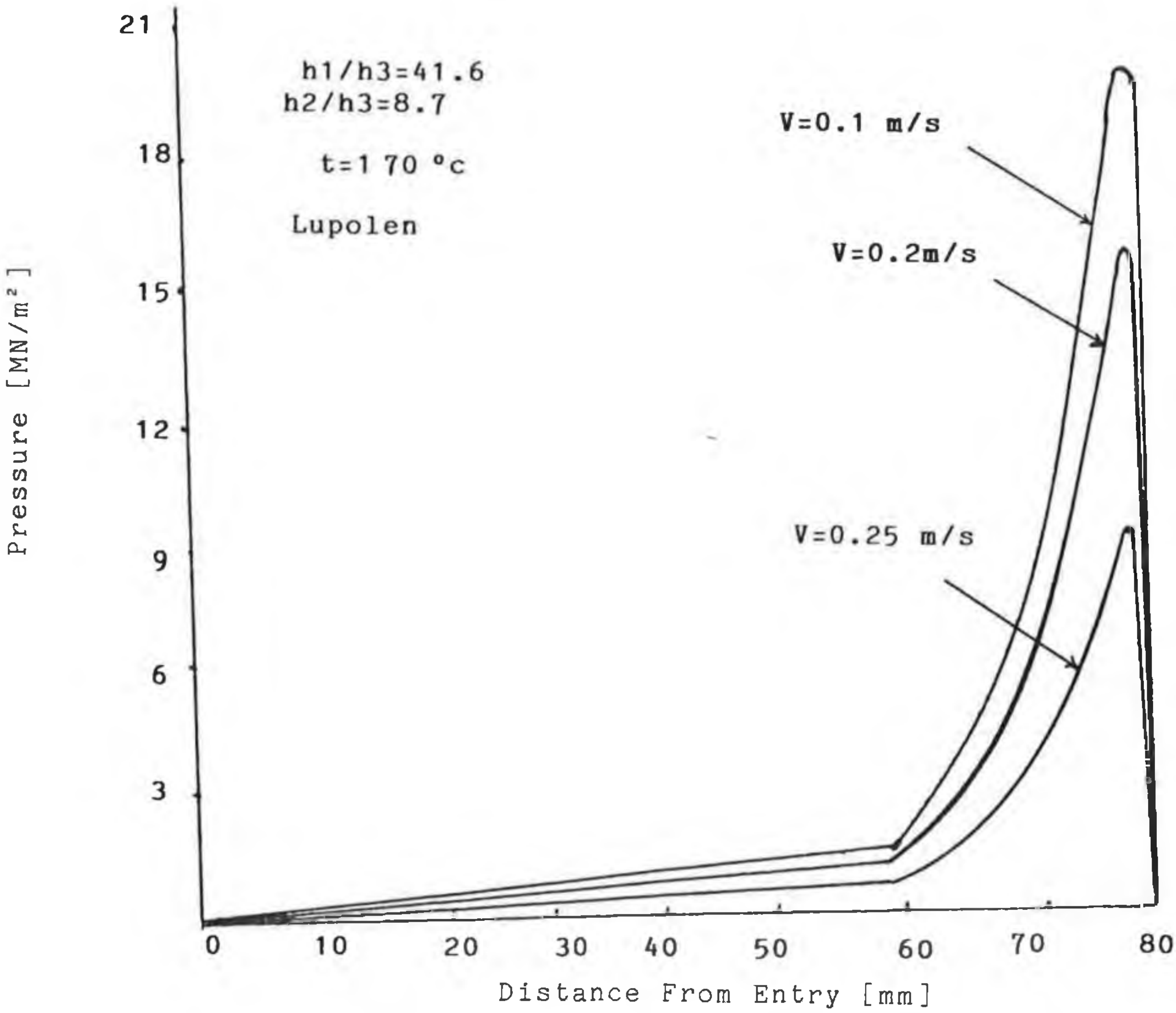

FIG(68) THEORETICAL RESULT OF PRESSURE DISTRIBUTION BASED ON PSEUDO-NEWTONIAN SOLUTION

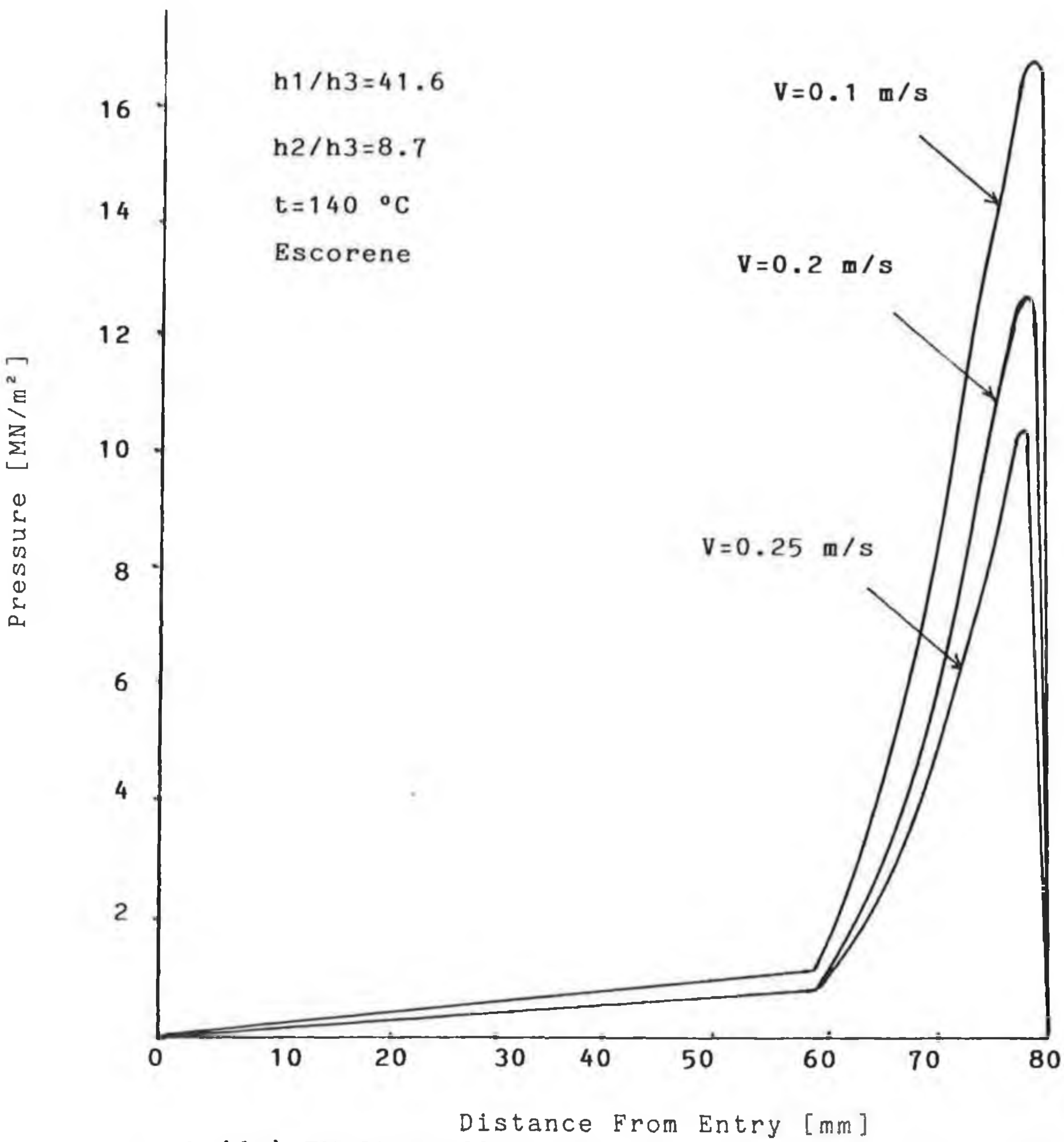

FIG (69) THEORETICAL RESULTS OF PRESSURE DISTRIBUTION BASED ON PSEUDO-NEWTONIAN SOLUTION

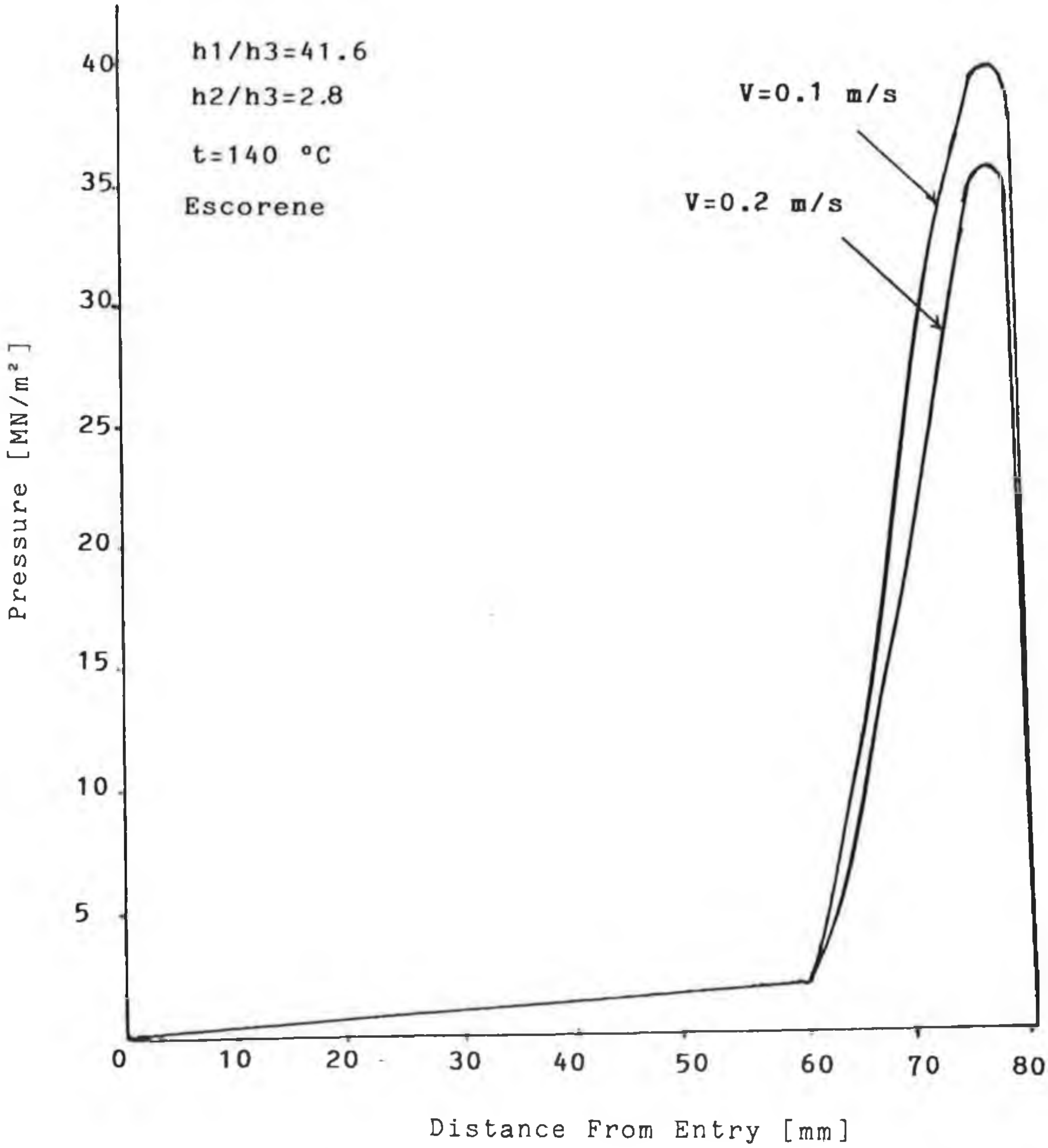

FIG(70) THEORETICAL RESULTS OF PRESSURE DISTRIBUTION BASED ON PSEUDO-NEWTONIAN SOLUTION

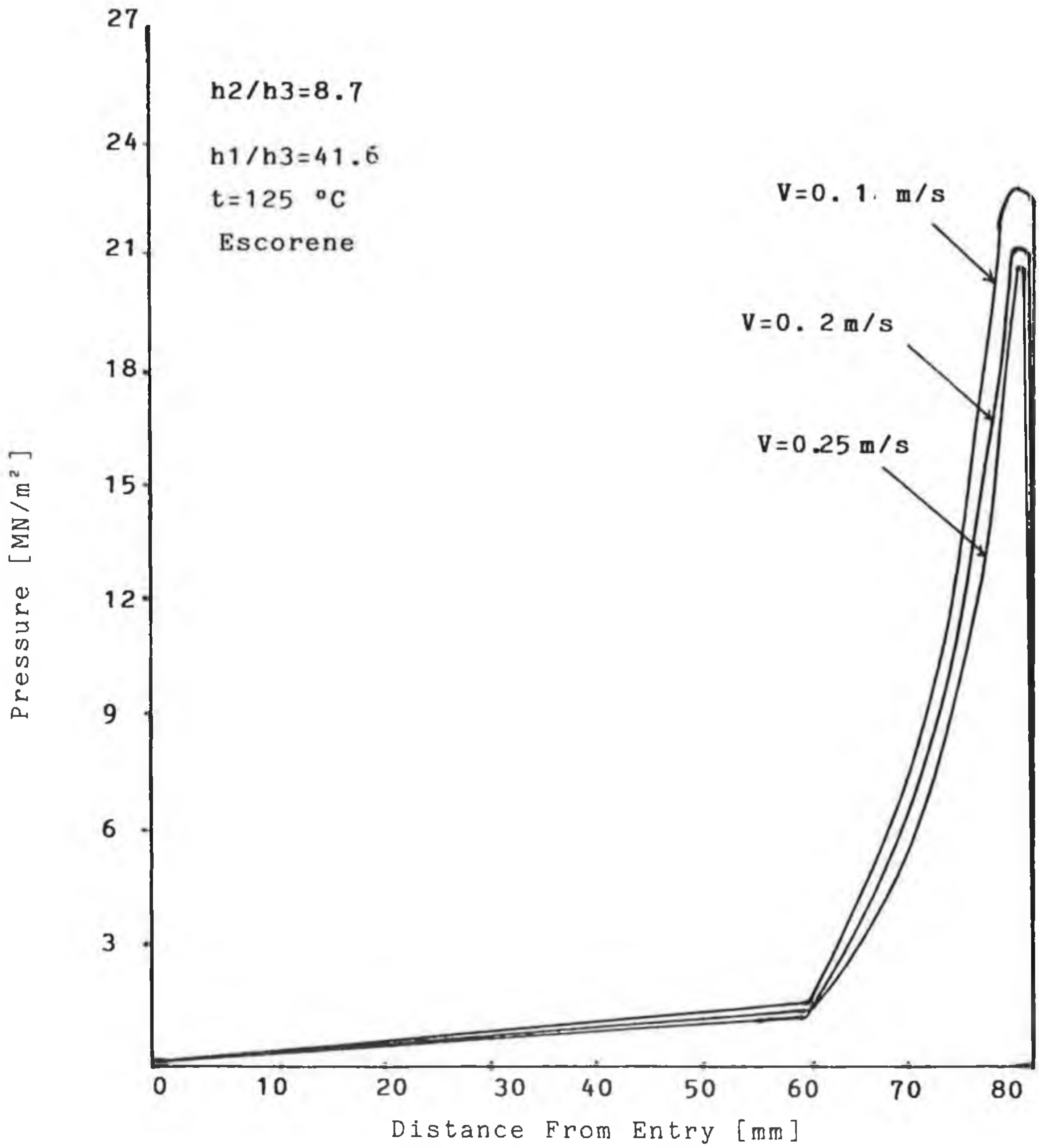

FIG(71) THEORETICAL RESULTS OF PRESSURE DISTRIBUTION BASED ON PSEUDO-NEWTONIAN SOLUTION

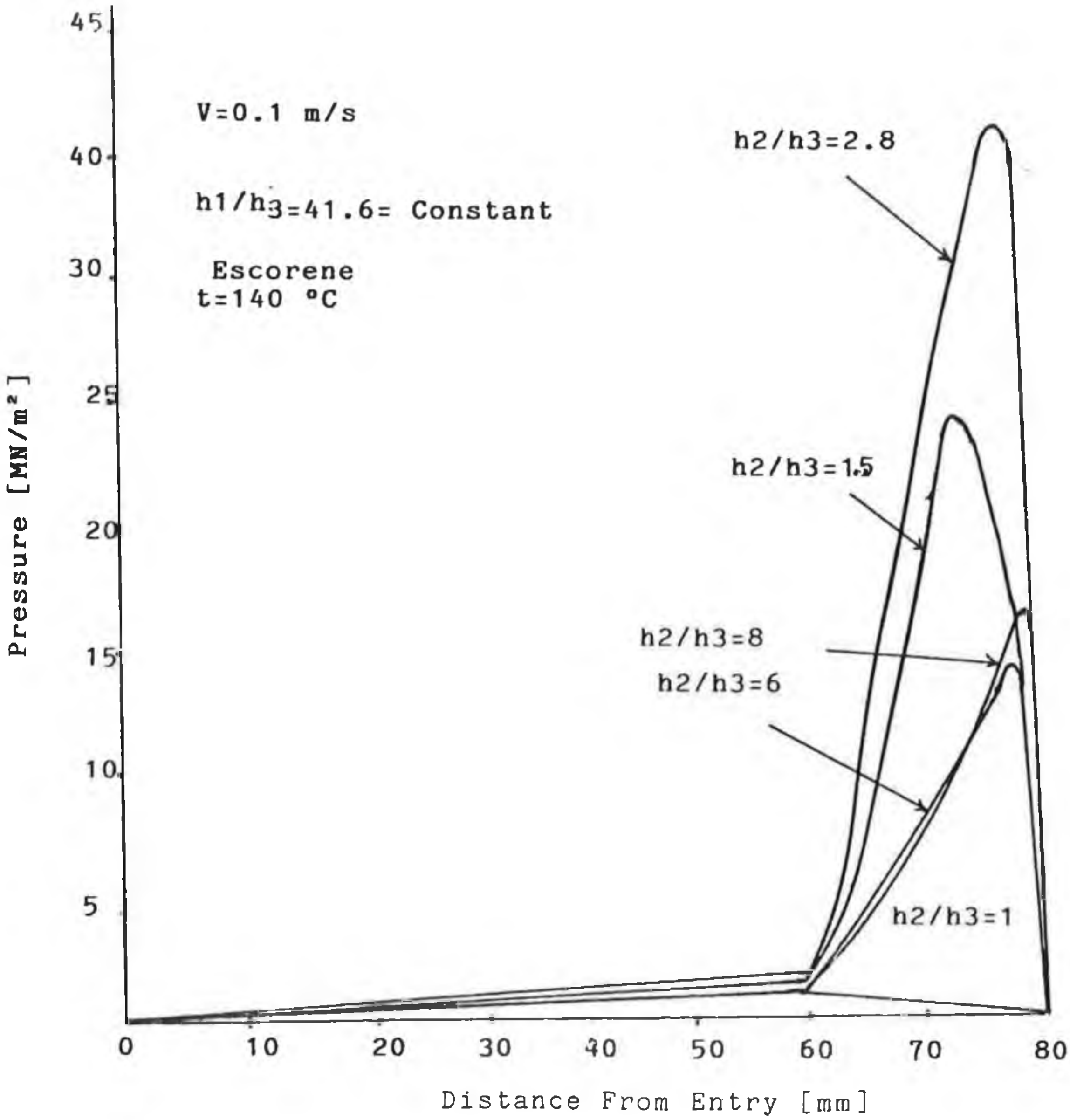

FIG(72) THEORETICAL EFFECT OF h2/h3 ON PRESSURE DISTRIBUTION BASED ON PSEUDO-NEWTONIAN SOLUTION

CHAPTER-6

DISCUSSION

6-1 Discussion On The Theoretical and Experimental Results

A new geometry of the pressure unit has been investigated in which a polymer melt is used in order to generate higher hydrodynamic pressure within the pressure unit which consists of combined parallel and taper bores. To investigate the performance of the unit, an extensive experimental and theoretical programme was conducted during which a considerable amount of data were obtained. Therefore, in this chapter, it is aimed to highlight the important results obtained experimentally and theoretically and to carry out a comparison of typical results.

6-2 Discussion On The Test Procedure and Experimental Results

A number of interesting results have been observed while carrying out the experimental tests, using this complex geometry pressure unit and polymer melt as the pressure medium. During the course of the experimental programme, parameters such as melt temperature, gap ratio of the pressure unit, polymer type drawing speed and wire material were varied in order to investigate their effect on the performance of the unit. The length ratio of the unit was kept constant throughout the tests. Two polymers having different densities and viscosities were selected as pressure mediums. One being polyethylene(Escorene) which has a relatively low melt temperature and the other being lupolen. The gap ratio h2/h3 and drawing speed were found to have the most significant effect on the performance of the unit. This effect is manifested in terms of the pressure distribution throughout the pressure unit and the shear rates on the viscosity of the polymer which leads to the condition of slip in the polymer at higher drawing speeds. Two types of flow of polymer were thought to occur as the drawing speed is increased. These are sub-critical and critical flow. It is possible that at low speeds the stick-slip phenomenon of the polymer melt along the surface of the wire produced a discontinuity in pressure generation. As the speed was increased, a critical shear stress value was surpassed which then caused slip to be continuous, producing a constant pressure independent of speed and hence the performance of the pressure unit was reduced.

Four location of pressure transducer were made on the pressure unit and for each speed increment the trace of pressure at each location was recorded on the as shown in Fig. 22 . Figures 24 to 51 show the measured pressure for different wire materials and polymer used for the test. In Fig. 26 for drawing speeds in excess of about 0.12 m/s the pressure readings were found to be approximately independent of speed at positions 2 and 3 whilst at position 4 the measured pressure decreased with increase in drawing speed. The reason for the sudden decrease in pressure was probably the transition from no-slip in the polymer melt ie., at low drawing speed (below 0.12 m/s) slip did not occur and high pressure was developed. As the speed was increased, a transition from no-slip to slip occured and the polymer melt was unable to develop such higher pressures since the velocity gradient became discontinuous. Apart from the shear rate, the magnitudes of the pressures generated during the drawing process are believed to be another reason for slip to occur. Maxwell and Jung (37) reported that when polystyrene was subjected to the pressure of 150 MN/m^2 the polymer acted like solid plastic material

Figures 48 and 49 indicate that for lower values of gap ratios h1/h3, h2/h3, higher pressure should be obtained. Figures 40 , 43 and 50 show effect of viscosity on pressure distribution. These figures indicate that for lower values of temperature and higher viscosity hence, higher pressure pressure should be obtained. When slip occured, the pressures reduced as the drawing speed was increased as shown in Fig. 39 . Figure 51 indicates that the maximum pressure is much higher in the complex geometry pressure unit than the pressure in stepped pressure unit at which h2=h3

6-3 Discussion On The Analysis and The Theoretical Results

A model has been developed based on the assumption that the pressure medium demonstrates ideal Newtonian characteristics. The following assumptions were made in order to simplify the analyses.

(1) The flow of the fluid pressure medium in the pressure unit is laminar.This seems to be a reasonable assumption since the drawing speeds of the wire are low, viscosity of the pressure medium is higher and the gaps are small.

(2) The flow of the fluid pressure medium is axial. Once flow through the pressure unit has commenced, little or no back flow is expected. This assumption allowed one dimensional flow to be considered.

(3) The thickness of the fluid layer is small compared to the dimensions of the pressure unit. This assumption enabled the analysis to be conducted in plane flow rather than cylindrical co-ordinates.

(4) The pressure in the fluid medium is uniform in the thickness direction. This assumption simplified calculation of the pressure in the pressure unit and allowed the viscosity be later as constant

(5) The pressure is isothermal. This assumption may introduce some error in the results since it is known

that the temperature of the wire increases during the drawing process due to plastic deformation and interlayer shearing in the fluid.

In addition to the above, the following assumption was made:

From the experimental results reported in reference (39) for similar type of polymer (low density polyethylene the following relationship can be used,

$$\mu_a=(A + B\ Pe^2)/\dot{\gamma}$$

where A and B are constants, Pe is excess pressure(over atmospheric) and $\dot{\gamma}$ is the shear rate. The accuracy of Westover's (36) results is not known and the polymer used for his experiments was not the same polyethylene. Therefore small errors may be involved in the determination of the constants A and B. The results of maximum pressure showed that:

(1) For smaller gaps of h1, h2 and h3 greater maximum pressures were predicted for a given drawing speed(see Figs 52 to 54)

(2) The values of h3 are more influential than the values of h1 and h2 on the maximum pressure in the pressure unit.

(3) The increase in the length L_1 in the first part of the pressure unit does not significantly affect the maximum pressure (see Fig 55)

(4) For higher values of the length L_2 of the pressure unit, greater maximum pressure is predicted for a given drawing speed (see Fig. 56).

(5) The maximum pressure increases as the viscosity of fluid is increased for a given drawing speed (see Fig. 57).

Theoretical results of predicted pressure distribution based on Newtonian analysis are shown in Figures 58 to 65 which indicate that smaller values of h_2/h_3 caused higher pressures (see Fig 60). This may be explained in terms of the pressure generated due to the geometry of the pressure unit. The predicted results also showed that there exists a gap ratio (optimum) for which the maximum pressure is the highest, everything else being the same. This maximum pressure occurs towards the exit end of the tapered part of the pressure unit. For greater or smaller values of the gap ratio than this optimum value, a decreased magnitude for the maximum pressure is obtained (see Fig. 61). The pressure increases as the length ratio L_1/L_2 is decreased for a given drawing speed when L1 is constant. However, there is very little change in the pressure distribution when L_1/L_2 was increased with L_2 being kept constant (see Fig. 62).

6-4 Comparison Between The Experimental and Theoretical Results

In the previous two sections a discussion of theoretical and the experimental results were carried out in which some discrepancies were apparent. In this section, it is aimed to point out these discrepancies and discuss the possible causes of such discrepancies. Figure 73 shows typical experimental results of the maximum pressure and theoretical results based on Newtonian analysis and pseudo-Newtonian solutions under similar condition. A reasonably close correlation was observed between the trends of the experimental results and the theoretical pseudo-Newtonian solutions, i.e., the maximum pressure decreased as the drawing speed was increased. The Newtonian analysis showed a different trend compared to the these results, i.e., the maximum pressure increased as the drawing speed was increased.The reason being that the viscosity was assumed to be constant in Newtonian analysis. The assumption of a Newtonian behaviour of the pressure fluid facilitated reasonably less cumbersome analytical solutions whilst providing satisfactory comparison of pressure distribution in complex and simples geometry pressure units. Fig. 74 shows the experimental and theoretical pressure distributions for Escorene polymer at 140 °C and at drawing speed of 0.2 m/s . Good agreement was observed between the pseudo-Newtonian solution and the experimental results.

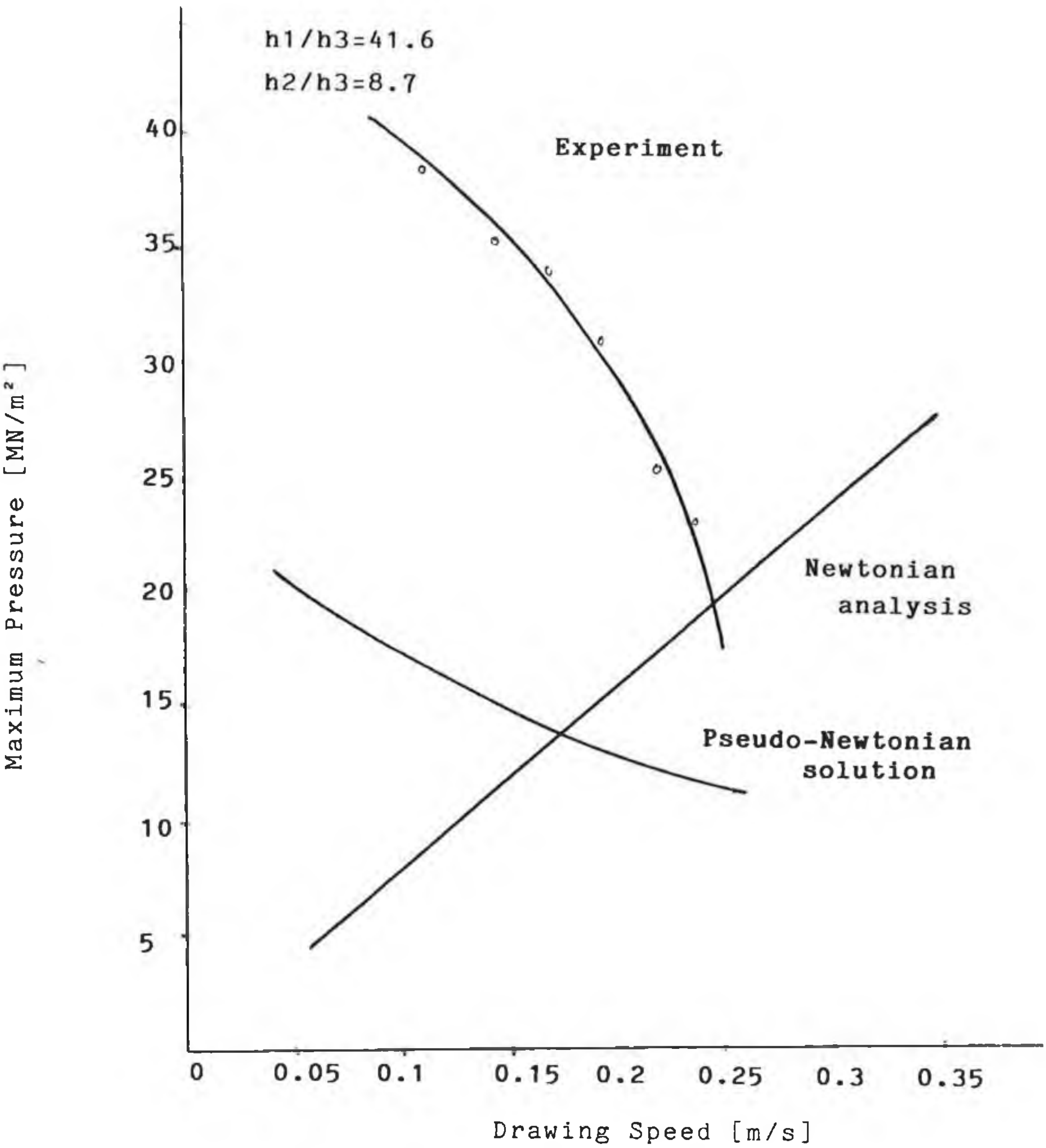

FIG. (73) COMPARISON BETWEEN EXPERIMENTAL AND THEORETICAL MAXIMUM PRESSURE

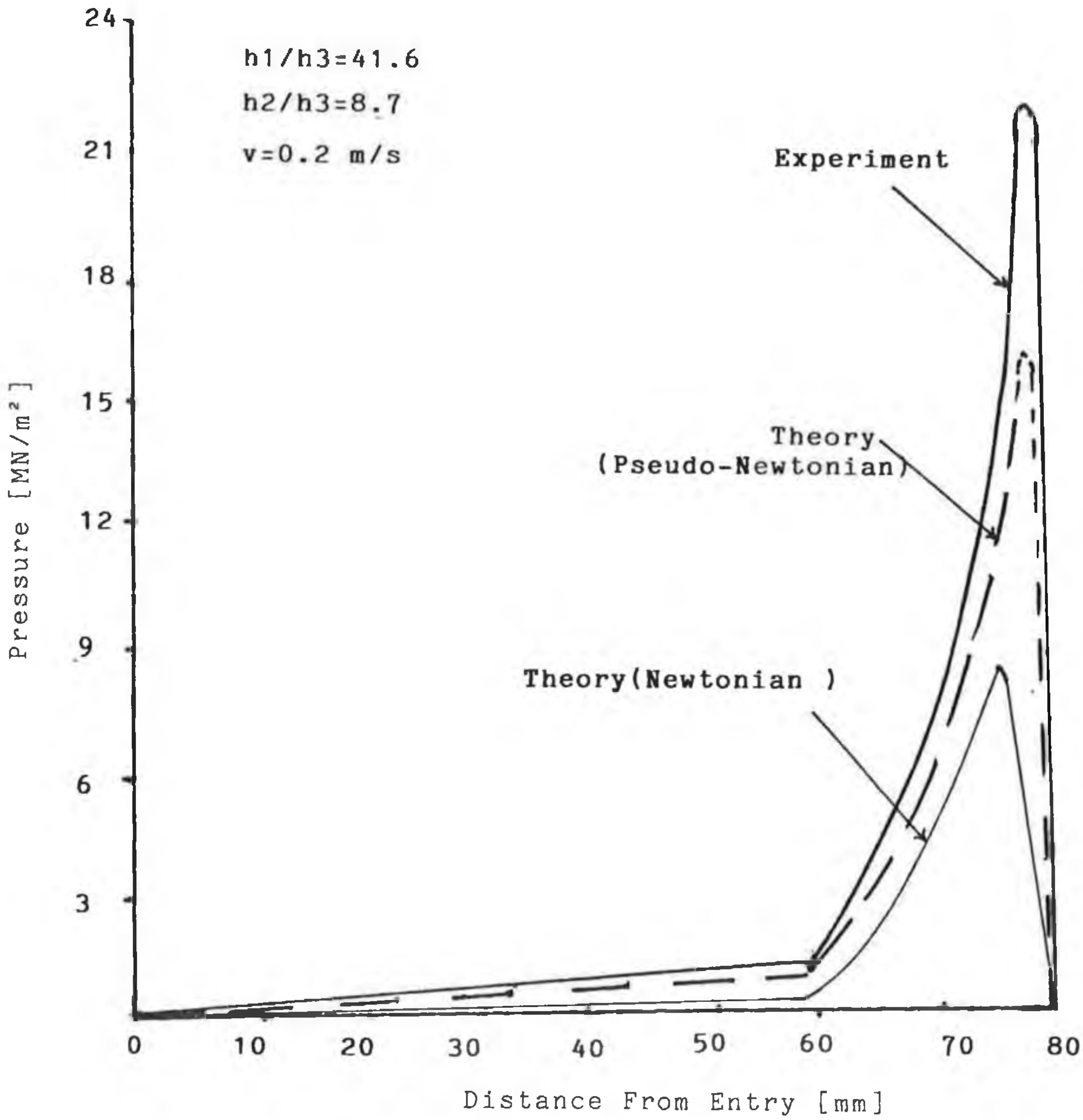

FIG.(74)COMPARISON BETWEEN EXPERIMENTAL AND THEORETICAL PRESSURE DISTRIBUTION

CHAPTER-7

CONCLUSION AND SUGGESTIONS FOR FUTURE WORK

7-1 Conclusions

A new pressure unit for a number of possible applications such as drawing processes, coating of wires, tubes, ropes and wire-ropes has been developed in which either the stepped bore pressure unit or tapered bore unit is replaced by complex geometry which consists of combined parallel and taper bore. According to the theoretical analysis developed for the geometry of this unit, the maximum pressure occurs after the step in the second part (tapered part) of the unit. This is not in line with previous studies which showed that the maximum pressure occurs at the step of the pressure unit. Theoretical and experimental results , showed that there is a gap ratio (optimum) for which the pressure is maximum. For values of the gap ratio greater or smaller than optimum value, a decreased magnitude for the maximum pressure is obtained. The maximum pressure at that gap ratio (optimum) is much higher compared to stepped or tapered bore units having similar geometrical parameters.

Experimental work has been carried out on different pressure units with similar external but different internal geometries to investigate the performance of the new pressure unit. Two different types of polymers were used as the pressure medium. These are Lupolen and Escorene (Polythylene). Experimental results showed that the maximum pressure decreases as the drawing speed is increased and hence the performance of the unit at higher speeds decreased. This might be due to the effect of a phenomenon referred to as the slip condition, where at a certain speed, the value of the pressure reaches a maximum and decreases suddenly which these is an increase in speed In this study an analytical model based on Newtonian characteristics and pseudo-Newtonian solution has been developed theoretically to investigate the performance of the unit and to optimise the process. The predicted results showed reasonable agreement with those observed experimentally in terms of the maximum pressure and pressure distribution.

7.2 Suggestions for Future Work

The new pressure unit developed in this work showed a limitation when experimentally lower pressure was obtained at higher drawing speed. In the analysis it was attempted to incorporate as many factors as possible, but further works could be usefully conducted in the following areas.

1- Experimentally

The performance of the new system depends on the geometry of the pressure unit and on the type of the pressure medium. Experimental results were obtained by using several geometries of the pressure unit. Further experimental investigation using other viscous pressure medium and geometry of the pressure unit should be carried out to verify the effectiveness of the the unit. It is well known that the polymer melts are shear thinning fluids and no polymer have been found to perform otherwise. However, in references (40) and (41) it was reported that certain polymer solutions are shear thickening (dilated). It is thought that use of a dilated pressure medium could remove the problem of slip and hence improve the performance of the pressure unit at higher drawing speeds.

2- Theoretically

In the present work, the theoretical analysis was developed assuming isothermal condition. The viscosity of fluids are known to be sensitive to temperature change, hence a relationship predicting the viscosity change due to the temperature variation may improve the theoretical results. The rheology of the pressure medium should be better understood with respect to the effect of pressure and temperature on viscosity and slip characteristics. This in turn

REFERENCES

1. WISTREICH,J.G "The fundamentals of wire drawing" METALLURGIGAL REVIEW, 1958,VOL.3,NO 10.

2. WISTREICH,J.G "ABC of better lubrication and cooling in steel wire drawing" WIRE,1959,NOV.,PG1486.

3. CHRISTOPHERSON,D.G. and NAYLOR,H "Promotion of lubrication in wire drawing" PRO.INSTN.MECH.ENGRS.169,PG.643-653(1955)

4. WISTREICH,J.G "Lubrication in wire drawing" WEAR,MARCH,PG. 505-511,1957

5. TATTERSALL,G.H. "Hydrodynamic lubrication in wire drawing" J.MECH.ENG.SCI., VOL.3, NO.4, PG.378, 1961.

6. CHU,P.S "Theory of lubrication applied to pressure nozzle design in wire drawing" Proc.inst.mech.eng., VOL.181,PG.3,(1966-1967)

7. KALMOGROV,V.L. AND SELISHCHEV,K.P. "Cold drawing tubes with improved lubrication" Stall in

english PG.830-831,9 (1962)

8. BLOOR,M.,DOWSON,D. AND PARSON,B."AN elasto-plasto-hydrodynamic analysis of the plane strain drawing process" J.MECH.SCI., VOL.12,NO.3,1970

9. SWAMY,S.T.N. PRABHU,B.S. AND RAO,B.V.A "Calculated load capacity of non- newtonian lubrication in finite width bearings" EAR,VOL.3, Pg.277-285, (1975)

10. THOMPSON, P.J. AND SYYONS,G.R. "A plasto-hydrodinamic analysis of the lubrication and coating using polymer melt during drawing" PROC.INST.MECH.ENG., VOL.191, 13/77, (1977)

11. STVENS,A.J."A plasto-hydrodynamic investigation of lubrication and coating of wire using a polymer melt during drawing "Ph.D Thesis,SHEFFILD city polytechnic, 1979

12. CRAMPTON,R."Hydrodynamic lubrication and coating of wire using a polymer melt during drawing" Ph.D Thesis, SHEFFIELD city,polytechnic, 1980

13. HASHMI, M.S.J, CRAMPTON,AND SYMMONS,G.R."Effects of strain hardening and strain rate sensitivity of

the wire material during drawing under non-Newtonian plasto-hydrodynamic lubrication conditions"
INT.J.MACH.TOOL.DES.RES.Pg.71-86, (1981)

14. CRAMPTON,R.,SYMMONS,G.R., AND HASHMI,M.S.J."A non-Newtonian plasto-hydrodynamic analysis of the lubrication and coating of wire using a polymer melt during drawing" Int.symposium, metal working lubrication, SAN-FRANSISCO, U.S.A Pg107, AUGUST(1980).

15. HASHMI, M.S.J., SYMMONS, G.R.AND PARVINMEHR,H. "A novel technique of wire drawing"
Inst.mech.engrs., Vol.24No.1, (1982)

16. M.I.PANWHAR, R.CRAMPTON AND M.S.J.HASHMI "Dieless tube sinking plasto-hydrodynamic analysis based on Newtonian fluid characteristics"

17. M.I.PANWHER "A novel technique for tube sinking" Ph.D Thesis, SHEFFIELD city polytechnic(1986)

18. G.R. SYMMMONS ,M.S.J.HASHMI AND YD.XIE "The optimisation of plasto-hydrodynamic wire-drawing process"

19. G.R.SYMMONS,YD.XIE AND M.S.J.HASHMI "Thermal effect on a plasto-hydrodynamic wire drawing process using a polymer melt"

20. DIENES.G.J "Journal Appl.phys."24, 779.(1953)

21. LENK.R.S "Plastics Rheology".inter. science.new york. (1968)

22. CRAWFORD.R.J "Plastics Engineering" published by pergamon press.

23. ABBAS.K.H and PORTER.R.S "J.Appl.Polymer Sci." 20, 289, (1976)

24. NASON.K.H "J.Appl.Phys."16, 338, (1945)

25. DILLON.R.E. and SPENCER.R.S "J.Colloid Sci".4,241,(1949)

26. BENBOW.J.J and LAMB.P."SPE Trans." Jan., (1963)

27. TORDELLA.J.P."Trans.Soc.Rheol." 1, 203, (1957)

28. TORDELLA.J.P."J.Appl.phys.",27,454, (1965)

29. PEARSON.J.R.A."Plastics Polymer",37, 285, (1969)

30. BRYDSON.J.A "Flow Properties Of Polymer Melts" published by Van nostrand reinhold, NEW YORK (1970)

31. CARLEY.J.F. "J.Modern Plastics",dec. (1961).

32. MACEDO.P.B. and LITOVITZ.T.A "J.Chem.Phys.", 42, 245, (1965)

33. NIELSON.L.E."Polymer Rheology " NEW YORK,(1977)

34. SANCHEZ.I.C."J.Appl.Phys.", 45,4204,(1974)

35. COHEN.M. and TURNBULL.D."J.Chem. Phys.",31, 1164, (1959)

36. WESTOVER.R.F. "Polymer Eng.Scie.",6,83,(1966)

37. MAXWELL.B. and JHNG.A."Modern Plastics", 35, 174, Nov.,(1957)

38. COGSWELL.F.N."Plastics and Polymers",Feb.,(1973)

39. WESTOVER.R.F."Effect of hydrostatic on polyethylene melt rheology" S.P.E. Technical Papers. 1960, Vol 6, series 80-1

40 GOGOS, G.G Principles of Polymer Processing" Pg. 147-149, 1979.

41. LENK ,R.S "Plastics Rheology" ,Interscience,New York, 1968

APPENDIX 1-LISTING OF THE COMPUTER PROGRAMME FOR THEORETICAL MODELS BASED ON NEWTONIAN FLUID CHARACTERISTICS

```
01 PRINT "THIS PROGRAMME CALCULATES THEORETICAL
          HYDRODYNAMIC"
02 PRINT "PRESSURE DISTRIBUTION THROUGH A CONFINED
          PASSAGE"
03 PRINT "USING POLYMER MELT AS A NON-NEWTONIAN
           FLUID"
10 READ H1,H2,H3,L1,L2,MU
20 DATA 1E-3,.5E-3,.05E-3,60E-3,35E-3,100
22 DATA 1.5E-3,.5E-3,.05E-3,60E-3,35E-3,100
24 DATA 2E-3,.5E-3,.05E-3,60E-3,35E-3,100
26 DATA 1E-3,.7E-3,.05E-3,60E-3,35E-3,100
30 DATA 1E-3,.9E-3,.05E-3,60E-3,35E-3,100
32 DATA 1E-3,.5E-3,.07E-3,60E-3,35E-3,100
35 DATA 1E-3,.5E-3,.09E-3,60E-3,35E-3,100
36 DATA 1E-3,.5E-3,.05E-3,65E-3,35E-3,100
40 DATA 1E-3,.5E-3,.05E-3,70E-3,35E-3,100
45 DATA 1E-3,.5E-3,.05E-3,60E-3,40E-3,100
48 DATA 1E-3,.5E-3,.05E-3,60E-3,35E-3,150
50 DATA 1E-3,.5E-3,.05E-3,60E-3,35E-3,50
55 DATA 99,0,0,0,0,0
57 IF H1=99 GO TO 400
58 GOSUB 300
```

```
60 PRINT "H1=";H1;"m","H2=";H2;"m","H3=";H3;"m"
62 PRINT "L1=";L1;"m","L2=";L2;"m","MU=";MU;
63 PRINT "N.sec/m^2"
68 GOSUB 300
70 FOR V=.1 TO 1 STEP .3
80 B=(H2-H3)/L2
90 A=(6*MU*H1*V/(2*B))
100 C=(1/H3^2)-(1/H2^2)
110 D=(6*MU*V/B)*((1/H2)-(1/H3))
120 E=(1+(H1^3*C/(2*B*L1)))
130 Pms=((A*C)+D)/E
140 HBAR=H1-((H1^3*Pms)/(6*MU*V*L1))
142 XDASH=(H2-HBAR)/B
145 hb=HBAR/2*H3^2
150 Pmax=(6*MU*V/B)*((1/(2*HBAR))-(1/H3)+ hb)
160 PRINT "V=";V;"M/sec","Pms=";Pms;"N/m^2"
163 RPINT "XDASH=";XDASH
165 PRINT "HBAR=";HBAR;"m","Pmax=";Pmax;"N/m^2"
167 GOSUB 300
170 PRINT "X[m]","Px[N/m^2]"
180 GOSUB 300
190 FOR X1=0 TO L1 STEP L1/4
200 Px=(Pms/L1)*X1
210 PRINT X1,Px
220 NEXT X1
230 FOR X2=0 TO L2 STEP L2/35
231 W1=(6*MU*V)/B
232 W2=1/(H2-(B*X2))
```

```
233 W3=HBAR/(2*(H2-(B*X2))**2)
234 W4=W2=W3
235 W5=(1/H3)-(HBAR/(2*H3^2))
236 Px=(W1*W4)-(W1*W5)
250 PRINT X2,Px
251 NEXT X2
252 GOSUB 300
260 NEXT V
270 GOTO 10
300 FOR QWE=1 TO 11
310 PRINT"*****"
320 NEXT QWE
330 PRINT
340 RETURN
400 END
```

APPENDIX A.2: **PAPER PUBLISHED**

PROC. SIXTH IMC CONFERENCE ON ADVANCED
MANUFACTURING TECHNOLOGY
DUBLIN CITY UNIVERSITY, AUGUST 1989.

DEVELOPMENT OF A COMPLEX GEOMETRY PRESSURE UNIT FOR HYDRODYNAMIC COATING APPLICATIONS

I. Al-Natour and M.S.J. Hashmi
School of Mechanical Engg., Dublin City University

ABSTRACT

In recent years a number of researchers have studied the application of hydrodynamic pressure in various metal forming process. These investigators have studied the hydrodynamic action in the drawing process by using either a stepped bore or a tapered bore pressure unit.

In this paper theoretical and experimental studies of hydrodynamic pressure distribution through a confined passage using a polymer melt as the pressure medium have been investigated. The pressure unit consists of combined parallel and taper bores. The pressure in the polymer is generated by hydrodynamic action produced by the motion of the wire through the pressure unit. The distribution of pressure is measured experimentally and predicated theoretically. The results of this study should be useful in optimisation of the design of the pressure unit for plasto-hydrodynamic die-less drawing and coating of wires, strips, tubes and composite wire ropes.

NOMENCLATURE

P'_1 Pressure gradient in the first part of the unit
P'_2 Pressure gradient in the second part of the unit
τ_1 Shear stress in the melt in the first part of the unit
τ_2 Shear stress in the melt in the second part of the unit
τ_{c1} Shear stress on the wire in the first part of the unit
τ_{c2} Shear stress on the wire in the second part of the unit
μ Viscosity of polymer melt
L_1 Length of the first part of the unit
L_2 Length of the second part of the unit
Q_1 Flow of polymer in the first part of the unit
Q_2 Flow of polymer in the second part of the unit
Pms Pressure at the step
Pmax Maximum pressure in the unit
h_1 Initial radial gap in the first part of the unit
h_2 Middle radial gap at the step of the unit
h_3 Final radial gap in the second part of the unit
u_1 Velocity of polymer melt in the first part of the unit
u_2 Velocity of polymer melt in the second part of the unit

1. INTRODUCTION

It has been observed experimentally (1-3) that when a wire is pulled through a stepped or conical gap, which is filled with a viscous fluid then a very high pressure is generated. The magnitude of this pressure depends on the type of fluid and the geometrical configuration of the gap called the pressure unit. A number of studies have been carried out applying this phenomenon to plastically reduce the diameter of steel, copper and aluminium wires and tubes by drawing through pressure units of stepped or tapered bore geometry.

The first attempt to employ hydrodynamic action in a metal forming process was described by Christopherson and Naylor (4). They published a paper which showed the development of hydrodynamic lubrication action in wire drawing. Subsequently, a number of studies have been carried out applying the hydrodynamic action in coating of wires, tubes, strips and wire ropes by using polymer melt. The use of a polymer melt as the coating material was suggested by Symmons and Thompson (5). They investigated the adherence of the polymer coat on to the drawn wire. Stevens (6) conducted some limited experimental work in wire drawing and polymer lubrication and investigated the coating features of the polymer. Crampton (7) carried out an in-depth study of the wire drawing process. The apparatus used in references (6) and (7) consisted of a pressure tube connected to the forward end of a conventional die. The polymer melt was dragged into the tube by the motion of the wire generating hydrodynamic action which resulted in high pressures and coating of the wire. Symmons et al (8 & 9) presented an analysis of a die- less wire drawing process using viscosity-pressure and viscosity-temperature relationships of experimental form. Their aim was to examine individually the effect of pressure and temperature on the viscosity of polymer melt and consequently on the performance of the process.

All the previous investigators have studied hydrodynamic action by using either stepped bore or tapered bore pressure unit. They found that for certain design of the geometry of the unit the maximum pressure could be up to 300 MN/m^2.

In this paper a theoretical and experimental study of the hydrodynamic pressure distribution through a pressure unit which consists of combined parallel and taper bores have been investigated. The aim of this study is to determine the optimum design of the pressure unit which will generate higher pressure than those observed in previous studies. Such high pressure is very important for plasto-hydrodynamic die-less drawing and coating of wires, strips, tubes and composite wire ropes.

2. ANALYSIS

In this section a theoretical model is developed in order to predict the pressure distribution within the combined geometry pressure unit.

To formulate the analysis, the following reasonable assumptions are made:

- (i) the fluid has the characteristics of a Newtonian fluid
- (ii) material of the wire is undeformed during the drawing process
- (iii) the flow of the fluid is laminar and axial
- (iv) the flow of fluid is isothermal
- (v) the thickness of the fluid layer is small compared to the bore of the pressure unit
- (vi) the pressure in the fluid is uniform in the thickness direction at any point along the length of the pressure unit.

In the first part of the unit, the relationship between the pressure and shear stress gradient is given by

$$(\partial P/\partial x)_1 = (\partial \tau/\partial y)_1 \qquad (1)$$

The relationship between the shear stress and the rate of shear for the Newtonian fluid may be given by,

$$\tau_1 = \mu(\partial u/\partial y). \tag{2}$$

Integrating equation (1) with respect to y and noting that $(\partial P/\partial x)$ is constant with y we have,

$$\tau_1 = P'_1\ y + \tau_{c_1}. \tag{3}$$

substituting τ_1 from equation (3) into equation (2) and integrating we have

$$u_1 = \tfrac{1}{2}\mu P'_1\ y^2 + \tau_{c_1} y/\mu + C_1/\mu. \tag{4}$$

Applying the boundary condition that at $y = 0$ $u_1 = v_1$ we have,

$$C_1 = \mu v_1 \text{ so that } u_1 = \tfrac{1}{2}\mu\ P'_1\ y^2 + \tau_{c_1}\ y/\mu + v_1. \tag{5}$$

Applying the boundary condition that at $y = h_1$, $u_1 = 0$ in equation (5) and rearranging we have,

$$\tau_{c_1} = -P'_1\ h_1/2 - \mu v_1/h_1. \tag{6}$$

The flow of the fluid in the first part of the unit, Q_1, is given by

$$Q_1 = \int_0^{h_1} u_1 dy\ ;$$

which upon substituting for u_1 from equation (5) and integrating gives

$$Q_1 = P'_1 \, h^3{}_1/6\mu + v_1 h_1 + \tau_{c_1} \, h^2{}_1/2\mu .$$

and substituting for τ_{c_1} from equation (6) into the above equation we get

$$Q_1 = -h^3{}_1/12\mu(\partial P/\partial x)_1 + v_1 h_1/2 . \qquad (7)$$

The continuity of the flow of fluid shows that,

$(\partial Q_x/\partial x) + (\partial Q_y/\partial y)+(\partial Q_z/\partial z)=0$ But $\partial Q_y/\partial y=\partial Q_z/\partial z=0$ hence $\partial Q_y/\partial x=0$. Thus, $\partial P/\delta x$ in equation (7) must be constant, Therefore,

$$\partial P/\partial x = P'_1 = P_{ms}/L_1 = \text{Constant} .$$

From the geometrical configuration as shown in Figure (1) the gap between the second part of the unit and the surface of the wire is given by:

$$h = h_2 - Bx_2 \text{ where } B = h_2 - h_3/L_2 , \qquad (8)$$

for Newtonian fluid the pressure gradient is given by:

$$(\partial P/\partial x)_2 = (\partial \tau/\partial y)_2 \qquad (9)$$

and the shear stress is expressed by

$$\tau_2 = \mu(\partial u/\partial y). \qquad (10)$$

Differentiating equation (10) with respect to y we obtain

$$(\partial \tau/\partial y) = \mu(\partial^2 u/\partial y^2) .$$

substituting above in equation (9) we have

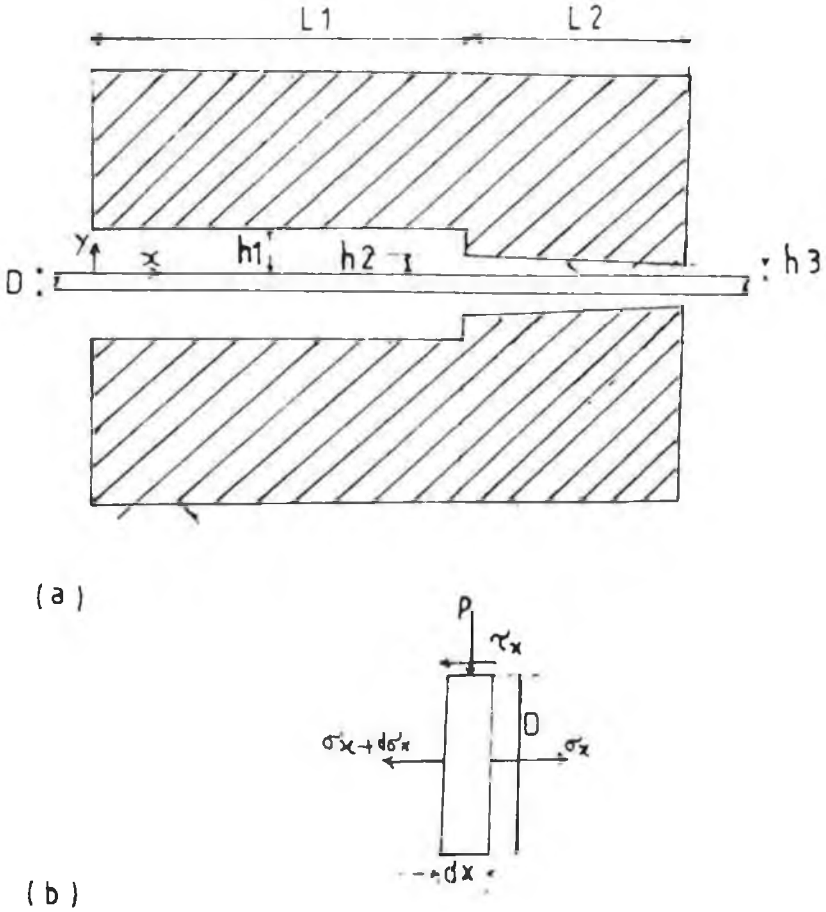

FIG.1 GEOMETRICAL CONFIGURATION OF THE PRESSURE UNIT AND THE WIRE

$$\partial^2 u/\partial y^2 = 1/\mu(\partial P/\partial x). \tag{11}$$

Integrating the above equation twice and noting that $\partial P/\partial x$ is assumed to be constant with Y we get

$$u_2 = 1/2\mu(\partial P/\partial x)\, y^2 + C_2 y + C_3\,, \tag{12}$$

Where C_2 and C_3 are constant.

Using the boundary condition that $u_2 = 0$ at $y = h$ and $u_2 = v_2$

at $y = 0$ and after rearrangement,

$$u_2 = 1/2\mu(\partial P/\partial x)\ (y^2 - hy) + v_2\ (1 - y/h). \tag{13}$$

the flow of the fluid is given by

$$Q_{x2} = \int_0^h u_2\, dy,$$

Which upon substituting for u_2 from equation (13) and integrating becomes

$$Qx2 = -\ h^3/12\mu(\partial P/\partial x) + v_2\ h/_2. \tag{14}$$

The continuity of the flow of the fluid shows that:

$\partial Qx/\partial x + \partial Qy/\partial Y + \partial Qz/\partial z = 0$ But $\partial Qy/\partial y = \partial Qz/\partial z = 0$, hence $\partial Qx/\partial x = 0$.

Differentiating equation (14) with respect to x and equating to zero and then integrating we obtain,
$h^3/\ 6\mu(\partial P/\partial x) = v_2 h + C_4$.

Using the boundary condition that the maximum pressure ($\partial P/\partial x = 0$) occurs at a point where $h = \bar{h}$ we have $C_4 = -v_2\bar{h}$ so that:

$$(\partial P/\partial x)_2 = 6\mu v_2(1/h^2 - \bar{h}/h^3), \tag{15}$$

which upon substitution for h from equation (8) gives:

$$(\partial P/\partial x)_2 = 6\mu v_2/(h_2 - Bx_2)^2 - 6\mu v_2\bar{h}/(h_2 - Bx_2)^3.$$

integrating the above equation we get

$$P = 6\mu v_2/B[1/(h_2 - Bx_2) - \bar{h}/2(h_2 - Bx_2)^2] + C_5; \tag{16}$$

but $P = 0$ at $x_2 = L_2$ where $(h_2 - Bx_2) = h_3$ hence

$$C_5 = -6\mu v_2 / B[1/h_3 - h/2h^2{}_3].$$

substituting above in equation (16) we get,

$$P = 6\mu v_2/B[1/(h_2 - Bx_2) - \bar{h}/2(h_2 - Bx_2)^2]$$

$$-6\mu v_2 / B[1/h_3 - \bar{h}/2h^2{}_3]. \qquad (17)$$

applying the boundary condition that $x_2 = 0$ at $h = h_2$,

$$P = P_{ms} = 6\mu v_2/B \{[1/h_2 - \bar{h}/2h^2{}_2]-[1/h_3 - h/2h^2{}_3]\}. \qquad (18)$$

for continuity of the flow we have $Qx_1 = Qx_2$ hence

$$-h^3{}_1/12\mu(\partial p/\partial x)_1 + v_1 h_1/2 = - h^3/12\mu(\partial P/\partial x)_2 + v_2 h/2.$$

but $v_1 = v_2 = v$ and $(\partial P/\partial x)_1 = P'_1 = P_{ms}/L_1$ therefore,

$$(\partial P/\partial x)_2 = h^3{}_1/h^3 (P_{ms}/L_1) - 6\mu v(h_1/h^3 - 1/h^2). \qquad (19)$$

Using the boundary condition that maximum pressure occurs at a point where $h = \bar{h}$ and $\partial P/\partial x = 0$ and substituting in equation (19) we get,

$$\bar{h} = h_1 - h^3{}_1 P_{ms}/6\mu v L_1. \qquad (20)$$

After solving equations (20) and (18) we obtain,

$$P_{ms} = \{(6\mu v h_1/2B)[1/h^2_3 - 1/h^2_2] + (6\mu v/B)[1/h_2 - 1/h_3]\}/$$

$$[1+(h^3_1/2BL_1)(1/h^2_3 - 1/h^2_2)], \qquad (21)$$

The maximum pressure occurs where $h=\bar{h} = h_2 - Bx_2$ which after substituting in equation (17) gives

$$P_{max} = (6\mu v/B)\ [1/2\bar{h} - 1/h_3 + \bar{h}/2h^2_3], \qquad (22)$$

3. EXPERIMENTAL PROCEDURE AND EQUIPMENTS

Experimental work was carried out using a purpose built wire drawing machine which incorporates the pressure unit and permits a wire drawing speed range of up to 20 m/sec. to be accomplished. The schematic diagram of the drawing machine is shown in Fig. (2). The pressure unit which consists of combined stepped and tapered bore cylinder, the melt chamber and the hopper are rigidy attached to the drawing machine bench. Details of the pressure unit is shown in the schematic diagram in Fig.(3). Pressure transducers and load cell were used in these experiments to measure the hydrodynamic pressure and drawing load respectively. The polymer melt chamber is attached to the pressure unit and is heated by electrical heater bands. The polymer was fed into the hopper and the melt chamber in granular form and sufficient time was allowed for the polymer melt to reach the set temperature. The diameter of mild steel wire used is 1.92 mm. A low density polyethylene (Escorene) and Lupolen were used as the pressure fluid.

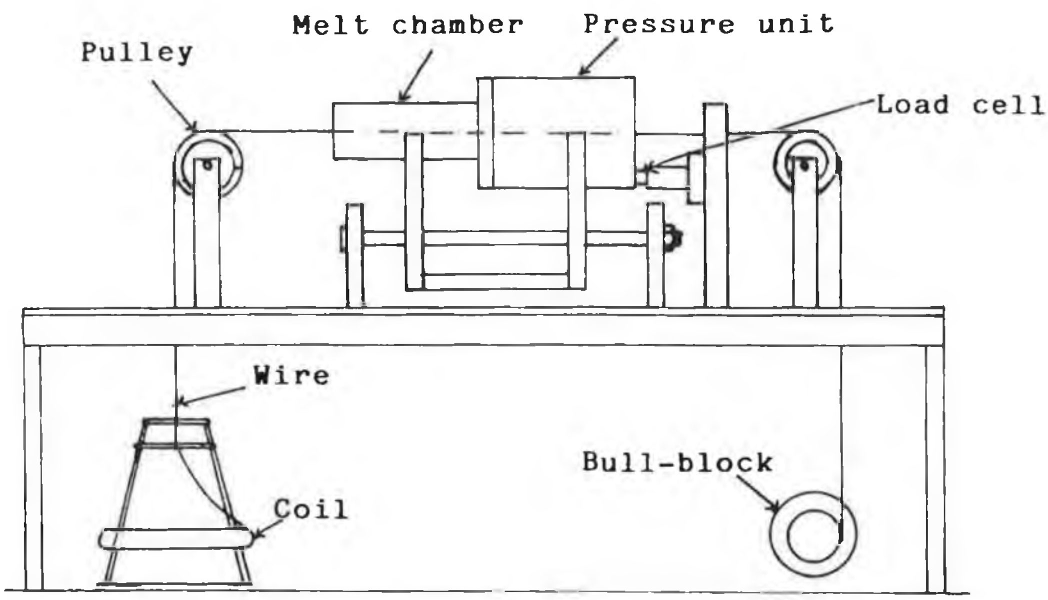

FIG 2 Schematic diagram showing the wire drawing arrangement

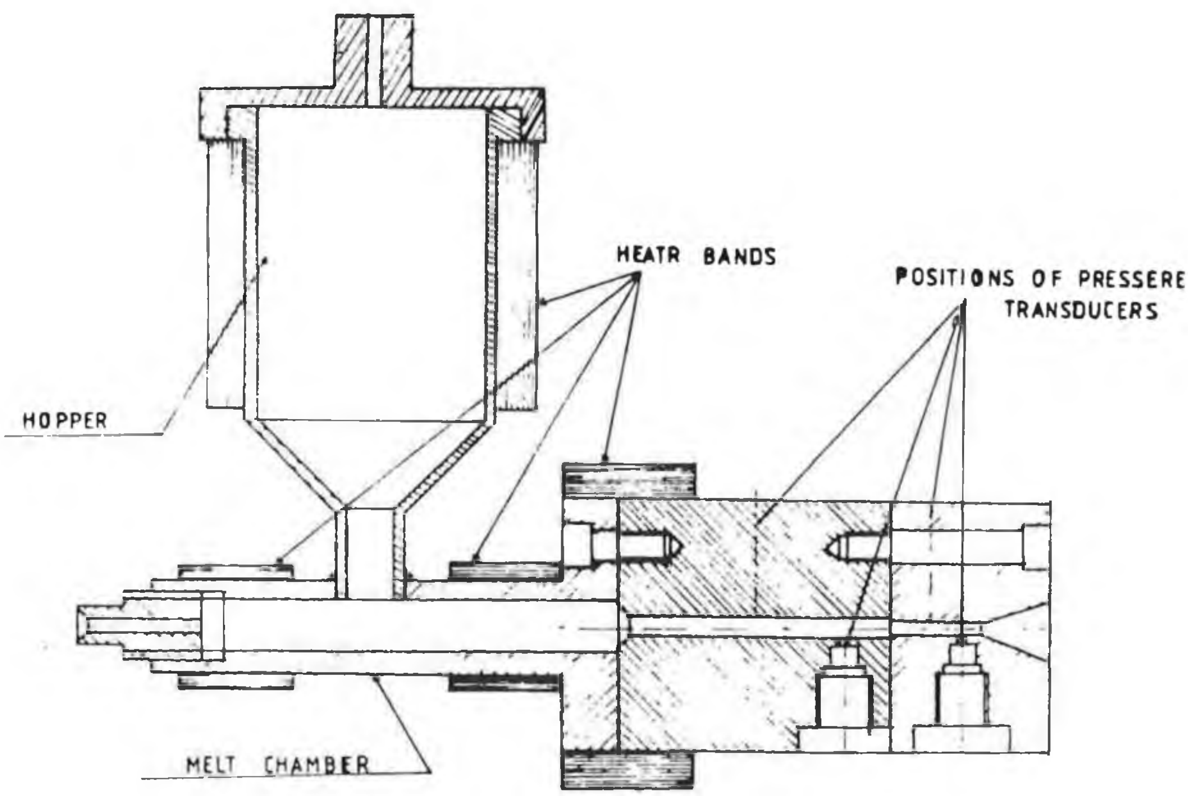

FIG. 3 Pressure unit assembly

To start a test run the wire is passed through the melt chamber and through the pressure unit before being attached to the motorised winding drum. When the process is started the wire while passing through the melt chamber drags along molten polymer into the pressure unit where hydrodynamic action generates high pressures. The magnitude of the pressure depends on the speed of drawing, the temperature of the fluid and the geometrical dimensions of the pressure unit.

4. EXPERIMENTAL AND THEORETICAL RESULTS

Mild steel wire of 1.92 mm diameter and brass wire of 2.04 mm diameter were used in this experiments. Figure (4) shows the results of pressure distribution when brass wire was drawn using lupolen polymer at melt temperature of 170° c and two different speeds but same gap ratio of h_2/h_3= 27.1. In all these cases the measured pressure was found to be the maximum just before the end of the unit (position number 4). The maximum pressure was found to vary between

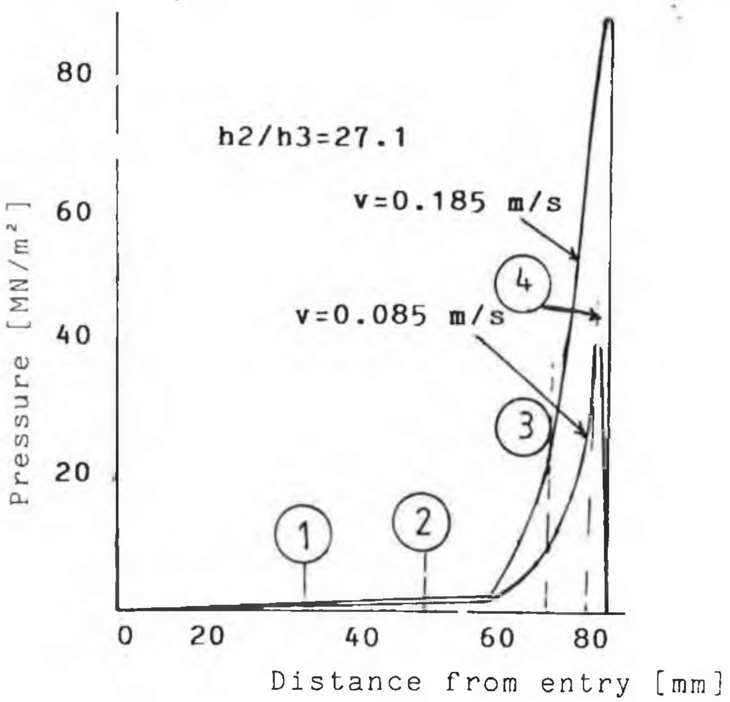

FIG. 4 Experimental result of pressure distribution for brass wire with lupolen at 170 °C

40-90 MN/m^2. Figure (5) shows the pressure profile when galvanised mild steel was drawn using lupolen polymer at speeds of 0.085, 0.11 respectively but the at same gap ratio of h_2/h_3= 8.7. Pressure profile showed very little change in the pressure as the drawing speed was increased.

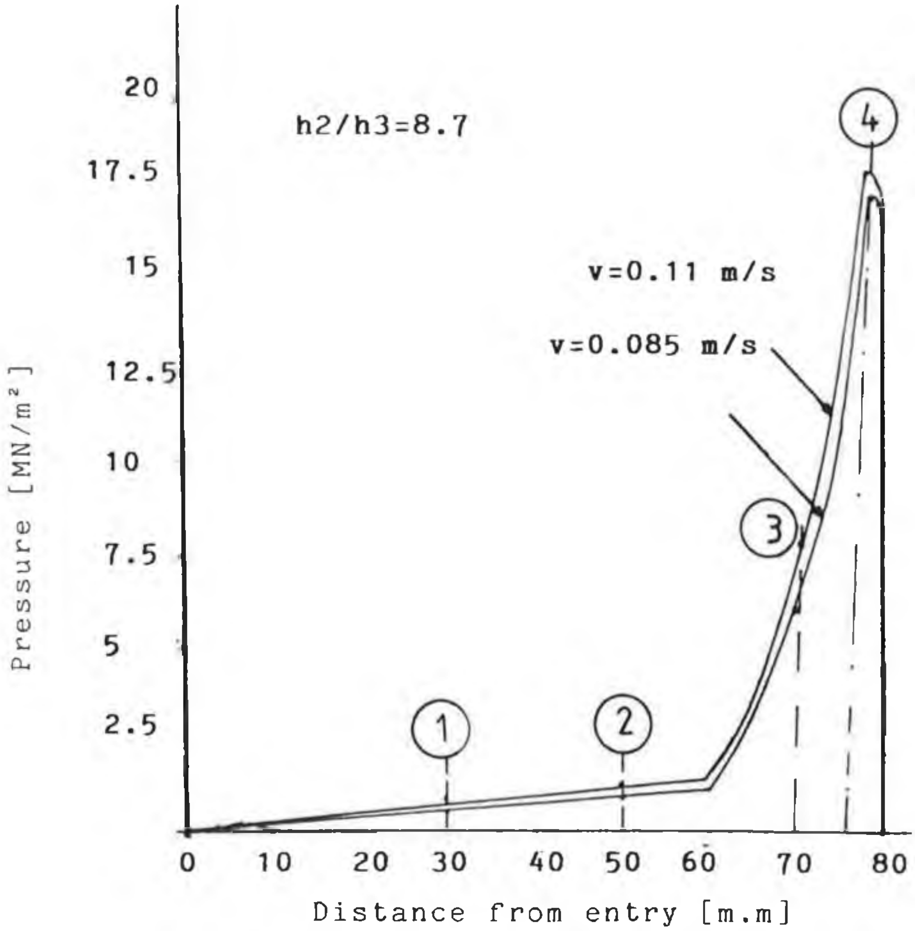

FIG. 5 Pressure distribution for mild steel wire with lupolen polymer at 170 °C

Figure (6) shows the measured pressures for brass wire versus speed with lupolen polymer at melt temperature of 170° c. The maximum pressure readings were measured at position number 4. At different drawing speeds for position numbers 1 and 2 the pressure readings were found to be approximately constant whilst at position 3 and position number 4 the measured pressure was observed to vary significantly with the drawing speed.

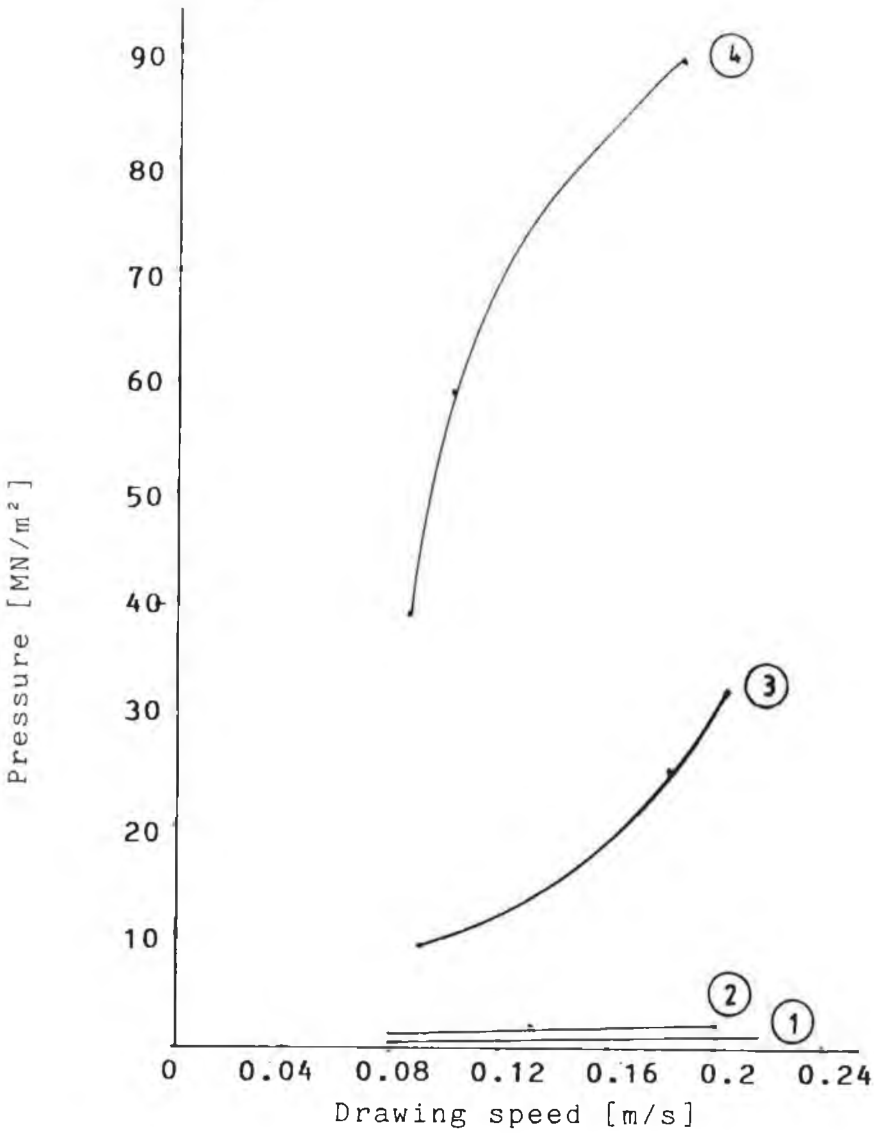

FIG.6 Pressure versus speed for brass wire with lupolen polymer at 170 °C

Figure (7) shows the comparison of theoretical and experimental hydrodynamic pressure distribution at drawing speed of 0.185 m/sec. Good agreement was observed between the theoretical and experimental results. Figure (8) shows the theoretical result of pressure distribution at different drawing speeds and at gap ratio $h_2 / h_3 = 8.7$. This figure shows that the pressure increases as the drawing speed is decreased while it was observed experimentally that only a little change in the pressure takes place as

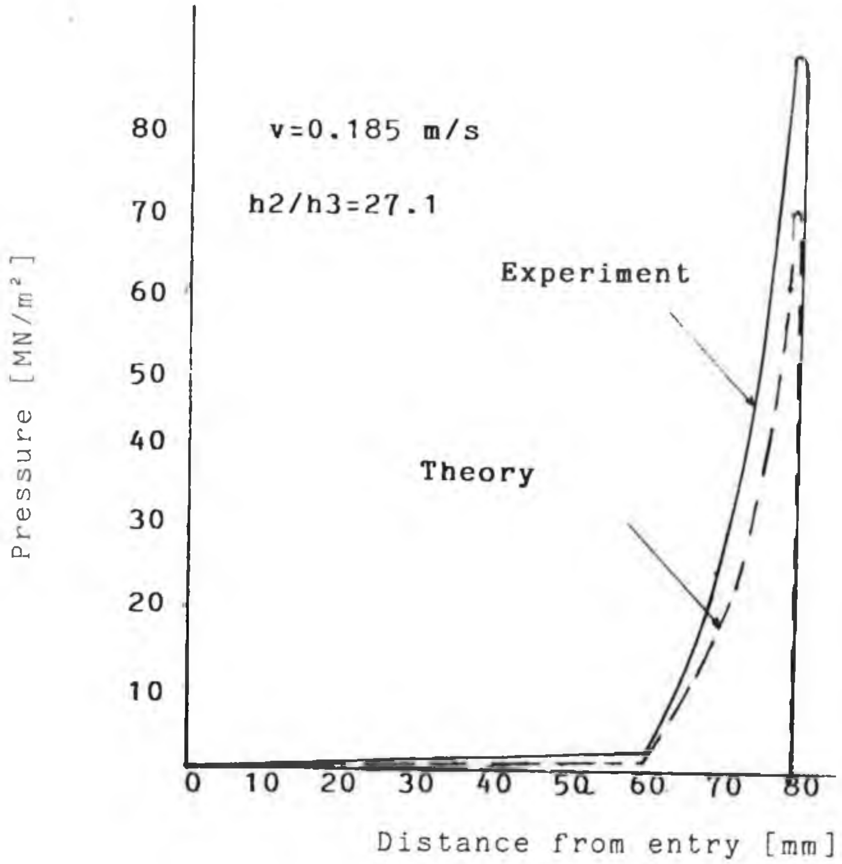

FIG.7 Comparison of theoretical and experimental results of hydrodynamic pressure distribution

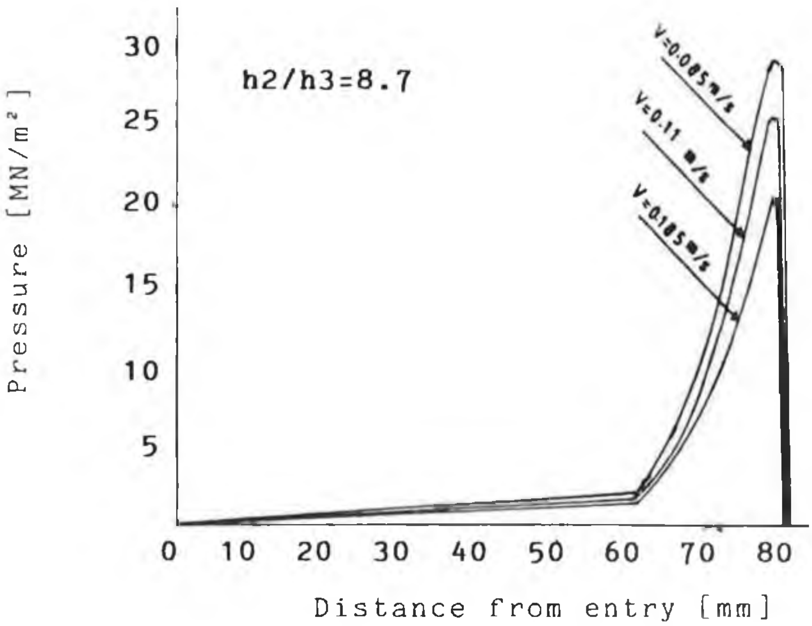

FIG.8 Theoretical results of pressure distribution debend on psudo-newtonian solution

the drawing speed is increased. Figure (9) shows the predicted pressure distributions for different gap ratios, h_2/h_3 at a drawing speed of 0.1 m/sc. This figure suggests that there exists a gap ratio (optimum) for which the pressure is maximum, everything else being the same. This maximum pressure occurs towards the exit end of the tapered part of the pressure unit. For greater or smaller values of the gap ratio than the optimum value, a decreased magnitude for the maximum pressure is obtained. For a gap ratio of unity (stepped bore) the maximum pressures occur at the step.

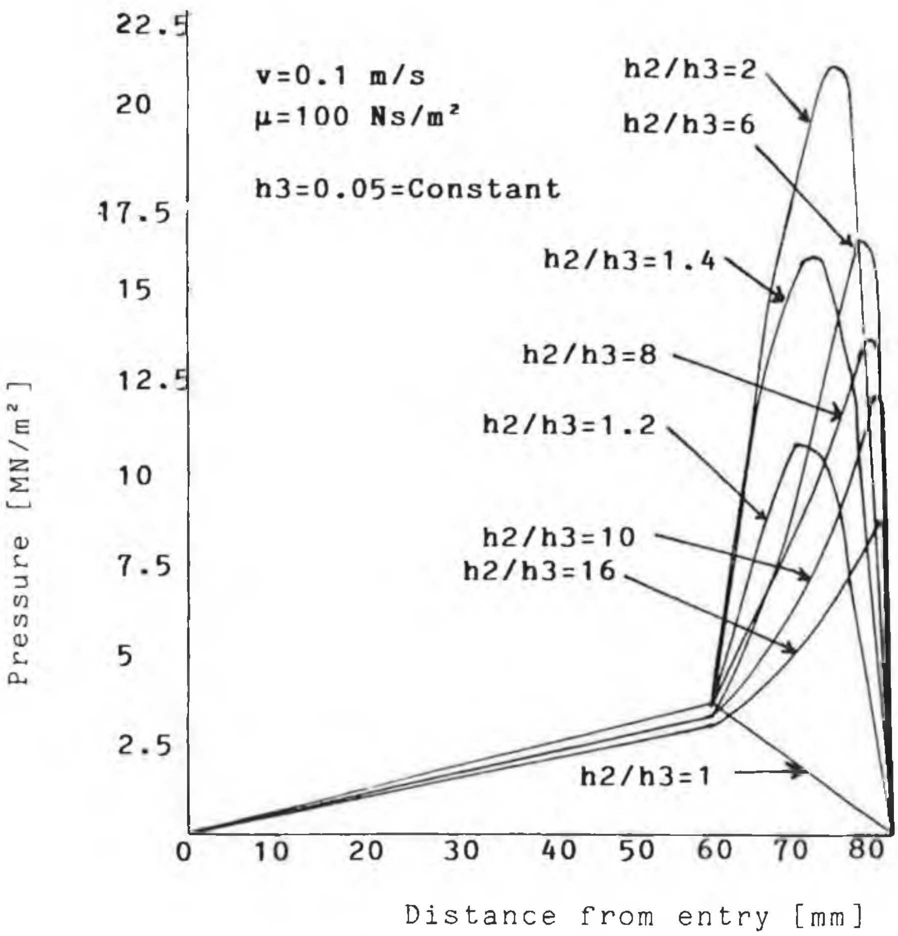

FIG.9 Theoretical effect of gap ratio h2/h3 on pressure distribution

5. CONCLUSIONS

Initial experiments have been carried out towards optimising a plasto-hydrodynamic pressure unit for drawing and/or coating of wires and tubes.

Theoretical prediction based on a Newtonian analysis suggests that certain combination of taper and parallel geometries for the unit exists which would generate larger pressure. Experimental results confirm this. Further extensive tests should be undertaken to validate the present and any modified theory.

REFERENCES

1. H. Parvinmehr, G.R. Symmons and M.S.J. Hashmi
   "A non-Newtonian plasto-hydrodynamic analysis of die-less wire-drawing process using a stepped bore unit"
   Int. J. Mech. Sci. Vol 29, No. 4, pp 239-257 1987

2. M.S.J. Hashmi and G.R. Symmons
   "A numerical solution for the plasto-hydrodynamic drawing of a rigid non-linearly strain hardening continuum through a conical orifice"

3. M.S.J Hashmi, G.R. Symmons and H. Parvinmehr
   "A novel technique for wire drawing"
   J. of Mech. Eng. Sci. Vol 24, P.1, 1982.

4. Christopherson, D.G. and Naylor, H. "Promotion of lubrication in wire drawing"

5. Thompson, P.J. and Symmons, G.R. "A plasto-hydrodynamic analysis of the lubrication and coating using polymer melt during drawing" Proc. Inst. Mech. Eng., vol. 191, 13177

6. Stevens, A.J. "A plasto-hydrodynamic investigation of lubrication and coating of wire using a polymer melt during drawing" PhD Thesis, Sheffield City Polytechnic, 1979

7. Crampton, R. "Hydrodynamic lubrication and coating of wire using a polymer melt during drawing" PhD Thesis, Sheffield City Polytechnic, 1980

8. Symmons, G.R., Hashmi, M.S.J. and Xie, Y.D. "The optimisation of plasto-hydrodynamic wire-drawing process"

9. Symmons, G.R. Xie, Y.D. and Hashmi, M.S.J. "Thermal effect on a plasto-hydrodynamic wire drawing process using a polymer melt"